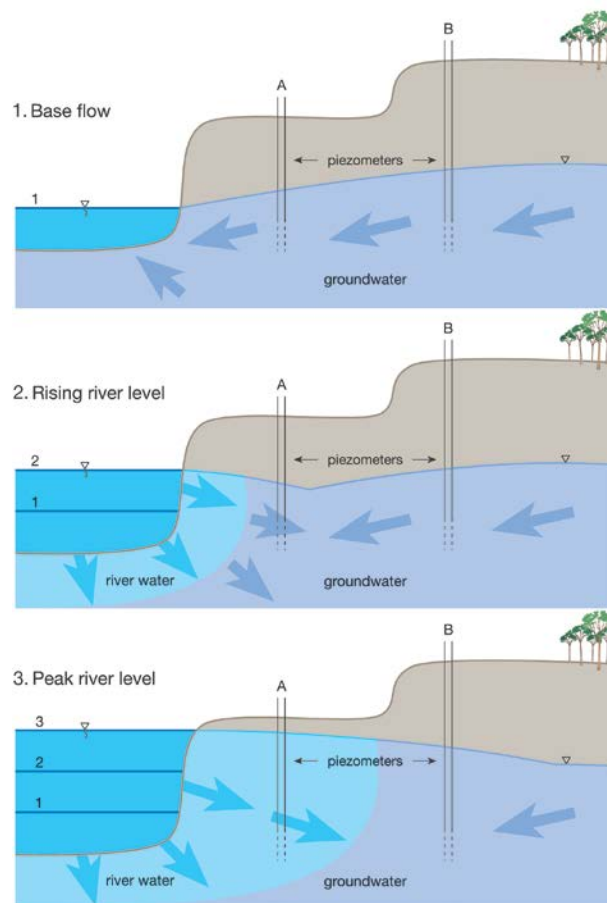


Evaluation of Bank Storage Using Pressure and Solute Propagation



Submitted by

Chani Welch

As a requirement in full for the degree of Doctor of Philosophy in the
School of the Environment, Flinders University of South Australia

2014

Table of Contents

Table of Contents.....	i
List of Figures	iv
List of Tables	vii
Summary.....	viii
Declaration of Originality.....	x
Co-authorship	xi
Acknowledgements	xii
1 Introduction	1
1.1 The research problem.....	1
1.2 Research aim.....	3
1.3 Structure of this thesis.....	4
2 Propagation of solutes and pressure into aquifers following river stage rise	6
2.1 Introduction	6
2.2 Analytical solution development	9
2.3 Numerical simulations	13
2.3.1 Model conceptualization and set up	13
2.3.2 Rapid increase in river stage	17
2.3.3 Sensitivity analysis for rapid increase in river stage	20
2.3.4 Sensitivity to hydrological processes	23
2.4 Example application to field data	29
2.4.1 Field setting.....	29

2.4.2	Determining travel times and travel distances.....	30
2.5	Discussion	32
2.6	Conclusions.....	35
3	Relative rates of solute and pressure propagation into heterogeneous alluvial aquifers following river flow events	37
3.1	Introduction.....	39
3.2	Methodology	41
3.2.1	Analytical solutions.....	42
3.2.2	Numerical simulations	43
3.3	Modelling Results	46
3.3.1	Process of pressure and solute propagation.....	46
3.3.2	Effects on travel time metrics.....	49
3.3.3	Comparison to analytical solutions	54
3.3.4	Estimating hydraulic conductivity and flux.....	56
3.3.5	Identifying heterogeneity from travel time ratios.....	60
3.4	Field application	63
3.4.1	Site Description.....	63
3.4.2	Analysis of field data.....	64
3.5	Discussion	67
3.6	Conclusions.....	70
4	Influence of hydraulic gradient on bank storage exchange, penetration distance and return time	72
4.1	Introduction.....	73

4.2	Methods.....	75
4.2.1	Analytical Solutions.....	76
4.2.2	Numerical Simulations.....	77
4.2.3	Initial Conditions and Metrics.....	78
4.3	Results.....	79
4.3.1	Process of Exchange.....	79
4.3.2	Aquifer and Wave Properties, Exchange and Return Time	82
4.3.3	River Shape and Aquifer Penetration	89
4.4	Discussion	92
4.5	Conclusions	96
5	Conclusions, Research Contribution and Future Work.....	97
	Appendix A Theoretical development of solute travel time.....	100
	Appendix B Analytical solutions for pressure propagation through a clogging layer.....	103
	Appendix C Synoptic sampling results from the Cockburn River	104
	Appendix D Time series data from the Cockburn and Mitchell Rivers	107
	Appendix E Groundwater chemistry and isotope results	109
	Appendix F Published conference proceedings.....	111
	References	116

List of Figures

Figure 2-1 Plot of a against c for commonly anticipated values in the context of bank storage investigations ($0 < c < 1$).....	11
Figure 2-2 Model set up.....	14
Figure 2-3 Comparison of analytical prediction and numerically simulated hydraulic heads against time at $x = 10$ m and $z = 5$ m for the base case for a) the simulation period and b) early time when t_p occurs.....	18
Figure 2-4 Propagation of a) hydraulic head (m), b) Darcy flux (m d^{-1}) and c) solute concentration into an aquifer due to a 1 m river stage rise.....	18
Figure 2-5 Stage increase-induced variation in a) hydraulic head (m), b) Darcy flux (m d^{-1}) and c) solute concentration with respect to time at $x = 10$ m and $z = 1, 5$ and 9 m.....	19
Figure 2-6 Sensitivity of solute and pressure travel time metrics to variation in K , b , S_y , and H	21
Figure 2-7 Sensitivity of solute travel time and travel distance to regional hydraulic gradients at a) at $x = 5$ m and $z = 5$ m with $K = 4.32 \text{ m d}^{-1}$, b) at $x = 10$ m and $z = 5$ m with $K = 4.32 \text{ m d}^{-1}$, and c) at $x = 10$ m and $z = 5$ m with $K = 43.2 \text{ m d}^{-1}$	23
Figure 2-8 Percentage difference between the base case (zero gradient) time travel metrics and travel time metrics for simulated positive (flow towards the river, gaining) and negative (flow away from the river, losing) regional hydraulic gradients.....	24
Figure 2-9 Hydraulic head and concentration plotted against time at $z = 5$ m, $x = 5$ and 10 m for a 50 day stage increase and the base case (infinite stage increase).....	26
Figure 2-10 Percentage difference between the base case (full penetration, or $P = 1$, river bed at $z = 0$ m) travel time metrics and travel time metrics for partial river penetration $P = 0.25$ (river bed at $z = 7.5$ m) and $P = 0.5$ (river bed at $z = 5$ m) at observation points at $x = 10$ m and $z = 2.5$ m, 5 m, and 7.5 m.....	27
Figure 2-11 Percentage difference between instantaneous rate of stage increase and normalized pressure travel time for a representative range of aquifer parameters.....	28

Figure 2-12 Continuous pressure and EC measurement throughout a flood event in September 2011 for the Cockburn River and two adjacent monitoring bores.....	30
Figure 3-1 Conceptual models of heterogeneity in alluvial aquifers, a) vertical clogging layer and b) horizontal sand string.....	42
Figure 3-2 Comparison of numerically simulated a) head and b) solute propagation into a heterogeneous aquifer with a 20 m thick clogging layer to two end-member homogenous aquifers.....	47
Figure 3-3 Spatial distribution of solute and pressure propagation into aquifers containing 1 m thick sand strings (white lines) with increasing contrast in string and aquifer hydraulic conductivities (numerical simulations).....	49
Figure 3-4 Comparison of numerically simulated pressure (t_p) and solute (t_s) travel times and their ratio (t_s/t_p) at increasing distances from the river bank for homogenous aquifers (solid lines) with low ($K_1 = 8.64 \text{ m d}^{-1}$) and high ($K_2 = 77.76 \text{ m d}^{-1}$) hydraulic conductivity and heterogeneous aquifers (dashed lines) with either a)- c) clogging layer 20 m thick or d)-f) sand string 1 m thick ($H = 5 \text{ m}$, $K_2/K_1 = 9$).	51
Figure 3-5 Comparison of numerical results for a) pressure travel times and b) solute travel times as a function of hydraulic conductivity contrast for different sand string thicknesses (b_2) ($K_2 = 77.76 \text{ m d}^{-1}$, $H = 5 \text{ m}$, $x = 30 \text{ m}$).	53
Figure 3-6 Comparison of pressure and solute travel times obtained from analytical solutions (equivalent homogenous, equations (3.1) and (3.2) and heterogeneous (equation B1)) with travel times obtained from numerical simulations of heterogeneous aquifers....	54
Figure 3-7 Comparison of a) hydraulic conductivities calculated with equation 3.1 (t_p) or equation 3.2 (t_s) and b) fluxes from solute and pressure travel times obtained from homogeneous aquifer simulations to actual (hydraulic conductivity) or model-derived (flux) values.....	57
Figure 3-8 Ratios of a), b) estimated to average hydraulic conductivity and c), d) estimated to simulated flux from river to aquifer for clogging layer and sand string scenarios.....	58

Figure 3-9 Numerically simulated solute and pressure travel times and their ratio at $x = 30$ m for a) clogging layers and b) sand strings of varying thickness across a range of hydraulic conductivity ratios ($K_2 = 77.76 \text{ m d}^{-1}$, $H = 5 \text{ m}$).....	61
Figure 3-10 Field data for May 2012 for piezometers at 15 m (GW1) and 30 m (GW2) from the river bank.	64
Figure 4-1 Conceptual model of river – aquifer system.	75
Figure 4-2 Velocity vectors from the simulation of a wave 1 m high with a period of 5 days under a hydraulic gradient of 0.01 depicting the process of river water movement into and out of an aquifer.....	80
Figure 4-3 Total volume of water exchange per unit width of aquifer and return times obtained from analytical solutions for a range of hydraulic conductivity (K), wave height (H) and wave period values at a range of hydraulic gradients.....	83
Figure 4-4 Dependency of total exchange per unit width of aquifer, penetration distance, and 90% return time on variation in hydraulic gradient and hydraulic conductivity (K), wave height (H) and period, and dispersivity (A).....	85
Figure 4-5 Percentage error in analytical results compared to numerical results for a) total flux and b) 90% return time.....	86
Figure 4-6 10%, 50% and 90% return times after commencement of river stage rise for variation in hydraulic conductivity (K), wave height (H) and period (d), dispersivity (A), and partial penetration with varying aspect ratios (AR).	87
Figure 4-7 Vertical distribution of exchange along the wetted perimeter on entry to the aquifer for a range of hydraulic conductivities at a) hydraulic gradient = 0 and b) hydraulic gradient = 0.01.....	88
Figure 4-8 Dependency of a) total exchange per unit width of aquifer, b) horizontal penetration distance, c) vertical penetration distance, and d) return time on variation in hydraulic gradient and partial penetration.	90

Figure 4-9 Close up of the spatial variation in penetration distance of the 0.5 concentration contour for a fully penetrating river (<i>FP</i> , black line), aspect ratio (<i>AR</i>) of 3 (red line) and 9 (blue line) with no hydraulic gradient present.....	91
Figure 4-10 Comparison of river flow events in a) 2012 and b) 2013 and the groundwater level (solid red line) and specific electrical conductivity (EC, dashed red line) at a field site adjacent to the Mitchell River in tropical north Queensland, Australia.....	94

List of Tables

Table 2-1 Model parameters for base case simulation.....	16
Table 3-1 Parameters used for generic model simulations.....	45
Table 4-1 Parameter variation.....	78

Summary

Bank storage is the process of river water mixing with near-river groundwater as a result of an increase in river stage due to a flow event. Such mixing causes temporal and spatial variation in near – river groundwater chemistry. However, the extent of the interaction is poorly defined. The extent of the interaction has important ramifications for biogeochemical cycling, contaminant mixing and degradation, and resource assessment techniques that differentiate between surface water and groundwater reservoirs. Previous assessments of bank storage have primarily relied on hydraulic methods, particularly pressure propagation, and chemistry measurements with limited temporal resolution. This work aimed to evaluate the relative rates of solute and pressure propagation and develop new assessment techniques for bank storage in a variety of hydrogeological environments.

In contrast to pressure propagation into homogeneous aquifers in response to river stage rise, the relationships between water propagation and aquifer properties were not well understood prior to this study. Practically, water movement is most readily measured using a conservative solute or tracer. Numerical assessment of a new analytical relationship between solute and pressure travel times and distances and aquifer and flow event characteristics determined that the solution may be used in variably saturated aquifers with errors generally less than 30%. In homogeneous aquifers the ratio of solute to pressure travel time is independent of hydraulic conductivity. Consequently, under certain hydrological conditions time series measurement of pressure and a solute (or proxy) and computation of pressure and solute travel times enables a first-order estimate of aquifer properties and the lateral extent of river water penetration into an aquifer.

In homogeneous systems river stage rise causes pressure to propagate faster and further into an aquifer than water (or solutes). Numerical testing of two conceptual models of alluvial heterogeneity indicated that pressure and solute propagation are unequally affected by aquifer heterogeneity. Hence, under certain conditions, substantial solute

change can be recorded in an aquifer before substantial pressure change. This may be identified by computing a solute travel time less than a pressure travel time. Flux estimates obtained from solute travel times using homogeneous solutions were determined to be more accurate than estimates obtained from pressure data. The error in estimates derived from pressure data was proportional to the contrast in hydraulic conductivity in a system.

Theoretical investigations of bank storage have not systematically quantified the influence of the hydraulic gradient between aquifer and river. In this work analytical and numerical techniques demonstrated that variation in the hydraulic gradient influences bank storage exchange, penetration distance and residence time, at a scale similar to substantial variation in hydraulic conductivity, wave height and period, dispersivity, and river partial penetration. Consideration of the hydraulic gradient is therefore integral to quantitative assessments of exchange.

Simultaneous measurement of pressure and solutes at high temporal resolution within rivers and adjacent aquifers is a useful technique for improving understanding of the spatial and temporal extent of river – aquifer exchange during flow events. The utility of the theory relies on contrasting river and aquifer chemistries. Future work should consider the use of alternative tracers to test residence time distribution theories, and geostatistics, spatial imaging, and uncertainty techniques to further understand the influence of heterogeneity.

Declaration of Originality

I certify that this thesis does not incorporate, without acknowledgment, any material previously submitted for a degree or diploma in any other university; and that to the best of my knowledge and belief it does not contain any material previously published or written by another person except where due reference is made in the text.

Chani Welch

Co-authorship

Chani Welch is the primary author on this thesis and all the enclosed documents. Chapters 2 to 4 were written as independent manuscripts in which the co-authors provided intellectual supervision and editorial comment. Neville I. Robinson completed the analytical derivation presented in Appendix A.

Acknowledgements

First and foremost I would like to acknowledge the contributions of my two supervisors to this PhD. I am grateful to Peter Cook for his generosity with his many ideas and time, for sharing his passion for hydrogeological process understanding, and for expecting the best. I appreciate the numerous lengthy conversations with Glenn Harrington about hydrogeology, modelling, and various completely unrelated topics, which, as much as anything, helped me work things out for myself. I would also like to express my gratitude to Marc Leblanc for coordinating all aspects of field work in the Mitchell River and being continually passionate about tropical hydrology, and Roki for the fresh perspective he brought at just the right time.

I gratefully appreciate assistance with field work provided by Jordi Batlle Aguilar, Roger Cranswick, Saskia Noorduijn, Rolf Kipfer, Michelle Irvine, Cameron Wood, Nick White, Lawrence Burke, Mark Trigg, Vincent Post, Nick Rockett, Tony Forsyth, Joel Bailey, and the NSW Office of Water.

Financial assistance consisted of an Australian Postgraduate Award and a scholarship from the National Centre for Groundwater Research and Training (NCGRT). Additional funding for this research was provided by the NCGRT, an Australian Government initiative, supported by the Australian Research Council and the National Water Commission. Funding for the installation of piezometer transects adjacent to the Cockburn River was provided through the SuperScience program. The Australian Wildlife Conservancy – Brooklyn provided site access and general assistance during field work on the Mitchell River.

On a personal note, I would like to thank my Adelaide family for the companionship, camping, food, and wine that have made the past few years so enjoyable, and my family and friends who stuck around for the journey, helping me maintain perspective.

Chani Welch 7 February, 2014

1 Introduction

1.1 The research problem

Quantifying the exchange of water and solutes between rivers and aquifers has become crucial in many water-limited environments as climatic conditions and human consumption stress surface water and groundwater systems simultaneously (Baillie et al., 2007). This situation has highlighted the interconnection between the two resources, and historical over-allocation of water in some areas (Nevill, 2009; Sophocleous, 2002). A variety of methods are available to quantify water fluxes between aquifers and rivers, but many are limited by the localised nature of the measurements, and spatial heterogeneity in hydrogeological properties (Kalbus et al., 2006). This can result in highly variable and uncertain volume estimates, and, where such values are subsequently used for management purposes, potential sub-optimal allocation of resources. In addition, estimates made using hydraulic and chemistry based methods often produce conflicting results (Kirchner, 2003).

Characterising the river-aquifer exchange processes occurring in a system is the first step to appropriately quantifying groundwater discharge or recharge. Exchange processes occur over a continuum of timescales and include hyporheic exchange (minutes to weeks), parafluvial flow (hours to months) and bank storage (hours to years). Hydrological, geological, and geomorphological controls on the significance of these processes vary throughout time and space, as do the drivers for the exchange (Winter, 1998). These short to medium term mixing processes occur, and therefore need to be considered, in the context of regional processes that occur over decades to millennia as a result of aquifer-wide recharge/discharge dynamics.

Chemical mass balance flux quantification methods are considered most appropriate on a scale potentially useful to water resource managers due to their ability to integrate processes over larger scales (Kalbus et al., 2006). However, interpretation of chemistry data

using simple models requires that processes are lumped, and hence, results can be highly dependent on the conceptual model and parameterisation. Lack of consideration of hyporheic exchange, for example, can significantly affect estimates of groundwater discharge to rivers (Cook et al., 2006). Furthermore, river aquifer exchange processes mix river water with groundwater. In many cases this creates a temporally and spatially variable zone of water around a river with a chemistry that is distinct from the wider aquifer. Lack of consideration of this temporal variability has rarely been considered but can lead to significant errors in estimates of groundwater discharge to rivers (McCallum et al., 2010).

Techniques that exploit temporal chemistry changes to determine, for example, travel times from rivers to aquifers, are increasing as measurement technologies improve, but existing analysis methods such as deconvolution (e.g., Cirpka et al., 2007; Vogt et al., 2010) and principal component analysis (Lewandowski et al., 2009; Page et al., 2012) cannot explicitly identify the influences of individual aquifer properties or processes.

Temporal changes in groundwater chemistry have many drivers. In aquifers connected to rivers, flow events are considered to be one of the main drivers. As the river level rises above that of the adjacent groundwater, river water moves into the aquifer, and mixes with the existing groundwater. As the flood wave passes, this mixture of water returns to the river. This process is termed bank storage (Todd, 1956). Bank storage occurs regardless of whether a river is gaining or losing water from the adjacent aquifer, as long as the river and aquifer are hydraulically connected.

Analytical solutions that relate pressure propagation as a function of river stage rise to aquifer properties, and from that estimate flux, have long been available for homogeneous systems (Cooper and Rorabaugh, 1963) and for rivers with clogging layers (Hall and Moench, 1972; Hantush, 1965). However, pressure change alone cannot be directly correlated to the extent of water movement into an aquifer. Conventional theory indicates that pressure propagates further and faster than water or any solutes it contains. However,

explicit relationships between solute propagation, river stage rise, and aquifer properties have not been described in analytical solutions. Consequently, solute data has been under-utilised. Similarly, numerical investigation of the process of bank storage has been predominantly hydraulic, and in homogenous systems, as pressure data is more readily available for model calibration and simulating solute transport is more numerically intensive. Field assessment of bank storage has also predominantly used hydraulic methods, or measurements of river chemistry obtained at low temporal resolution. Systematic assessment of the movement of water and solutes during bank storage was required to facilitate exploitation of increasingly available high temporal resolution solute data for the purposes of improved management of surface water and groundwater resources.

1.2 Research aim

The aim of this research was to increase bank storage process understanding in general, evaluate the relative rates of pressure and solute propagation during bank storage, and develop new techniques for assessment of river – aquifer exchange during flow events. The research was based on two hypotheses:

- i. River stage rise and fall induces a predictable variation in near-river groundwater chemistry, the spatial and temporal extent of which is dependent on key aquifer properties and the degree of stage change; and
- ii. Continuous measurement of a solute (or proxy) in addition to pressure in near-river groundwater will assist with the determination of additional aquifer properties (compared to solely measuring pressure) and the conceptual model of the river-aquifer interface.

In order to address these hypotheses this work aimed to:

- use analytical and numerical methods to explore relationships between water (which can be represented by a generic conservative solute) and pressure travel

- time and distance and aquifer and wave characteristics in variably saturated aquifers with a wide range of characteristics and conceptual models;
- provide a preliminary assessment of the influence of heterogeneity structures on the relative rates of solute and pressure propagation identified for homogenous aquifers using transient numerical flow and transport simulations;
 - examine the relationships of bank storage exchange, penetration distance and return time to aquifer properties, river – aquifer conceptual models, and hydraulic gradients; and
 - verify the practical application of theoretical findings using data collected in distinct hydrogeological environments. Field sites were instrumented in semi-arid northern New South Wales on the Cockburn River and tropical north Queensland on the Mitchell River.

1.3 Structure of this thesis

This thesis consists of a broad overview (Chapter 1), three pieces of work published in or submitted to international peer-reviewed journals (Chapters 2 – 4) and overarching conclusions of the research, including the research contribution and recommendations for further work (Chapter 5). The three manuscripts included are:

- (1) **Welch, C.**, P. G. Cook, G. A. Harrington, and N. I. Robinson (2013), Propagation of solutes and pressure into aquifers following river stage rise, *Water Resources Research*, 49, 5246–5259, doi:10.1002/wrcr.20408 [Chapter 2];
- (2) **Welch, C.**, G. A. Harrington, M. Leblanc, J. Battile-Aguilar, and P. G. Cook (2014), Relative rates of solute and pressure propagation into heterogeneous alluvial aquifers following river flow events, *Journal of Hydrology*, 511, 891-903, doi: 10.1016/j.jhydrol.2014.02.032 [Chapter 3]; and

(3) **Welch, C.**, G. A. Harrington, and P. G. Cook (under review), Influence of hydraulic gradient on bank storage exchange, penetration distance and return time, submitted to *Groundwater* [Chapter 4].

Supplementary information for Chapters 2-4 is contained in appendices, as are conference papers which resulted directly from this research.

2 Propagation of solutes and pressure into aquifers following river stage rise

ABSTRACT

Water level rises associated with river flow events induce both pressure and solute movement into adjacent aquifers at vastly different rates. We present a simple analytical solution that relates the travel time and travel distance of solutes into an aquifer following river stage rise to aquifer properties. Combination with an existing solution for pressure propagation indicates that the ratio of solute to pressure travel times is proportional to the ratio of the volume of water stored in the aquifer before the river stage rise and the volume added by the stage rise, and is independent of hydraulic conductivity. Two-dimensional numerical simulations of an aquifer slice perpendicular to a river demonstrate that the solutions are broadly applicable to variably saturated aquifers and partially penetrating rivers. The solutions remain applicable where river stage rise and fall occur, provided that regional hydraulic gradients are low and the duration of the river stage rise is less than pressure and solute travel times to the observation point in the aquifer. Consequently, the solutions provide new insight into the relationships between aquifer properties and distance and time of solute propagation and, in some cases, may be used to estimate system characteristics. Travel time metrics obtained for a flood event in the Cockburn River in eastern Australia using electrical conductivity measurements enabled estimates of aquifer properties and a lateral extent of river-aquifer mixing of 25 m. A detailed time series of any soluble tracer with distinctly different concentrations in river water and groundwater may be used.

2.1 Introduction

Despite intensive investigation of the processes by which rivers and aquifers exchange water and solutes at a variety of scales, theoretical developments have predominantly focused on hydraulic methods, and the use of pressure data to determine aquifer

properties. Advancements in water chemistry measurement technology provide the potential for increased use of time series chemistry data in the quantification of river and aquifer exchange at the event time scale, and impetus for theoretical development in this area. While pressure propagation is largely determined by aquifer diffusivity (ratio of transmissivity to storativity), water velocity, and hence solute transport, is a function of the ratio of hydraulic conductivity to aquifer porosity. Theoretical methods that incorporate chemistry measurements could exploit the different mechanisms that govern transport of water as opposed to pressure through aquifers to develop estimates of aquifer properties.

Observations of the propagation of head changes from river stage rise to adjacent aquifers have been used for decades to estimate aquifer properties. Early analytical solutions modified equations for heat conduction (e.g., Carslaw and Jaeger, 1959) to estimate aquifer diffusivity from the time and distance of pressure propagation into an aquifer induced by step increases in river stage (Hantush, 1961; Rorabaugh, 1960; Rowe, 1960). Subsequent analytical solutions developed relationships that incorporated single sinusoidal flood wave inputs and semi-infinite aquifers (Cooper and Rorabaugh, 1963) and arbitrary river stage input and semi-pervious stream banks (Hall and Moench, 1972). Assumptions common to the majority of analytical solutions include temporally constant aquifer diffusivity, homogeneity of aquifer properties, free surface Dupuit assumptions, vertical banks, and saturated flow (Doble et al., 2012; Sharp Jr, 1977). Numerical solutions have been applied to assess some of these limitations. Improvements that have been investigated include variable hydraulic conductivity and aquifer geometry (Whiting and Pomeranets, 1997), anisotropy and heterogeneity (Chen et al., 2006; Chen and Chen, 2003), and sloping banks and explicit inclusion of unsaturated flow (Doble et al., 2012). In many cases, these analytical and numerical methods have also been used to estimate aquifer transmissivity and storativity (e.g., Pinder et al., 1969). Recently, pressure propagation due to river stage fluctuation has been used to determine the heterogeneity of aquifer hydraulic conductivity (Yeh et al., 2009).

Time series solute datasets have predominantly been used to determine travel times of river water into aquifers in losing environments, generally where flow is induced by pumping (Cirpka et al., 2007; Hunt et al., 2005; Vogt et al., 2010). Data interpretation has relied on interpretation of tracer arrival times directly, or through cross correlation or deconvolution, with analysis rarely extended to estimation of aquifer properties. Examples of the use of numerical models to explicitly examine solute transfer induced by flow events are limited. Squillace (1996) used a 2D numerical simulation to confirm that river stage rise and fall was a plausible explanation for observed variations in groundwater chemistry at a site contaminated by atrazine. A generic analysis of the effects of river stage rise and fall and aquifer parameters on the spatial extent of river-aquifer exchange fluxes was presented by Chen and Chen (2003) using particle tracking. McCallum et al. (2010) explicitly simulated solute movement during river stage rise and fall in order to examine the temporal variation in groundwater chemistry at the river-aquifer interface, and its sensitivity to aquifer parameters for a general case, but did not specifically assess the movement of the pressure and solute fronts into the aquifer. In systems where river and aquifer electrical conductivities (EC) (or temperatures) are distinctly different, collection of detailed time series data is relatively simple and cost effective. Sawyer et al. (2009) presented time series data for pressure, EC and temperature in shallow piezometers adjacent to a river affected by regular dam-induced stream-stage fluctuations, however only the pressure data was used to estimate aquifer properties.

In this study we develop a simple equation that relates aquifer properties to the travel time and travel distance of water into an aquifer as the result of a unit increase in river stage. This analytical solution is combined with an existing solution for pressure propagation to create ratios between water and pressure travel times and travel distances that are independent of hydraulic conductivity. The applicability of these simple analytical relationships to variably saturated aquifers is evaluated by comparison with results from 2D numerical simulations of flow and mass transport in an aquifer slice. A range of aquifer

parameters are tested, as are the effects of the duration of maximum river stage, regional hydraulic gradients, degree of river penetration, and rate of river stage rise. Concentration change of a generic solute is used to represent water movement. The method by which the solutions may be used to estimate aquifer thickness and hydraulic conductivity and the lateral extent of river-aquifer mixing from simultaneous measurement of pressure and EC is demonstrated using extended time series data from a field site on the Cockburn River in eastern Australia.

2.2 Analytical solution development

In one dimension, propagation of head h in an aquifer of constant hydraulic conductivity K , in terms of distance x and time t can be described by the equation

$$\frac{\partial^2 h}{\partial x^2} = \frac{S}{Kb} \frac{\partial h}{\partial t}, \quad (2.1)$$

for both confined and unconfined aquifers with some provisos on the constant value parameters S and b (Bear, 1972). In a confined aquifer S is storativity and b is constant aquifer thickness. In an unconfined aquifer, equation (2.1) is one of two standard linearisations of the Boussinesq equation in which $S = S_y$ is specific yield and b is average saturated thickness. The analytical solution of equation (2.1) for an instantaneous river stage (head) increase is given by (Carslaw and Jaeger, 1959)

$$h = h_0 + H \cdot \operatorname{erfc} \left(\sqrt{\frac{x^2 S}{4 K b t}} \right), \quad (2.2)$$

where h_0 is initial head in the river and aquifer, H is stage change in the river, and $\operatorname{erfc}()$ is the complementary error function. In this paper we will assume that a conservative solute travels at the same rate as a water particle and define the solute (or water particle) travel velocity v_s by Darcy's Law:

$$v_s = -\frac{dx}{dt} = -\frac{K}{\theta} \frac{\partial h}{\partial x}, \quad (2.3)$$

where ϑ is aquifer porosity. This approach neglects diffusion and dispersion of the solute.

In order to develop a distance-time relationship for solutes, the partial x derivative of h in equation (2.3) is formed from equation (2.2), and then the first order differential of the last equality of equation (2.3) is solved. Detailed analytical development is presented in Appendix A. The solute travel time t_s at any distance x from a river bank becomes

$$t_s = \frac{x^2 S}{a^2 K b}, \quad (2.4)$$

where a is a constant determined by the gradient of the straight line plot of x against $\sqrt{Kbt/S}$.

It may be shown that a is a function of c (Figure 2-1; Appendix A), where c is a constant described in the formation of the partial x derivative of h :

$$c = \frac{HS}{b\theta}. \quad (2.5)$$

A metric for travel time related to pressure t_p is defined by setting $(h - h_0)/H$ equal to 0.5, approximating $\text{erfc}^{-1}(0.5)$ as 0.5, and rearranging equation (2.2) as:

$$t_p = \frac{x^2 S}{4Kb[\text{erfc}^{-1}(0.5)]^2} \approx \frac{x^2 S}{Kb}. \quad (2.6)$$

The metric is defined this way for two reasons. Firstly, one half of the head rise is a simple and common representation for averaging a time dependent head rise. Secondly, the replacement of $\text{erfc}^{-1}(0.5)$ by 0.5 is not only a good approximation, but removes the complementary error function from consideration. The error introduced by this approximation is 4 %, which is small relative to our ability to measure the parameters in this equation.

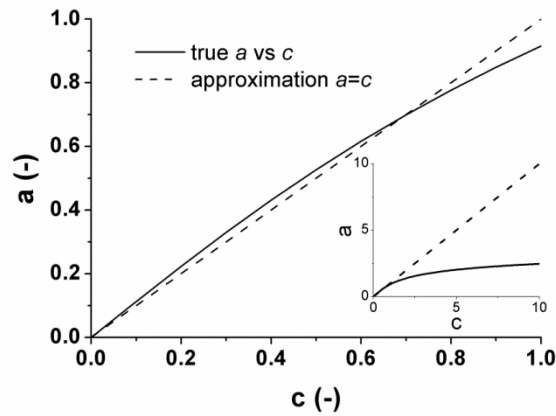


Figure 2-1 Plot of α against c for commonly anticipated values in the context of bank storage investigations ($0 < c < 1$). The insert depicts the range up to $c = 10$. The parameter α is a constant determined by the gradient of the straight line plot of x against $\sqrt{Kbt/S}$, where K is hydraulic conductivity, b is saturated thickness, t is time and S is storage. The parameter $c = HS/b\vartheta$, where H is the magnitude of river stage change and ϑ is porosity.

Combination of equations (2.4) and (2.6) yields the ratio of solute and pressure travel times t_s/t_p :

$$\frac{t_s}{t_p} \approx \frac{1}{a^2}. \quad (2.7)$$

Relationships between lateral distances travelled by solute and pressure are readily obtained for a given time t . From equation (2.4), with $t_s = t$ and $x = x_s$:

$$x_s = a \sqrt{\frac{Kbt}{S}}, \quad (2.8)$$

and from equation (2.6), based on a 50% increase in pressure, with $t_p = t$ and $x = x_p$:

$$x_p \approx \sqrt{\frac{Kbt}{S}}. \quad (2.9)$$

Combination of equations (2.8) and (2.9) yields the ratio of lateral travel distances x_s/x_p :

$$\frac{x_s}{x_p} = a. \quad (2.10)$$

Typical aquifer parameter ranges for H , S , b and θ in the context of bank storage indicate that the common range of c would be $0 < c < 1$. In this range c is approximately equal to a (Figure 2-1), whereas at larger values of c the relationship between a and c is clearly non-linear (Figure 2-1 insert). Consequently, the travel time of solute t_s as a function of distance into an aquifer x may be approximated by substituting c for a in equation (2.4) for the range $0 < c < 1$. By rearrangement t_s is obtained in terms of aquifer properties and river stage:

$$t_s \approx \frac{b\theta^2 x^2}{SH^2 K} , \quad (2.11)$$

and the ratio of solute and pressure travel times t_s/t_p as a function of aquifer properties and river stage rise becomes:

$$\frac{t_s}{t_p} \approx \left(\frac{b\theta}{HS} \right)^2 . \quad (2.12)$$

Interestingly, in the braces of the right side of equation (2.12) the numerator represents the volume of water present in the aquifer before the pressure wave (when multiplied by aquifer width and length), while the denominator represents the addition (or reduction) of water to (or from) the aquifer after the change in river stage.

Also, an approximate expression for the lateral travel distance of solute x_s as a function of aquifer properties and time is given by

$$x_s \approx \frac{H}{\theta} \sqrt{\frac{SKt}{b}} . \quad (2.13)$$

For the range $0 < c < 1$, approximation of the parameter a by aquifer properties (represented by the parameter c) introduces errors to the travel time metrics t_s and t_s/t_p of $\pm 20\%$. Over the same range, the error introduced to the travel distance metrics x_s and x_s/x_p varies from -13% to $+9\%$. The travel distance metrics are less sensitive to the approximation because they are directly proportional to a , whereas the travel time metrics

are proportional to $1/a^2$. Henceforth our analysis of the utility of the new analytical solutions is based on the simple approximation that $a = c$, that is, equations (2.11), (2.12) and (2.13).

2.3 Numerical simulations

Numerical simulations were conducted to test the applicability of the analytical solutions to pressure and solute propagation in variably saturated aquifers across a range of typical aquifer property values and system behaviours. Assumptions of the analytical solution that were tested numerically include 1) temporally constant transmissivity, 2) saturated flow, 3) instantaneous river stage rise, 4) neglecting dispersion and diffusion, 5) no ambient hydraulic gradient, and 6) fully penetrating river.

2.3.1 Model conceptualization and set up

The river-aquifer system was conceptualized as a two-dimensional aquifer slice perpendicular to a river (Figure 2-2). A numerical model was constructed using the finite element code FEFLOW as it has the capacity to explicitly model unsaturated zone pressure and solute transport processes (Diersch, 2009). The model was constructed as a variably saturated media model, in which the head-based (standard) form of the Richard's equation for flow and the convective form of the transport equation were solved across unsaturated and saturated portions of the model simultaneously. In the fully penetrating river case, the total model domain was 20 m in height, 2000 m in length, and 1 m in width, with an initial head h_0 equivalent to the initial saturated aquifer thickness b . For partially penetrating river cases, the model domain was extended by the distance w (from river bank to midpoint) at height h_p . The initial water table was flat, except where the effects of a regional hydraulic gradient were investigated. An unsaturated zone at least 4 m thick was maintained in order to explicitly simulate water and solute movement in this zone. The thickness of the unsaturated zone was sufficient to avoid boundary effects on the capillary fringe, and hence flow regimes. No-flow boundaries were applied along the base of the model, the right hand boundary, the top of the model, the left hand boundary above h_{max} , and in

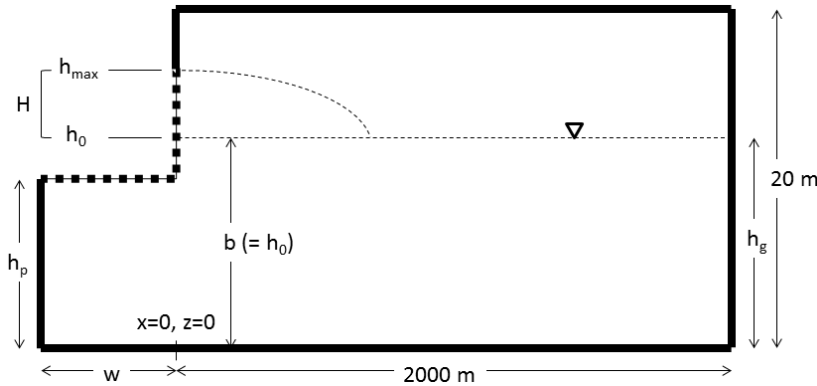


Figure 2-2 Model set up. The no-flow boundary condition is symbolized by the thick black line and the time varying head and concentration boundary conditions by the thick square dotted line. The water table before and after river stage rise are indicated by the dashed line. Generally, the initial water table height h_0 was set equal to the saturated thickness b . The magnitude of river stage rise H was the difference between the initial and maximum river stages. In order to obtain a regional gradient a constant head boundary condition was applied from $z = 0$ to $z = h_g$. h_g was set below h_0 to create a negative gradient and above h_0 to create a positive gradient. For the fully penetrating base case the river width w and height of penetration h_p are zero and the boundary conditions extend to $(0, 0)$.

partially penetrating cases, from $z = 0$ to h_p . In order to simulate a regional hydraulic gradient, the no-flow boundary on the right hand side of the model was replaced with a constant head boundary $h = h_g$ from $z = 0$ to $z = h_g$. The model was first run to steady state to obtain a head distribution throughout the aquifer. This head distribution was used as the initial condition for application of the river stage increase.

The river was represented by a time varying head (TVH) boundary applied from $z = 0$ to $z = h_{max}$ at $x = 0$ (fully penetrating) and from $z = h_p$ to $z = h_{max}$ at $x = -w$ to $x = 0$ (partially penetrating). For simulations involving a rising river stage only, the head boundary was varied according to

$$h(0, t) = \begin{cases} h_0, & t = 0 \\ h_0 + \frac{(h_{max} - h_0)}{2} \left[1 - \cos\left(2\pi \frac{t}{t'}\right) \right], & 0 < t \leq \frac{t'}{2} \\ h_{max}, & \frac{t'}{2} < t \leq t_{max} \end{cases} \quad (2.14)$$

where h is hydraulic head, t is time, t' is wave period, h_0 is head at $t = 0$, h_{max} is maximum head, which occurs at $t = t'/2$, and t_{max} is the simulation time of 200 days. This generates the rising limb of a cosine-shaped wave between $t = 0$ and $t = t'/2$, with amplitude $(h_{max} - h_0)$ that is maintained at the maximum head until t_{max} . The increase in head was set at 1 m (that is, $h_{max} - h_0 = 1$ m), except where sensitivity to the magnitude of river stage was examined. t' was set at 0.02 d, except where sensitivity to the rate of stage rise was examined. For simulations of a rising and falling river stage, and in order to investigate the duration of maximum river stage t_l independently of wave shape, the head boundary was varied as

$$h(0,t) = \begin{cases} h_0, & t = 0 \\ h_0 + \frac{(h_{max} - h_0)}{2} \left[1 - \cos\left(2\pi \frac{t}{t'}\right) \right], & 0 < t \leq \frac{t'}{2} \\ h_{max}, & \frac{t'}{2} < t \leq t_l \\ h_0 + \frac{(h_{max} - h_0)}{2} \left[1 - \cos\left(2\pi \frac{t}{t'}\right) \right], & t_l < t \leq t_l + \frac{t'}{2} \\ h_0, & t_l + \frac{t'}{2} < t \leq t_{max} \end{cases} \quad (2.15)$$

where t_l varied between 5 and 100 days, giving wave periods of 5.02 – 100.02 days.

The initial solute concentration throughout the model domain (saturated and unsaturated) was specified as $C = 1$. A constant (specified) concentration boundary condition was used to represent river water transport into the aquifer. The boundary condition allowed mass to enter the model by both advection and dispersion, and was applied at the same boundary as the TVH at a constant concentration of $C = 0$. A minimum mass-flux constraint was applied to this solute boundary condition to ensure that where flow reversal occurred, water was able to move from the aquifer to the river (out of the model) at an unspecified concentration; that is, the boundary condition was removed for negative flux across this boundary. The solute was designated as conservative.

The mesh was discretised in order to appropriately capture solute transport and unsaturated zone flow processes in the simulations. Given that the largest concentration gradients occur at the left hand boundary representing the river, the sizes of the triangular elements increased in the x direction (away from the river) from an average element diameter of 0.1 m between the boundary and $x = 10$ m, to 0.15 m from $x = 10$ m to $x = 100$ m, and to a maximum of 0.3 m from $x = 100$ m to $x = 2000$ m. Unsaturated zone processes occurring as the pressure wave propagated into the aquifer necessitated reasonably small element sizes throughout the model domain. The model contained a single 1 m wide cell in the Y direction (perpendicular to the direction of flow). Observation points were located at intervals small enough to capture wave propagation into the aquifer and also at sufficient distance to confirm that boundary conditions were not influencing results.

Unsaturated zone parameterization assumes a loam and the van Genuchten-Mualem parametric model as applied in FEFLOW (Diersch, 2009). Model parameters for the base case are assumed to be isotropic and homogenous (Table 2-1). Both travel time and travel distance metrics were defined by a 50% change in the respective variable at an observation point. That is, solute travel metrics were defined as the time (t_s) or distance (x_s) at which $C = 0.5(C_{\text{aquifer}} - C_{\text{river}})$ ($C = 0.5$ for the generic assessment), and pressure travel metrics were defined as the time (t_p) or distance (x_p) at which $h = h_0 + 0.5H$.

Table 2-1 Model parameters for base case simulation.

Parameter	Notation	Value	Unit
Initial river stage	h_0	10	m
Maximum river stage	h_{max}	11	m
Stage increase	H	1	m
Porosity	θ	0.4	
Maximum saturation	S_{max}	1	
Residual saturation	S_r	0.1	
Fitting coefficient in capillary head curve	A	6	m^{-1}
Fitting exponent in capillary head curve	n	1.35	
Hydraulic conductivity	K	4.32	m d^{-1}
Specific storage	S_s	0.0001	m^{-1}
Longitudinal dispersivity	α_L	0.5	m
Transverse dispersivity	α_T	0.05	m
Molecular diffusion		10^{-9}	$\text{m}^2 \text{s}^{-1}$

2.3.2 Rapid increase in river stage

Hydraulic head results from the base case numerical model are marginally lower than those predicted by the analytical solutions for the majority of the simulation time (e.g., < 0.1% at 10 days after simulation commencement, Figure 2-3a). However, head propagates more rapidly in the variably saturated numerical model at early time. Close inspection of the data at $x = 10 \text{ m}$, $z = 5 \text{ m}$ when $h = h_0 + 0.5H$ ($h = 10.5 \text{ m}$) indicates the value for t_p is 25% less than for the analytical solution (Figure 2-3b). The value for specific yield used in the analytical solution was computed from the difference between total porosity and initial moisture content at a matric potential of -1 m (Bear, 1972). Comparison with results from the Hall and Moench (1972) solution for a time-varying source demonstrates that the more rapid head rise in the numerical model is not attributable to the input function (Figure 2-3b). Instead, it is a function of explicitly simulating the unsaturated zone, which necessarily results in time-varying storage. Comparison simulations with thicker aquifers indicate that this behaviour is independent of the ratio H/b and hence is not a product of the change in aquifer thickness as a result of the river stage rise (not shown). This highlights the limitations of representing storage in an unconfined model with a constant value for specific yield when modelling unsaturated zone flow.

The difference between both the time and distance of pressure propagation versus solute propagation into the aquifer is substantial (Figure 2-4). One day after the rapid increase in head at the river bank the head increase has propagated over 30 m into the aquifer, whereas the reduction in solute concentration is limited to less than 3 m; at 10 days the head increase has propagated over 100m, while the solute reduction is limited to 8 m. The head increase drives the development of the velocity profile, which in turn drives solute transport and change in concentration. With time the head gradient reduces in the zone of the model where solute transport is occurring, the velocity slows, and this reduces the rate at which solutes are transported into the aquifer.

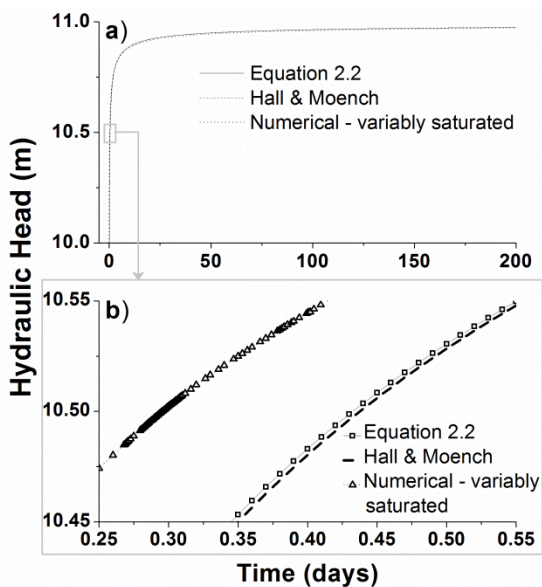


Figure 2-3 Comparison of analytical prediction and numerically simulated hydraulic heads against time at $x = 10$ m and $z = 5$ m for the base case for a) the simulation period and b) early time when t_p occurs. Equation 2.2 is the analytical solution and depicts a step increase in river stage. A cosine-shaped wave input is applied to obtain the Hall & Moench (1972) analytical solution and the numerical simulations. The analytical solution uses $b = 10$ m and $S_y = 0.17$.

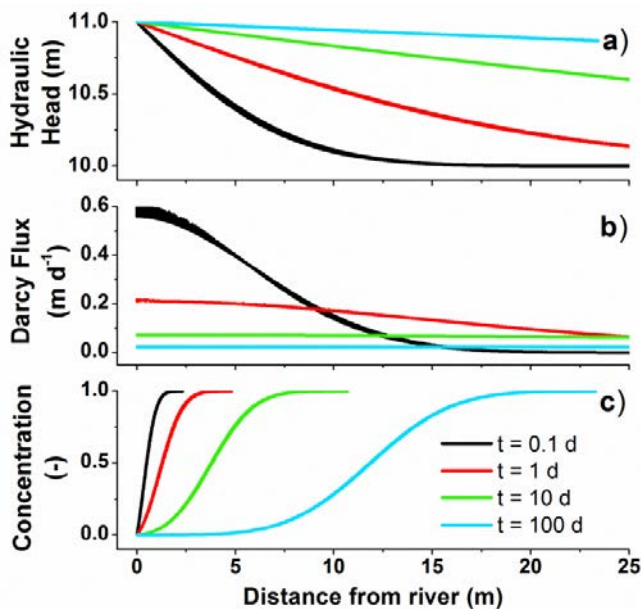


Figure 2-4 Propagation of a) hydraulic head (m), b) Darcy flux ($m d^{-1}$) and c) solute concentration into an aquifer due to a 1 m river stage rise. This figure uses the maximum value of each of these parameters at each x . Positions at 0.1 day, 1 day, 10 days and 100 days are presented to illustrate the rapidity of the head propagation in comparison with the solute concentration reduction and the vast difference in lateral extent over which the changes may be observed in the aquifer.

Head propagation is not vertically uniform throughout the domain, particularly at early time when it occurs least rapidly close to the phreatic surface due to a lag induced by the unsaturated zone (Figure 2-5a). The development of vertical hydraulic gradients as a result of explicitly including the unsaturated zone in simulations of bank storage has been previously reported (McCallum et al., 2010). Consequently, flow velocities are greatest at early time at the interface with the unsaturated zone and reduce towards the base of the aquifer (Figure 2-5b). A higher velocity at early time leads in turn to faster propagation of low concentration water into the aquifer (Figure 2-5c). This rapid propagation at early time results in a more rapid reduction in concentration at later time (Figure 2-5c) and a vertical solute concentration gradient opposite to that of head. At the time concentration change is observed the velocity difference across the model domain is minimal (inset of Figure 2-5b). The retarding effect of the unsaturated zone is a function of the moisture characteristics of the unsaturated zone, a complete assessment of which is beyond the scope of this study.

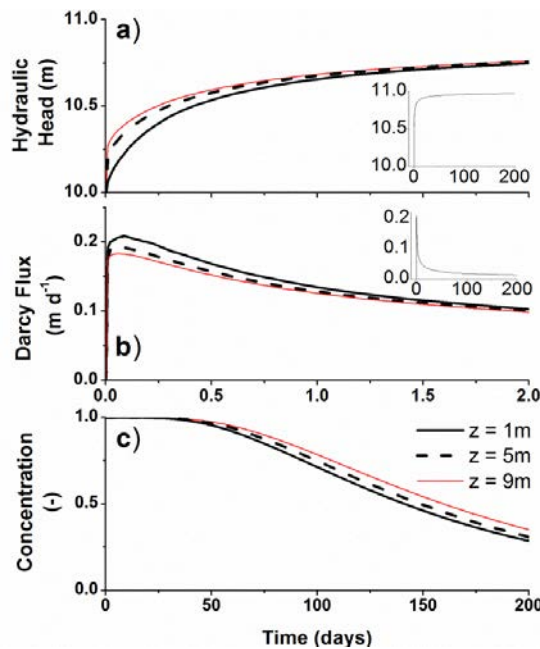


Figure 2-5 Stage increase-induced variation in a) hydraulic head (m), b) Darcy flux (m d^{-1}) and c) solute concentration with respect to time at $x = 10 \text{ m}$ and $z = 1, 5$ and 9 m . Data from the observation location at $x = 10 \text{ m}$ and $z = 5 \text{ m}$ approximates the median value. Note the difference in timescales between hydraulic head/Darcy flux and concentration (inserts show full simulation time). The vertical differences in hydraulic head and Darcy flux are not discernible when viewed over the full simulation time.

2.3.3 Sensitivity analysis for rapid increase in river stage

A sensitivity analysis was conducted by varying model parameters from the base case.

Changes were initially analysed by comparing the travel time metrics t_s , t_p , and t_s/t_p at an observation point at $x = 10$ m and $z = 0.5h_0$. t_0 was defined as the commencement of the simulation as the imposed stage rise could be considered essentially instantaneous.

The relationships for travel time predicted by the analytical solution are approximately maintained in the system that explicitly simulates the unsaturated zone (Figure 2-6). Solute travel time is sensitive to all parameters, whereas pressure travel time is most sensitive to K , b and S_y . The ratio of the two is sensitive to b , S_y , and H , and in contrast is relatively insensitive to K . There is some discrepancy in absolute values. For the base case, the percentage differences between the analytical and numerical solutions are 45% for t_s , 30% for t_p , but only 10% for t_s/t_p . Values for c for the simulations range from 0.02 to 0.425, with the base case at 0.0425. Approximation of the parameter a by aquifer properties contributes 20% error to values of t_s and t_s/t_p (refer Section 2.2). Percentage differences between analytical and numerical results for t_s were substantially lower for higher (relative to the base case) values of specific yield (25%), thinner aquifers (-15 – +20%) and larger river stage rises (0 – 20%).

Notable deviations from the types of relationships predicted for the travel time metrics and model parameters occur for S_y and b . The specific yield value is a single estimate obtained from the model's application of the moisture characteristics of the unsaturated zone used to represent a highly non-linear process. With respect to t_s and t_s/t_p , deviation is most pronounced at values of S_y below 0.15, where the metrics cease to increase as predicted by the analytical solution. This lower limit may vary with different combinations of van Genuchten parameters or alternative parametric models. Values for t_p exhibit a parabolic increase with increasing values for S_y , in contrast to the linear trend produced by the analytical solution. Deviation from the analytical solution for t_s values observed for changing b is attributable to violation of the assumption of constant saturated thickness at

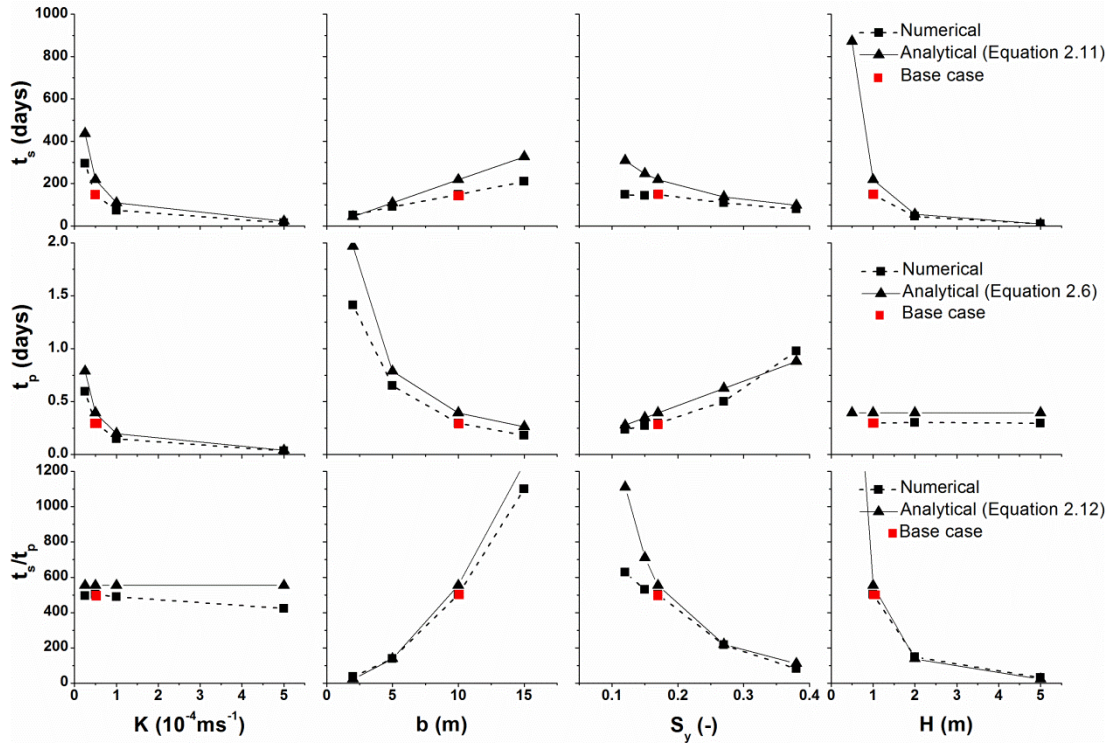


Figure 2-6 Sensitivity of solute and pressure travel time metrics to variation in K , b , S_y , and H .

Results of the numerical simulations in a variably saturated aquifer are compared to analytical solutions (Equation 2.6, Equation 2.11, and Equation 2.12). S_y is defined as the difference between porosity and water content at a matric potential of -1 m.

low aquifer thicknesses ($H/b \geq 0.5$), and the complex relationship between saturated aquifer thickness and storage as aquifer thickness increases ($H/b \leq 0.1$). Results have not been plotted for porosity as in a variably saturated system, it is not possible (nor sensible) to independently test this parameter separately from specific yield, as the specific yield is a function of the porosity, and thus changes as the porosity changes.

The sensitivities of the travel distance metrics to variations in aquifer properties were assessed for the same range of model parameters as the travel time metrics and also found to generally conform to the relationships predicted by the analytical solutions. x_0 coincided with the river bank. For the range of parameters assessed, the solute travel distance is typically under-predicted by the analytical solution (median percentage difference of -16%), whereas the pressure travel distance is typically over-predicted (median percentage

difference of 14%). Similar to travel time metrics, exceptions to these typical differences are observed for thin aquifers and at low values of specific yield.

In theory, any one of four aquifer properties can be estimated by rearranging equation (2.12), provided that each of the other parameters is known. The error associated with such an estimate can be determined from inspection of Figure 2-6. Taking saturated aquifer thickness and a t_s/t_p of 500 as an example, we would obtain $b = 10$ m from the numerical simulation, and $b = 9.3$ m from equation (2.11). This results in a percentage error for b of -7%. Similarly, estimates of S_y or H would be obtained with errors of approximately -10%. Subsequently, K may be estimated from equation (2.6) and/or equation (2.11), and would carry over the error associated with the estimated parameter(s) on which it is based. The lateral extent of river-aquifer mixing may then be estimated using equation (2.13) and a desired range of times post river stage increase. Using the base case example, the error in estimation of x_s is 2 - 8% for the period 0.5 – 200 days after river stage increase, assuming that aquifer parameters are precisely known. The estimate is relatively insensitive to errors in individual aquifer parameters. For example, if the error from the estimation of b is incorporated into the estimation of x_s only a slight increase in uncertainty is observed (2 – 12%).

Simulations were also conducted to assess the sensitivity of the travel time and travel distance metrics to changes in specific storage and dispersivity. In this unconfined setting specific storage is a small component of specific yield (Bear, 1972), and so when specific storage is maintained at realistic values ($< 10^{-4}$), the metrics are insensitive to its change. Increasing longitudinal and transverse dispersivity values causes t_s values to reduce below the value predicted by the analytical solution. This result is somewhat expected as the analytical solution does not consider dispersion. As long as longitudinal dispersivity is less than 2 m (with transverse dispersivity maintained at 10% of the longitudinal value), reduction in t_s and t_s/t_p at a distance of 10 m from the river bank is less than 20%, which is

small relative to the sensitivity to other model parameters (Figure 2-6). This range of dispersivity values is considered appropriate for the observed flow path lengths (Gelhar et al., 1992).

2.3.4 Sensitivity to hydrological processes

2.3.4.1 Regional hydraulic gradient

The influence of the regional hydraulic gradient R on travel time and distance metrics was assessed for $R = \pm 0.001, 0.002$ and 0.004 ($h_g = 12, 14$, and 18 respectively for positive gradients and $8, 6$, and 2 m respectively for negative gradients). The presence of a positive regional gradient increases the solute travel time and reduces the total travel distance into the aquifer (Figure 2-7). For example, a 50% decrease in solute concentration (t_s) occurs at $x = 5$ m for the base case after 40 d, for $R = 0.001$ after 50 d, and for $R = 0.002$ after 71 d, but does not occur for $R = 0.004$. At $x = 10$ m a decrease in solute concentration only occurs for the base case simulation after 149 d and for $R = 0.001$ after 233 d; in other cases t_s may not be defined. Hydraulic gradients induce percentage differences in t_s of 25% to 55% with $R = 0.001$, and up to 80% with $R = 0.002$ (Figure 2-8).

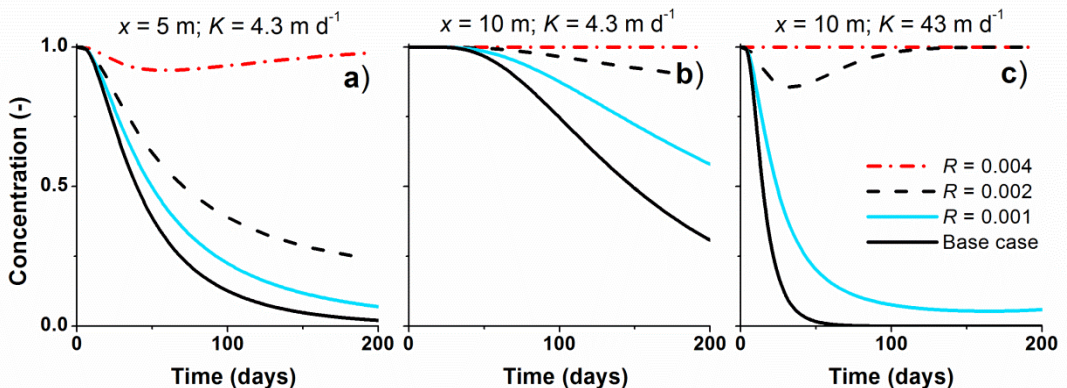


Figure 2-7 Sensitivity of solute travel time and travel distance to regional hydraulic gradients at a) at $x = 5$ m and $z = 5$ m with $K = 4.32$ m d^{-1} , b) at $x = 10$ m and $z = 5$ m with $K = 4.32$ m d^{-1} , and c) at $x = 10$ m and $z = 5$ m with $K = 43.2$ m d^{-1} . Gradients are expressed as m/m .

Percentage differences increase with increasing distance of the observation point from the river bank. This is due to the positive regional hydraulic gradient limiting the extent of

pressure propagation into the aquifer. At first, head within the aquifer increases until it is equal to the maximum river stage. During this early phase the direction of flow in the aquifer is from the river to the aquifer in the vicinity of the river, but towards the river beyond the influence of the pressure wave. Once head within the aquifer at least equals that of the river the positive regional gradient once again becomes the sole driver of flow. This regional flow returns water of a higher concentration towards the river. The initial decrease in solute concentration up to 50 days and subsequent increase back towards the initial groundwater concentration is demonstrated at $x = 5$ m for $R = 0.004$ (Figure 2-7a). This process occurs for all cases, albeit at simulation times longer than those shown. Increasing the hydraulic conductivity accelerates both the initial propagation of low concentration water into the aquifer and the subsequent return of regional water with higher concentration (e.g., compare Figure 2-7b and Figure 2-7c for $R = 0.002$). The former aspect reduces t_s and increases the number of locations at which it may be defined (e.g., compare Figure 2-7b and Figure 2-7c for $R = 0.001$).

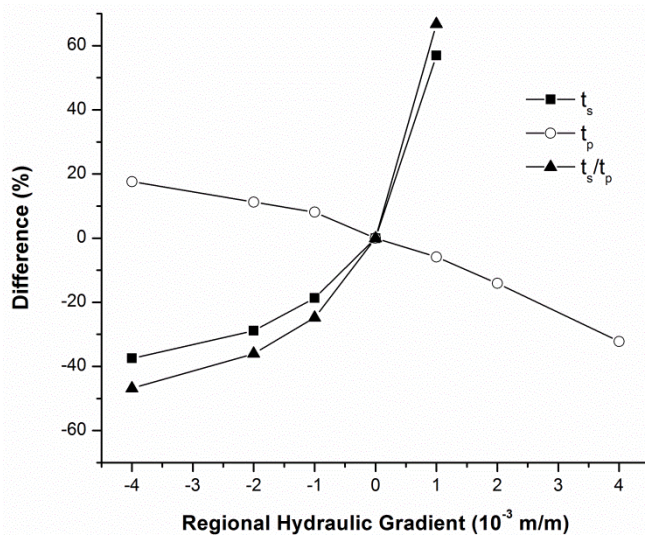


Figure 2-8 Percentage difference between the base case (zero gradient) time travel metrics and travel time metrics for simulated positive (flow towards the river, gaining) and negative (flow away from the river, losing) regional hydraulic gradients. The base case has a regional hydraulic gradient of 0, and is used as the reference point in for the error calculation.

In contrast, application of a negative regional gradient slows pressure propagation relative to the base case, which increases t_p and maintains a higher head gradient for longer than the base case. The longer duration of an elevated head gradient induces a higher flow velocity into the aquifer, thereby accelerating the propagation of river water into the aquifer and resulting in lower values for t_s . The effects of negative gradients on the metrics are far less extreme than the strongly limiting positive gradient (Figure 2-8). Consider, for example, percentage differences in t_s values of -20% for $R = -0.001$ against 55% for $R = 0.001$.

Regardless of the difference induced by the application of a regional hydraulic gradient, results of simulations with the hydraulic conductivity of the aquifer increased by an order of magnitude (Figure 2-7c) indicate that the tenfold reduction in t_s predicted by equation (2.11) still occurs, so long as t_s may be defined. The pressure travel time metric is particularly stable, with percentage differences limited to $\pm 20\%$ for $R = -0.004$ to $R = 0.002$. In summary, the analytical solutions are still applicable to systems with regional hydraulic gradients, provided positive gradients are small.

2.3.4.2 Duration of maximum river stage

A series of simulations examined the effects of river stage rise and fall, and the duration of the maximum river stage. Results indicate that the lateral extent of solute transport into the aquifer is highly dependent on the duration of maximum river stage. The base case, effectively a wave of infinite length, represents the maximum extent of propagation. For waves of finite length, both pressure and solute propagation occur as per the base case up to the time when the river stage decreases, at which time they diverge due to the reversal of the driving head gradient (Figure 2-9). An increase in solute concentration commences almost immediately after the head reversal, although the rate of increase is a function of how far the solute front has propagated beyond the observation point at the time of head reversal. In the event that the duration of maximum river stage is less than t_s for a particular distance from the river, t_s is undefinable. Thus, the time axis on a plot of x_s

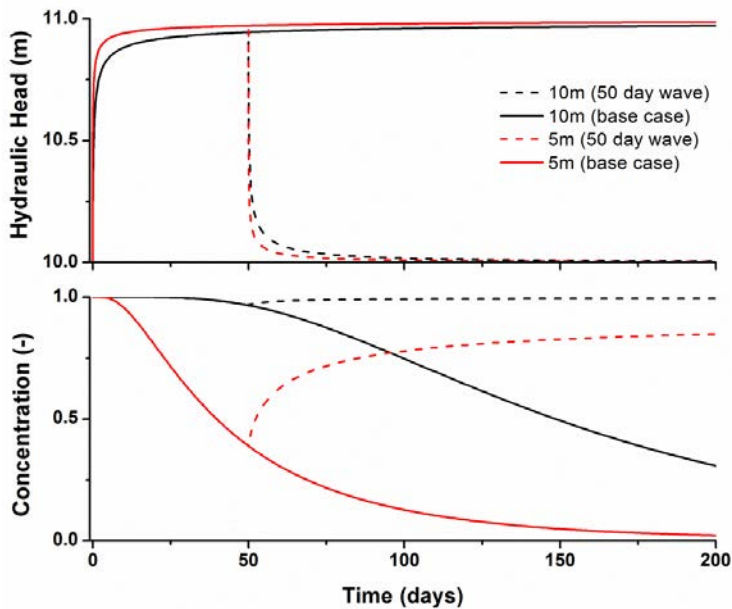


Figure 2-9 Hydraulic head and concentration plotted against time at $z = 5$ m, $x = 5$ and 10 m for a 50 day stage increase and the base case (infinite stage increase). Note the sharp departure from the infinite case at the time when the river stage falls.

against t may be interpreted as the duration of maximum river stage required to achieve t_s at any distance from the river. Furthermore, this analysis indicates that although the method solely analyses data induced by a river stage rise, a subsequent drop in river level does not invalidate the results.

2.3.4.3 River penetration

The effects of partial penetration on the travel time and travel distance metrics were investigated for degrees of penetration $P = (h_0 - h_p)/h_0 = 0.25$ and 0.5 . Partial penetration results in increased values for t_p due to head propagation first through the base of the river then out into the aquifer (in comparison to the fully penetrating base case). The percentage difference between the fully penetrating and partially penetrating values for t_p consistently reduces as the degree of penetration increases and is most pronounced at observation points below and adjacent to the river bed and where $P < 0.5$ (Figure 2-10). Values for t_s are relatively insensitive to the degree of penetration, so long as the observation point is not far below the base of the river, as are values for t_s/t_p (Figure 2-10).

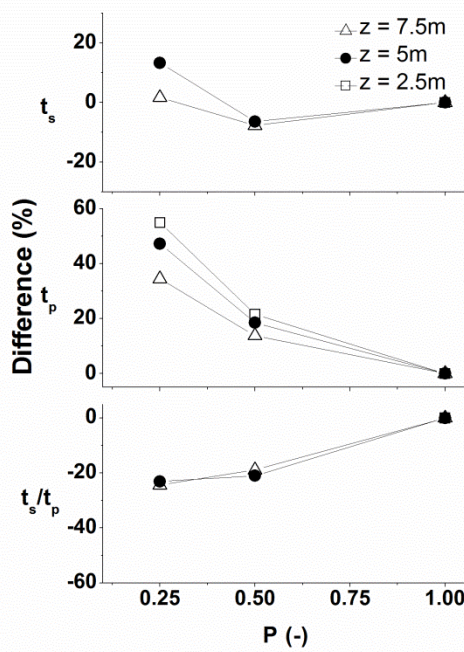


Figure 2-10 Percentage difference between the base case (full penetration, or $P = 1$, river bed at $z = 0$ m) travel time metrics and travel time metrics for partial river penetration $P = 0.25$ (river bed at $z = 7.5$ m) and $P = 0.5$ (river bed at $z = 5$ m) at observation points at $x = 10$ m and $z = 2.5$ m, 5 m, and 7.5 m. Note that t_s (and hence also t_s/t_p) were not measurable at $z = 2.5$ m.

The lateral distance of solute propagation is also relatively insensitive to the degree of penetration, with the proviso for solute travel time, that the observation point is located adjacent to or not far below the elevation of the river bed. Of course, partial penetration does substantially increase the complexity of the solute propagation pattern. Solute does not propagate evenly over the aquifer cross-section; rather, minimal penetration is observed below the river bed, whether directly below the river, or in the adjacent aquifer. Similar patterns were observed by Chen and Chen (2003). The lateral distance of pressure propagation for partially penetrating cases is consistently lower than the fully penetrating base case.

2.3.4.4 Rate of river stage rise

The sensitivity of travel time metrics to the time it takes for maximum river stage rise to occur was assessed for stage rise durations ranging from $t'/2 = 0.1$ d to $t'/2 = 5$ d. t_0 was defined as the time when $h_{river} = h_0 + 0.5H$ in order to normalize results, as the river stage

rise could no longer be considered instantaneous. Solute travel times are relatively unaffected by the duration of river stage rise, as values for t_s are generally much greater than the duration of river stage rise. Percentage errors for t_s range from -5% to 10% up to a duration of stage rise equal to the solute travel time (i.e. $t'/2 : t_p \leq 1$). Pressure travel times are significantly influenced by the duration of river stage rise. The percentage error increases in a parabolic manner as the ratio of $t'/2 : t_p$ increases (Figure 2-11). Percentage errors reduce at greater distances from the river simply because the travel times are longer (not shown). In summary, as long as t_p is greater than or equal to the duration of river stage rise, the metric is not significantly affected (percentage error < 10% where $t'/2 : t_p \leq 1$); otherwise values for t_p will be significantly longer than predicted by the analytical solution which assumes an instantaneous increase in river stage.

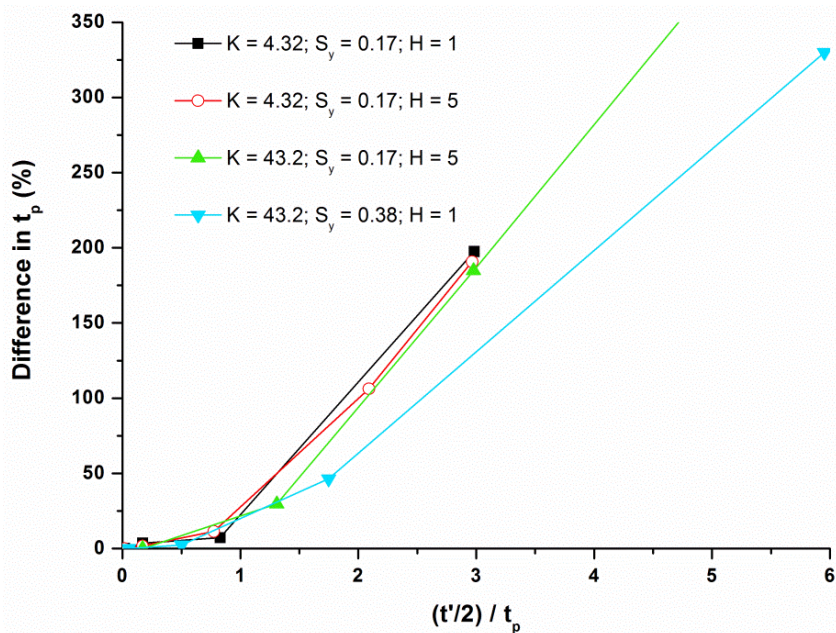


Figure 2-11 Percentage difference between instantaneous rate of stage increase and normalized pressure travel time for a representative range of aquifer parameters. The difference is plotted as a function of the ratio of the duration of river stage rise to the normalized pressure travel time metric for each scenario. Units for aquifer parameters are K (m d^{-1}), S_y (-), and H (m).

Solutions for head propagation into aquifers as a result of variable input functions are available (e.g., Hall and Moench, 1972), however such an extension is not possible for travel

times. Direct application of the proposed analytical solution that is a ratio of solute and pressure travel times is therefore limited to systems where the duration of river stage rise is smaller than the time it takes for pressure to propagate to an observation point within an aquifer. Alternatively, the pressure travel time could be calculated using a different method and then combined with the solute travel time, as the latter does not appear to be substantially affected by the duration of river stage rise after normalization.

2.4 Example application to field data

2.4.1 Field setting

The Cockburn River is situated in eastern Australia and has a total catchment area of 1130 km². The upper part of the catchment is underlain by fractured rock, while the lower section spreads out over an alluvial floodplain. The surficial aquifer consists of interbedded silty sands, sands, and gravel in clay. Rainfall in the catchment predominantly occurs in the months of September to April. River discharge ranged from 5 m³ d⁻¹ to 26,000 m³ d⁻¹ in 2011. Further information on river and aquifer interaction in the Cockburn River may be found in Cook et al. (2006) and McCallum et al. (2010). Pressure and electrical conductivity were continuously measured in two monitoring bores on the alluvial floodplain at 12 m (GWA) and 27 m (GWB) laterally from an essentially vertical, 4-m high river bank and screened across an interval coincident with the elevation of the riverbed. Drilling logs indicate that the river does not fully penetrate the aquifer at this location, with weathered granite bedrock encountered at 7 m below ground level close to the river (3 m below the base of the river). The river width at this location is approximately 30 m. The ratio of maximum in-bank river stage rise (4 m) to aquifer thickness (7 m) indicates that the majority of flood events at this site are likely to fall within the range of applicability of our analytical solutions.

Continuous pressure and EC measurement during a river flow event that occurred in September 2011 is presented for both the river and the adjacent monitoring bores (Figure 2-12). This dataset represents a river stage rise that results in rapid propagation of pressure

into the aquifer, and substantially lagged propagation of solutes, as anticipated from the numerical simulations and analytical solutions. The reduction in EC is greatest and most enduring at the monitoring bore closest to the river (GWA), and shorter and less pronounced at greater distance (GWB).

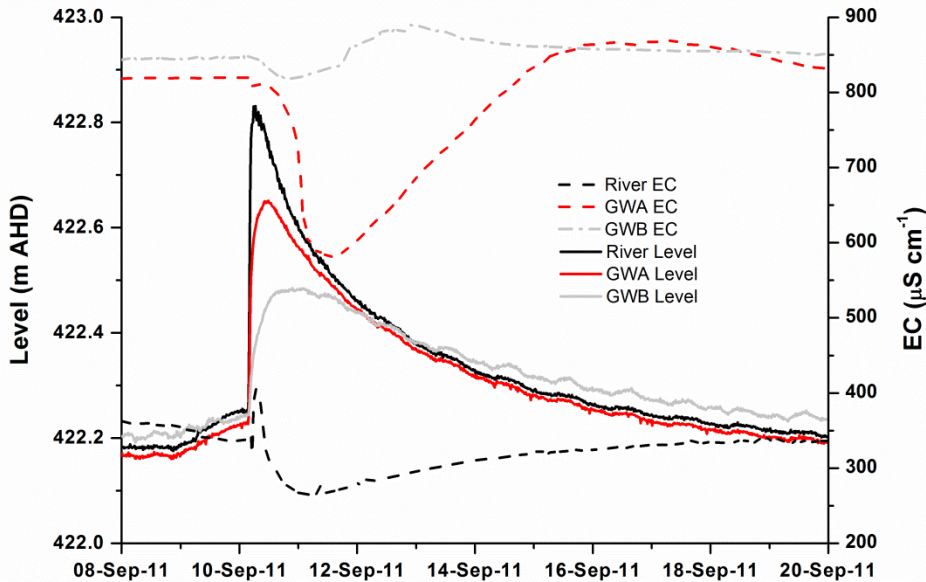


Figure 2-12 Continuous pressure and EC measurement throughout a flood event in September 2011 for the Cockburn River and two adjacent monitoring bores. All EC values are corrected to 25°C.

2.4.2 Determining travel times and travel distances

Travel time metrics can be obtained where the change in head at an observation point is greater than $0.5H$ (for t_p) and the change in solute concentration is greater than $0.5(C_{\text{aquifer}} - C_{\text{river}})$, where river and aquifer concentrations represent pre-event values (for t_s). It is assumed that EC approximates a conservative solute, as in other similar studies (e.g., Cirpka et al., 2007). Inspection of the observation data indicated that travel time metrics could be defined for the flood wave in September 2011 at GWA. The river wave amplitude, or H , for this event was 0.58 m. Groundwater head increased from 422.225 m AHD to 422.65 m AHD at the observation location, an increase of 0.425 m. t_p could be defined because this increase was more than $0.5H$ (0.29 m). The pre-event river EC was $350 \mu\text{S cm}^{-1}$. Groundwater EC reduced from a pre-event groundwater value of $820 \mu\text{S cm}^{-1}$ to $580 \mu\text{S cm}^{-1}$.

¹ during the event, a reduction of 240 $\mu\text{S cm}^{-1}$. t_s could be defined because this value is more than 50% of the difference between the pre-event groundwater and river values ($470 \mu\text{S cm}^{-1}$).

The first step in obtaining travel times is defining the time at which the river stage increase occurs, that is, t_0 . Given that the river stage increase cannot be considered instantaneous, we assume that t_0 occurs at the time when $h_{river} = h_0 + 0.5H$, as per the numerical simulations of variable river stage rise. As previously, t_p was defined as the time at which $h_{obs} = h_0 + 0.5H$ (here $h_{obs} = 422.515 \text{ m AHD}$) and t_s was defined as the time at which $C_{obs} = 0.5(C_{aquifer} - C_{river})$ (here $C_{obs} = 585 \mu\text{S cm}^{-1}$). We thus obtain $t_p = 0.025 \text{ d}$, $t_s = 1.16 \text{ d}$, and $t_s/t_p = 46$.

It is important to consider measurement errors and the effects of hydrological processes on these metrics. Uncertainty associated with obtaining travel time metrics from field data is a function of the recording frequency of the data loggers. For this field data a record is obtained each 15 minutes, or 0.01 day, which corresponds to 40% of the value obtained for t_p and less than 1% of the value obtained for t_s . Reduction in the recording interval would therefore reduce the uncertainty in t_p estimation, but have little effect on t_s estimation. A regional hydraulic gradient of 0.0003 was obtained by comparing the water level in the river and at GWB. According to Figure 2-8 this value indicates that the influence of regional hydraulics may be neglected. Inspection of the water levels in the river and the groundwater also indicated that the driving hydraulic gradient was towards the groundwater until after the time at which the reduction in EC occurred. Both monitoring bores used as observation points are screened at the level of the river bed and hence the degree of river penetration is unlikely to substantially affect t_s . A value of $t'/2 = 0.03$ was obtained and used to assess the potential influence of the rate of river stage rise on t_p . The resulting ratio of $t'/2 : t_p$ is 1.2 (or 1 and 1.5 for upper and lower limits of t_p). This is in the range where a percentage error in t_p of 10% (maximum value) to 50% (minimum value) may

be expected (Figure 2-11). Estimates of the pressure travel time therefore vary between 0.01 and 0.027 days, and the travel time ratio between 116 and 43.

Using equation (2.12) and the calculated value of t_s/t_p (46) yields $c = 0.15$. Subsequently, the aquifer thickness may be estimated using equation (2.12) and an estimate of the ratio of specific yield to porosity, which, given the aquifer materials, is likely to range between 0.25 and 0.75. A saturated aquifer thickness range of $b = 1 - 3$ m is obtained. This result compares reasonably well to the measured thickness of 3.5 – 4 m obtained from drilling logs and water level observations. By simultaneously solving equation (2.6) and equation (2.11) for this range of aquifer thicknesses and porosity values of 0.3 and 0.4, K values of $430 \text{ m d}^{-1} - 580 \text{ m d}^{-1}$ were calculated. Results are not significantly different when the maximum estimate of t_p is used; where the minimum estimate of t_p is used, estimates of b range from 1.5 m to 5 m, and estimates of K range from 690 m d^{-1} to 920 m d^{-1} .

The lateral extent of mixing of river water into the aquifer for the range of wave durations and amplitudes anticipated in the Cockburn River may be estimated with these values for aquifer properties. In the Cockburn River maximum amplitudes of up to 5 m occur, and the river level exceeds the groundwater level for up to five days. This combination results in an estimated lateral mixing zone for river water and groundwater approximately 25 m wide. In contrast, estimates of the lateral extent of pressure propagation range from 170 m to 270 m from the river bank. Estimates using this method should only be considered first-order estimates where significant local aquifer heterogeneity is believed to be present.

2.5 Discussion

The lateral extent of river – aquifer mixing caused by a rapid increase in river stage and the time that it takes for mixing to occur may be related to aquifer properties and the magnitude of river stage increase through the simple analytical relationships developed here. Although based on assumptions of constant transmissivity and storage, predicted relationships between travel time and travel distance metrics and aquifer parameters

generally apply in variably saturated aquifers. At ranges of values likely to be encountered in practical application, solute travel time and solute travel distance are most sensitive to the magnitude of river stage change, which is easily measured, whereas pressure travel time is most sensitive to saturated thickness and storage. Both metrics are equally sensitive to hydraulic conductivity. The independence of the ratio of solute travel time to pressure travel time from hydraulic conductivity is a key strength of our new relationships. In certain situations, measurement of the travel time ratio may enable the estimation of aquifer properties, and subsequently, the estimation of the lateral extent of river – aquifer mixing and pressure propagation. Knowledge of the lateral extent of mixing may be useful, for example, when evaluating the representativeness of bore data for use in chemical mass balances for the quantification of groundwater – river water exchange flux (Guinn Garrett et al., 2012).

The method presented in this paper is most applicable where large, discrete, surface flow events with rapid river stage rises occur and regional groundwater hydraulic gradients are low. A rapid river stage rise minimizes the violation of the assumption of an instantaneous head rise that is inherent in the analytical solution. Multiple consecutive flow events complicate definition of t_s by not allowing complete flushing out of river water between events. The incomplete flushing of the aquifer creates a zone of water in the aquifer with a concentration intermediate to river water and groundwater (McCallum et al., 2010; Simpson and Meixner, 2012). Where EC is used as the sole tracer, it is not always possible to differentiate between water introduced by the flow event being considered and one that occurred previously. Use of tracers that reflect water residence time in the subsurface (including the vadose zone) may assist in clarifying this source of uncertainty (Bertin and Bourg, 1994; Solomon et al., 2010). Large positive regional hydraulic gradients (strongly gaining rivers) limit the actual extent of mixing (Simpson and Meixner, 2012) and rapidly increase solute travel times. Short duration river stage rises also limit the extent of mixing. Due to the rapid propagation of head, the influences of these hydrological processes will

not significantly affect pressure metrics. Consequently, solely relying on pressure observations to identify exchange flux with no consideration of actual water movement is likely to lead to a vast over-estimate of the zone in which river-aquifer mixing occurs (Lewandowski et al., 2009; Yeh et al., 2009). The solutions developed in this paper provide a simple way of addressing this issue.

Useful proxies for water movement may include changes in solute concentrations or water velocity measurements (Lewandowski et al., 2009). Although we have used EC, this method may be applied using any tracer with a difference in river – aquifer concentration that is large relative to 1) the measurement error, and 2) changes caused by other perturbations to the system. Furthermore, the solute must be able to be measured at a temporal resolution that minimizes errors in calculation of travel time metrics. The use of temperature data with our solutions requires further analysis given its non-conservative behaviour in the river-aquifer environment (Vogt et al., 2010). Specific ion electrodes that measure, for example, chloride, nitrate, and fluoride, may be useful in some systems. Recent developments in time series measurement of ^{222}Rn (Gilfedder et al., 2012) and noble gases (Mächler et al., 2012) in groundwater and surface water will increase the scope for measurement of solute concentration changes at the event scale.

The nature of heterogeneity present in any particular system will have an as yet unexplored influence on travel time metrics and the ability of the solutions to estimate aquifer properties and the likely extent of river – aquifer mixing. Theoretical investigations using geostatistical distributions of hydraulic conductivity have indicated that not only heterogeneity, but also the connectivity of high hydraulic conductivity zones, can severely impact on pressure and solute flow paths (Knudby and Carrera, 2006; Renard and Allard, 2013). Influences on solute travel times may occur due to pore-scale mixing and plume-scale spreading of river water as it enters the aquifer (Dentz et al., 2011). Although they have been developed for homogenous systems, the analytical solutions inform conceptual

understanding of the influences of individual aquifer parameters on solute and pressure travel times and distances. Preliminary simulations with a sand string in a silty aquifer indicate that where the contrast in hydraulic conductivity is less than a factor of three, uncertainty in the travel time ratio is relatively small, and within the range of other sources of uncertainty (that is, the uncertainty in estimates of other aquifer properties, and that due to simplification of hydrological processes). The solutions can therefore be best viewed as a first-order assessment tool.

Factors not considered in this study that may further complicate interpretation of travel distance and travel time metrics include river bank slope, and spatially distributed aquifer recharge. Results presented by Doble et al. (2012) indicate that low bank slopes reduce water influx velocities. Lowering velocities tends to reduce water and solute travel times and the lateral extent of mixing but has little effect on pressure metrics. Furthermore, bank slope creates a non-unique set of starting points for measuring travel distances. The spatial and temporal distribution of recharge within a catchment relative to the flow event in the river may also influence the metrics by inducing temporal variation in hydraulic gradients. It can be difficult to separate changes in groundwater head due to river propagation from that due to vertical infiltration from rainfall. River stage change may occur independently of recharge, for example, in catchments where precipitation or snowmelt is concentrated in upper reaches and observations are made downstream. Bore transects that include bores close to and at some distance from the river assist in separating recharge from river responses in bore hydrographs, and permit more accurate estimation of travel time metrics.

2.6 Conclusions

The simple analytical solutions presented here that relate the travel time and travel distance of pressure and solutes to aquifer properties and the magnitude of river stage rise are broadly applicable to variably saturated aquifers. The solutions provide new insights into the relationships between travel time, distance, aquifer properties and river stage rise.

In some cases it will be feasible to estimate aquifer properties and to delineate the lateral extent of river and aquifer mixing through continuous collection of high resolution pressure and solute data in the river and aquifer. Such estimation relies on the ratio of travel times which is insensitive to variation in hydraulic conductivity. This new method is most applicable to rivers with relatively steep bank slopes, small regional hydraulic gradients, and where rapid, large, discrete flow events occur. The method may be applied to any river flow event, so long as the time it takes for maximum river stage to be reached is shorter than the computed travel time metrics. The analysis presented in this paper should facilitate greater exploitation of time series solute data in assessments of surface water – groundwater interactions.

Acknowledgements

The authors appreciate the constructive reviews provided by Brian Smerdon, Graham Sander, Daniel Fernàndez-Garcia, Jörg Lewandowski, and five anonymous reviewers. The NSW Office of Water assisted with obtaining the field data.

3 Relative rates of solute and pressure propagation into heterogeneous alluvial aquifers following river flow events

ABSTRACT

Conventional theory for homogeneous aquifers states that pressure propagates more rapidly into aquifers than solutes following river stage rise. We demonstrate through numerical simulations of two-dimensional aquifer slices that the relative timing of pressure and solute responses in alluvial aquifers is a function of subsurface structures. Two generic conceptual models of heterogeneity are investigated, a vertical clogging layer and a horizontal sand string. Independent of the conceptual model, the hydraulic conductivity contrast is the primary controlling variable on the rates of pressure and solute transport from a river to an observation point. Conceptual models are compared using metrics for pressure and solute travel time that represent propagation of 50% change in each variable from river to observation point. While not possible in a homogeneous system, a solute travel time less than a pressure travel time can occur in the presence of both types of heterogeneity, and indicates that heterogeneity is controlling propagation from the river to the aquifer. Less than one order of magnitude contrast in hydraulic conductivities is sufficient to create a travel time ratio less than one. Contrasts of this magnitude are often exceeded in alluvial environments and thus simultaneous measurement of solute and pressure has the potential to constrain estimates of exchange flux in a way not possible with pressure measurements alone. In general, flux estimates derived from solute travel times provide more accurate estimates than those derived from pressure responses in heterogeneous environments. The magnitude of error in estimates derived from pressure responses is proportional to the hydraulic conductivity contrast. Travel times calculated from time series pressure and EC data collected in the Mitchell River in northern Australia are used to demonstrate application of this combined approach.

Notation

A	fitting coefficient in capillary-head curve, m^{-1} .
b	saturated aquifer thickness, m.
b_2	thickness of sand string, m.
D	aquifer diffusivity, $\text{m}^2 \text{d}^{-1}$.
h_0	initial height of river, m.
H	magnitude of river stage rise, m.
K	aquifer hydraulic conductivity, m d^{-1} .
K_1	low hydraulic conductivity part of aquifer, m d^{-1} .
K_2	high hydraulic conductivity part of aquifer, m d^{-1} .
K^N	equivalent homogenous hydraulic conductivity where flow is normal (perpendicular) to layers of different hydraulic conductivity, m d^{-1} .
K^P	equivalent homogenous hydraulic conductivity where flow is parallel to layers of different hydraulic conductivity, m d^{-1} .
L_1	width of clogging layer with hydraulic conductivity K_1 , m.
L_2	width of aquifer between clogging layer and observation point, m.
n	fitting exponent in capillary-head curve, -.
S	storativity, -.
S_r	residual saturation, -.
S_s	specific storage, m^{-1} .
S_y	specific yield, -.
t_s	solute travel time, time it takes for 50% of the difference between river and aquifer concentration change to occur at an observation point, d.
t_p	pressure travel time, time it takes for 50% of the river stage rise to occur at an observation point, d.
x	distance from river boundary to observation point, m.

3.1 Introduction

Accurate assessment of river – aquifer exchange flux is vital for water resources management and as a basis for contaminant transport investigations. Interpretation of head data obtained during floods is often a key component in such assessments (Meyboom, 1961; Todd, 1956; Winter, 1998). However, the extent of river water movement into an aquifer cannot be determined solely from head data as head change measures energy propagation whereas water is a physical substance that advects, disperses and diffuses. The extent of water movement is more appropriately captured through measurement of solute concentrations or isotope ratios in aquifer and river. Analytical solutions that describe the differing influences of homogenous aquifer properties on rates of pressure and solute transport into a homogenous aquifer following a river flow event were recently presented (Welch et al., 2013). However, previous studies in heterogeneous systems have demonstrated limited correlation between techniques that estimate aquifer properties from metrics that represent solute and pressure transport (Trinchero et al., 2008). These studies also acknowledge a disconnect between the effective aquifer properties obtained for heterogeneous aquifers and the physical systems they purport to represent. Hence, there is a need to improve understanding of the physical processes that govern pressure and solute propagation in heterogeneous aquifer systems. Improved understanding of the influences of heterogeneity on observation data and methods of interpretation may help identify when heterogeneity needs to be incorporated into assessments of river – aquifer exchange flux.

Conceptualisations of a river in an alluvial aquifer commonly include either a clogging layer at the interface between river and aquifer created by deposition of fine particles, or horizontal layers of differing hydraulic conductivity deposited over time by changing river conditions, commonly interbedded silts, sands, and clays (Woessner, 2000). Adequate characterization of hydraulic conductivity zones in near-river environments is necessary for adequate estimates of exchange flux. However, at larger scales of interest to water

managers, compromises in data collection and model complexity become necessary (Fleckenstein et al., 2006). Thus, while alluvial aquifers often contain heterogeneity within clogging layers, sand strings, and surrounding aquifers, generic models that capture two dominant zones have the potential to inform process understanding and hence interpretation of head and solute measurements. Systematic assessment of the influence of generic subsurface structures on rates of water and solute flux across the river-aquifer interface has not previously been attempted.

In order to obtain estimates of exchange flux from river flow events, head data has traditionally been interpreted alone, either through analytical solutions or complex numerical simulations (e.g., Engdahl et al., 2010). Analytical solutions for head propagation in homogenous aquifers and in the presence of a clogging layer have long been available (Hall and Moench, 1972; Hantush, 1965; Zlotnik and Huang, 1999), but in practice tend to incorporate the effects of other near-river processes rather than providing specific characterisation of the clogging layer (Barlow et al., 2000; Ha et al., 2007). Analytical solutions are not available for sand strings, or, until recently, for solutes. Measuring and analysing solute data during flow events presents one method by which confidence in flux estimates can be increased. Sparse solute data is most commonly used as an adjunct to head data in the calibration of numerical models (Hill and Tiedeman, 2007). However, the use of complex numerical models is not always warranted or possible. Methods such as principal component analysis (PCA) provide alternatives for using groundwater head and electrical conductivity (EC) data to infer river water infiltration, and to identify zones of differing hydraulic conductivity along a river (Page et al., 2012), but cannot identify the mechanisms governing pressure and solute transport. However it demonstrates that methods that combine observations of head change and solute change in aquifers during flow events have the potential to delineate changes in exchange flux resulting from subsurface heterogeneity without the need for complex numerical models or analysis.

In this paper we systematically examine the effects of clogging layers and sand strings on pressure and solute propagation into aquifers following river stage rise using numerical simulations and analytical solutions. Contrary to behaviour observed in homogenous systems, we establish that both types of alluvial structure can result in the rate of solute propagation exceeding the rate of pressure propagation. Thus, significant change in solute concentration may be observed before significant change in pressure propagation at locations within the aquifer. In general, estimates of exchange flux derived from solute travel times contain less error than those derived from pressure data. Subsequently we demonstrate how co-measurement of pressure and EC can be used to identify the dominating presence of subsurface structures and constrain estimates of aquifer properties and exchange flux using field data from an alluvial system in tropical North Queensland, Australia.

3.2 Methodology

Two conceptual models of subsurface alluvial architecture were investigated:

1. vertical clogging layer with low hydraulic conductivity adjacent to the river bank (Figure 3-1a); and
2. horizontal sand string with high hydraulic conductivity contiguous with the river (Figure 3-1b).

The physical processes controlling pressure and solute propagation into alluvial aquifers with these characteristics during flow events were investigated through numerical simulations of a river that fully penetrates an aquifer. That is, all flow is considered to pass through the river bank. The influence of subsurface structures on the relative rates of pressure and solute propagation were assessed through comparison of results obtained from analytical solutions, numerical simulations, and field data. The numerical assessment was designed to extend analysis to a greater range of scenarios than possible with analytical solutions, including sand strings and variably saturated aquifers.

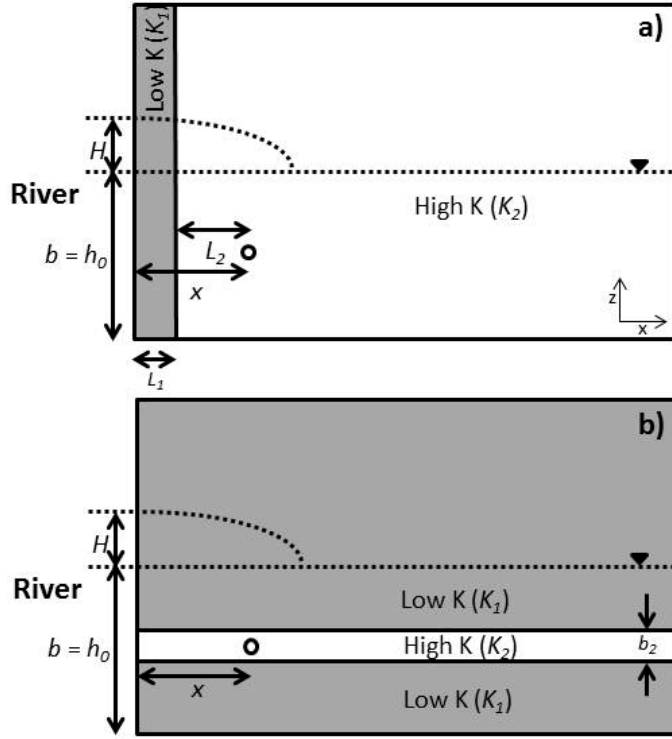


Figure 3-1 Conceptual models of heterogeneity in alluvial aquifers, a) vertical clogging layer and b) horizontal sand string. The shaded area corresponds to low hydraulic conductivity (K_1) and white areas correspond to high hydraulic conductivities (K_2).

3.2.1 Analytical solutions

Approximate analytical solutions for travel times for pressure t_p and solute t_s propagation into a homogeneous aquifer following an instantaneous river stage increase H were recently presented by Welch et al. (2013):

$$t_p \approx \frac{x^2 S_y}{Kb} , \quad (3.1)$$

$$t_s \approx \frac{b \vartheta^2 x^2}{S_y H^2 K} , \quad (3.2)$$

where S_y is specific yield, K is aquifer hydraulic conductivity, b is saturated thickness, ϑ is the porosity of the aquifer, and x is the distance of observation from the river bank. These travel times are defined as the time at which 50% of the total change at the river boundary occurs in the respective variable (pressure or solute) at an observation point in the aquifer.

One approach to estimating solute and pressure travel times in models with heterogeneous hydraulic conductivity fields is to compute average hydraulic conductivity values and use these in solutions for homogenous systems. Where flow is normal (perpendicular) to n layers of different K the harmonic mean K^N applies (Bear, 1972)

$$K^N = \left(\frac{L}{\sum_{m=1}^n \frac{L_m}{K_m}} \right), \quad (3.3)$$

where L is the total length of aquifer considered and m specifies the layer number. This averaging method applies to the clogging layer conceptual model. In this case $n = 2$, subscript 1 denotes the clogging layer, subscript 2 denotes the aquifer, and x is the total length of aquifer L . L_1 is thus the thickness of the clogging layer and L_2 is the thickness of the aquifer, which is equal to the distance between the clogging layer and the observation point (i.e., $L_2 = x - L_1$; Figure 3-1a).

Where flow is parallel to n layers of different K the arithmetic mean K^P applies,

$$K^P = \sum_{m=1}^n \frac{K_m b_m}{b}, \quad (3.4)$$

where b is the total aquifer thickness. This averaging method applies to the sand string conceptual model. Subscript 1 denotes the aquifer and subscript 2 denotes the sand string. b_2 is thus the thickness of the sand string (Figure 3-1b).

Exact analytical solutions exist for head change for the clogging layer scenario, and are described in detail in Appendix B. However, such solutions do not exist for the sand string scenario, or for solute propagation.

3.2.2 Numerical simulations

The model domain was a rectangle 20 m in height, 2000 m in length, and 1 m in width, representing a vertical slice of aquifer perpendicular to a fully penetrating river with a

vertical bank as the left hand model boundary. A vertical bank was simulated as bank slope has previously been shown to minimally affect river – aquifer bank storage flux unless slopes are very low (Doble et al., 2012). Both the vertical clogging layer and horizontal sand string were continuous throughout the domain (Figure 3-1). Clogging layer thickness ranged from 0.1 m to 2000 m. The 2000m thick clogging layer is equivalent to a homogeneous aquifer with low hydraulic conductivity. String thicknesses were 0.2 m, 1 m and 5 m. The models were constructed using the numerical code FEFLOW which solves the head-based (standard) form of the Richard's equation for flow and the convective form of the transport equation concurrently across the unsaturated and saturated domains (Diersch, 2009) for matrix flow only. The van Genuchten-Mualem parametric model as applied in FEFLOW was selected to describe the saturation – conductivity relationship in the unsaturated zone.

The river was represented by a time varying head (TVH) boundary imposed from $z = 0$ to $z = h_0 + H$ at $x = 0$ (left hand model boundary). The remaining boundaries were no flow boundaries. The length of the domain was selected to avoid influence of the right hand model boundary on pressure and solute propagation. Initially the water level in the river and aquifer were set to $h_0 = b = 10$ m, that is, the water table was flat. A specified concentration boundary was applied over the same portion as the TVH boundary and assigned a value of $C = 0$ to represent fresh river water. The initial solute concentration throughout the domain was set to $C = 1$. $C = 1$ and 0 are arbitrary normalised values that represent distinct water chemistries in rivers and aquifers. A longitudinal dispersivity value of 0.5 m and transverse dispersivity value of 0.05 m were used. Density effects were ignored.

Models for clogging layer and sand string scenarios were individually discretized. Average element diameters within the clogging layer model increased from 0.1 m within 20 m of the river up to 0.4 m. For each of the three thicknesses of sand strings element sizes were small both within 20 m of the river and across zone boundaries; average element diameters

ranged from 0.025 m to 0.1 m across the string within 20 m of the river, increasing to 0.05 m to 0.4 m at further than 20m.

Simulations were performed for homogenous aquifers and both conceptual models of heterogeneity using a range of system parameter values considered reasonable for alluvial environments (Table 3-1). The hydraulic conductivity ratio for heterogeneous models was typically varied by adjusting the conductivity of the low hydraulic conductivity layer K_1 (clogging layer in clogging layer conceptual model and surrounding aquifer in sand string conceptual model) and maintaining a constant value for the zone with the highest hydraulic conductivity K_2 . To test the generality of results, K_2 was also varied across three orders of magnitude while holding first K_1 and then the ratio K_2/K_1 constant. For comparison with analytical models the approximate specific yield was defined as the difference between porosity and moisture content at a matric potential of -1 m to correspond to a river stage rise of 1 m. For consistency this value was maintained for all river stage rises. Specific yield was varied by altering the van Genuchten parameters (Carsel and Parrish, 1988). Aquifer properties were isotropic and homogeneous within each zone.

Table 3-1 Parameters used for generic model simulations.

Parameter Range	Clogging Layer Model	Sand String Model
Structure thickness (m)	0.1 – 2000	0.2, 1, 5
Hydraulic conductivity, K_2 (m d^{-1})	7.76, 77.76, 777.6	77.76, 777.6
K_2/K_1 (-)	1 – 9000	1 – 9000
Soil type* (Approximate specific yield, S_y (-))	Sand (0.38), sandy loam (0.3), sandy clay loam (0.17)	Sand (0.38), sandy clay loam (0.17)
Porosity (-)	0.2, 0.3, 0.4	0.2, 0.4
Specific storage, S_s (m^{-1})	10^{-4}	$10^{-5} – 10^{-4}$
River stage rise, H (m)	1, 2.5, 5	1, 5

* Soil types were represented by van Genuchten parameters (Carsel and Parrish, 1988): sand ($A=15$, $n=3$, $S_r=0.04$), sandy loam ($A=7$, $n=1.8$, $S_r=0.07$), and sandy clay loam ($A=6$, $n=1.35$, $S_r=0.1$).

River stage rises were essentially instantaneous; a cosine wave with a time to peak of 0.01 d was implemented to minimise numerical instabilities that arise from sudden shifts in boundary conditions. A maximum river stage rise equivalent to half the saturated thickness

$(H/b = 0.5)$ was used to avoid unacceptable violation of linearisations inherent in the analytical solutions (Hornberger et al., 1970).

Results obtained from the numerical simulations were assessed using travel time metrics consistent with the definitions of travel times in equations (3.1) and (3.2), that is, the time it took for 1) 50% of the stage change in the river to propagate to the observation point, t_p , and 2) a concentration of 0.5 to be observed at the observation point, t_s . Hydraulic conductivity was estimated from travel times by rearranging equations (3.1) and (3.2). Flux was estimated on a per unit length of river basis from the hydraulic conductivity estimate and the gradient calculated between the river stage and groundwater head at an observation point. In the theoretical analysis the estimated flux was compared to the simulated flux across the river bank obtained from the numerical model. Observation points between $x = 1$ m and $x = 500$ m were used.

3.3 Modelling Results

First we present results from numerical simulations to describe the physical processes that occur as solute and pressure propagate into heterogeneous aquifers following river stage rise. Second we describe the influences of these processes on travel time metrics obtained from numerical simulations of each conceptual model of heterogeneity, and assess the extent to which available analytical solutions reproduce these influences. Third, we demonstrate the ability of solute travel times to reduce error in estimates of river – aquifer flux. Fourth, we explore the potential to identify heterogeneity in aquifers from the ratio of solute and pressure travel times by comparing numerical travel time results from both conceptual models.

3.3.1 Process of pressure and solute propagation

3.3.1.1 Vertical clogging layer

To demonstrate the impact of a clogging layer on the process of pressure and solute propagation into an aquifer we present a comparison to homogenous aquifers with high (K_2) and low (K_1) conductivity (Figure 3-2).

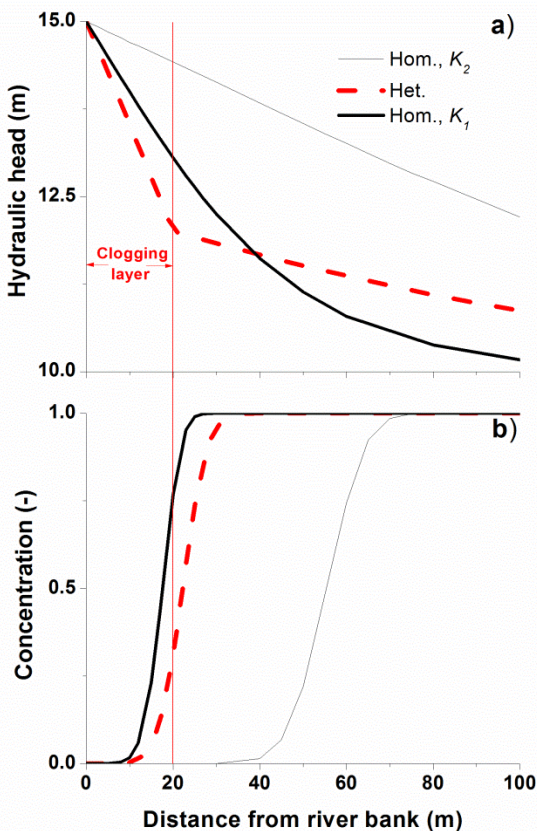


Figure 3-2 Comparison of numerically simulated a) head and b) solute propagation into a heterogeneous aquifer with a 20 m thick clogging layer to two end-member homogenous aquifers. The homogenous aquifers have hydraulic conductivities of the clogging layer (K_1 , 8.64 m d^{-1}) and aquifer (K_2 , 77.76 m d^{-1}). Head and solute contours are plotted five days after the commencement of a 5 m river stage rise. Initial concentrations were $C = 1$ in the aquifer and $C = 0$ in the river. The head gradient for the heterogeneous case is steeper than both the homogenous cases within the clogging layer and flatter for some distance beyond the interface because head dissipates more quickly into the wider aquifer than it propagates through the clogging layer.

The presence of a clogging layer with a lower hydraulic conductivity (K_1) than the aquifer (K_2) results in pronounced retardation of pressure propagation, and less pronounced retardation of solute propagation. In the heterogeneous aquifer a distinct change in head gradient is observed at the interface between the two hydraulic conductivity zones (Figure 3-2a). The steep head gradient within the clogging layer is partly caused by slower pressure propagation as a result of lower aquifer diffusivity ($D = Kb/S$), and partly caused by the presence of the hydraulic conductivity boundary. Compared to the low hydraulic

conductivity homogenous aquifer, the head gradient in the heterogeneous aquifer is not only steeper within the clogging layer, but also flatter for some distance beyond the interface. These conditions arise because pressure dissipates more quickly into the wider aquifer than it propagates through the clogging layer. The increase in head in the wider aquifer reduces the pressure difference across the boundary, which further slows pressure propagation. Retardation is exacerbated by increasing the contrast in hydraulic conductivities between the two zones (refer to Section 3.3.4). The rate of solute propagation in the heterogeneous aquifer is intermediate to the homogenous end-member aquifers (Figure 3-2b) because the higher head gradient in the clogging layer partially compensates for the retarding effect of low hydraulic conductivity on water velocity.

3.3.1.2 Horizontal sand strings

As is commonly understood, the presence of a sand string with high hydraulic conductivity (K_2) in an aquifer of lower hydraulic conductivity (K_1) results in water flowing preferentially through the sand string. This is reflected in the pattern of solute distribution throughout the surrounding aquifer (Figure 3-3). As the hydraulic conductivity of the aquifer is reduced (i.e., K_2/K_1 increases) the rate and distance of solute movement into the aquifer reduces, whereas solute propagates slightly further into the sand string (compare Figure 3-3a and Figure 3-3b). Conversely, pressure propagates reasonably evenly through the entire cross-section of the aquifer, at least until the contrast in hydraulic conductivities is large enough for the section of aquifer over-lying the sand string to become a semi-confining layer. Once this occurs, head propagates more rapidly within and below the sand string and heads measured at observation points in the high hydraulic conductivity sand string are not a reflection of the phreatic surface (Figure 3-3c). Once confined conditions are firmly established the rate of solute transport within the sand string also reduces, primarily because rapid pressure propagation reduces the driving head gradient (compare Figure 3-3b and Figure 3-3c).

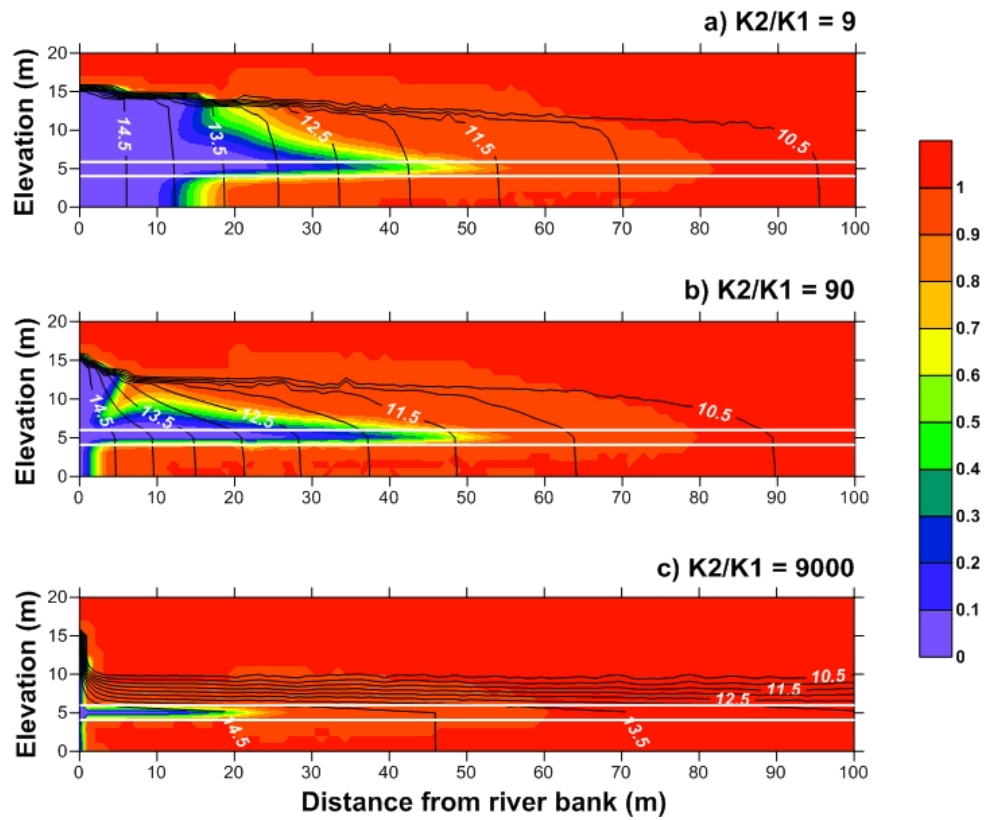


Figure 3-3 Spatial distribution of solute and pressure propagation into aquifers containing 1 m thick sand strings (white lines) with increasing contrast in string and aquifer hydraulic conductivities (numerical simulations). Head (black lines) and solute concentration (colour filled) contours are plotted five days after the commencement of a 5 m river stage rise. Initial concentrations were $C = 1$ in the aquifer and $C = 0$ in the river; $K_2 = 77.76 \text{ m d}^{-1}$ in all cases.

3.3.2 Effects on travel time metrics

3.3.2.1 Vertical clogging layer

To demonstrate the impact of a clogging layer on numerically simulated pressure and solute travel times we present a comparison to results from homogenous aquifer simulations (Figure 3-4a-c). Both solute and pressure travel times increase with distance from the river bank. Close to the river, values for the heterogeneous system are representative of the low hydraulic conductivity of the clogging layer (K_1). At greater distances values are representative of the high conductivity of the aquifer (K_2). However, the pattern between these two extremes is markedly different for t_p and t_s (Figure 3-4a, b).

Pressure travel times are greater than those obtained from the homogeneous aquifer with low hydraulic conductivity (K_1) where the observation point is at a distance between 50% and 200% of the thickness of the clogging layer (between 10 m and 40 m for the scenario on Figure 3-4a). The distance of 40 m corresponds to the distance where head is lower in the heterogeneous system than the low conductivity homogeneous system at all times (i.e., as depicted at 5 d on Figure 3-2a). The maximum pressure travel time is observed when the observation point is at the boundary of the clogging layer (i.e., $L_1 = x$, 20 m on Figure 3-4a). This occurs regardless of clogging layer thickness for all combinations of system parameters tested (not shown).

Solute travel times increase from a value representative of the clogging layer to one representative of the aquifer at observation points further than approximately ten times the thickness of the clogging layer from the river (Figure 3-4b). The ratio of travel times (t_s/t_p) is consistently less than that predicted for homogenous systems at observation points located more than 50% of the thickness of the clogging layer distant from the river (Figure 3-4c). The lower ratio and non-linear variation with distance demonstrate that the influence of the clogging layer on solute travel time and pressure travel time is not equal.

The general travel time trends are consistent for all hydraulic conductivity contrasts. For all clogging layer thicknesses the magnitudes of travel times at a given observation distance are inversely proportional to the hydraulic conductivity contrast K_2/K_1 . As the clogging layer thickness increases, a smaller contrast is required to obtain the same travel time. In other words, when the hydraulic conductivity of the clogging layer approaches that of the aquifer (low contrast), the thickness of clogging layer required to substantially retard the propagation of pressure and solute into an aquifer is large; a thin clogging layer with a large contrast has the same effect (discussed further in Section 3.3.4).

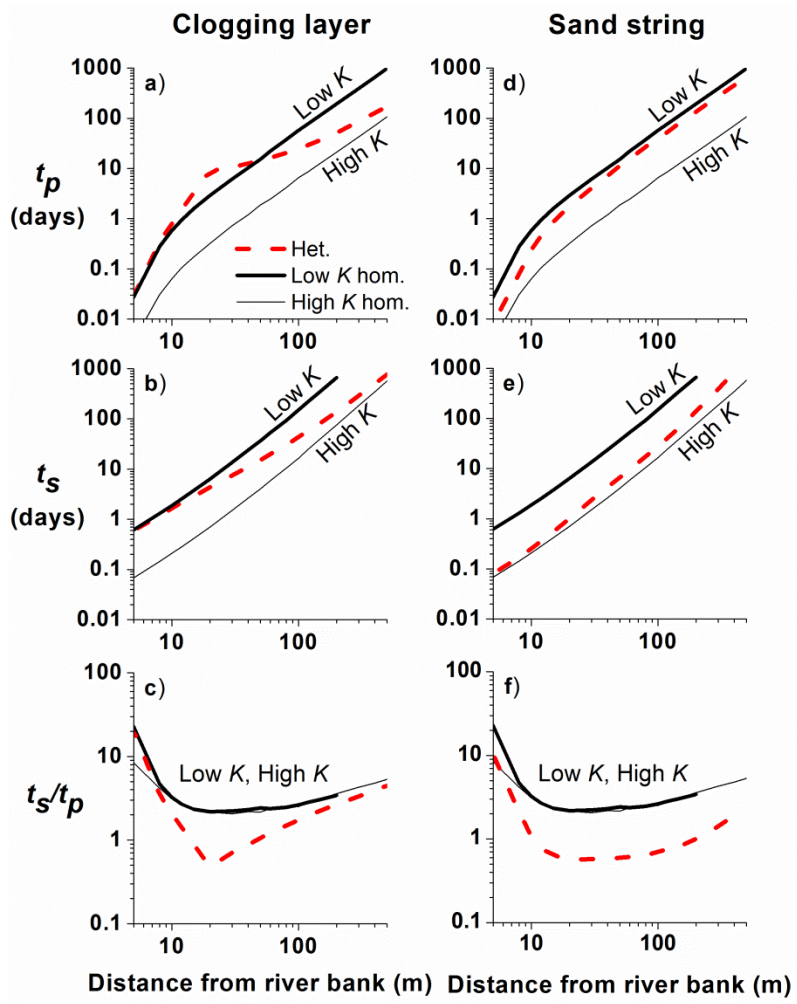


Figure 3-4 Comparison of numerically simulated pressure (t_p) and solute (t_s) travel times and their ratio (t_s/t_p) at increasing distances from the river bank for homogenous aquifers (solid lines) with low ($K_1 = 8.64 \text{ m d}^{-1}$) and high ($K_2 = 77.76 \text{ m d}^{-1}$) hydraulic conductivity and heterogeneous aquifers (dashed lines) with either a)- c) clogging layer 20 m thick or d)-f) sand string 1 m thick ($H = 5 \text{ m}$, $K_2/K_1 = 9$). The sand string is unconfined.

3.3.2.2 Horizontal sand strings

Two distinct types of solute and pressure travel time responses may be measured in a sand string. The type of response is a function of the hydraulic conductivity contrast. When the hydraulic conductivity contrast is small (sand string is unconfined, Figure 3-4), pressure travel times are controlled by average hydraulic conductivity (between homogenous K_1 and K_2 , Figure 3-4d) and solute travel times are controlled by the hydraulic conductivity of the string (close to K_2 , Figure 3-4e). As noted for the clogging layer conceptual model, the ratio

of travel times is less than that observed for homogeneous systems, indicating that the relative influence of the sand string on pressure and solute propagation is not equal (Figure 3-4f). Alternatively, when the hydraulic conductivity contrast is large (sand string is semi-confined, Figure 3-5), pressure travel times are significantly less than for a homogenous aquifer with high hydraulic conductivity (compare t_p at $K_2/K_1 = 450$ to t_p at $K_2/K_1 = 1$ on Figure 3-5a). In this region t_p is dependent on the value of specific storage, and there is minimal change in the phreatic surface with change in head in the sand string (Figure 3-3c). When the sand string is semi-confined solute travel time is long (Figure 3-5b). However, under such conditions the ratio of travel times is much larger than for the homogenous case primarily because of the change in pressure travel time.

The shift to semi-confined conditions in a sand string corresponds to the hydraulic conductivity contrast above which pressure travel times are no longer inversely proportional to average hydraulic conductivity (Figure 3-5a). Above this value of K_2/K_1 , pressure propagation transforms to being solely dependent on the transmissivity of the sand string and the total thickness of the aquifer, and independent of the hydraulic conductivity of the surrounding aquifer (from equation (3.4), $K^P = K_2 b_2 / b$). Although this is consistent for all string thicknesses, the shift occurs at increasingly lower values of K_2/K_1 for higher ratios of string thickness to saturated thickness (b_2/b) (Figure 3-5a). The trend to lower values of K_2/K_1 occurs because there is less change in the average hydraulic conductivity of an aquifer when the sand string is a larger proportion of the total saturated thickness. Hence, while thick aquifer layers with similar values of hydraulic conductivity result in minimal variation in t_p , less of a contrast between aquifer and sand string hydraulic conductivity is required for pressure propagation to become essentially independent of the hydraulic conductivity of the surrounding aquifer.

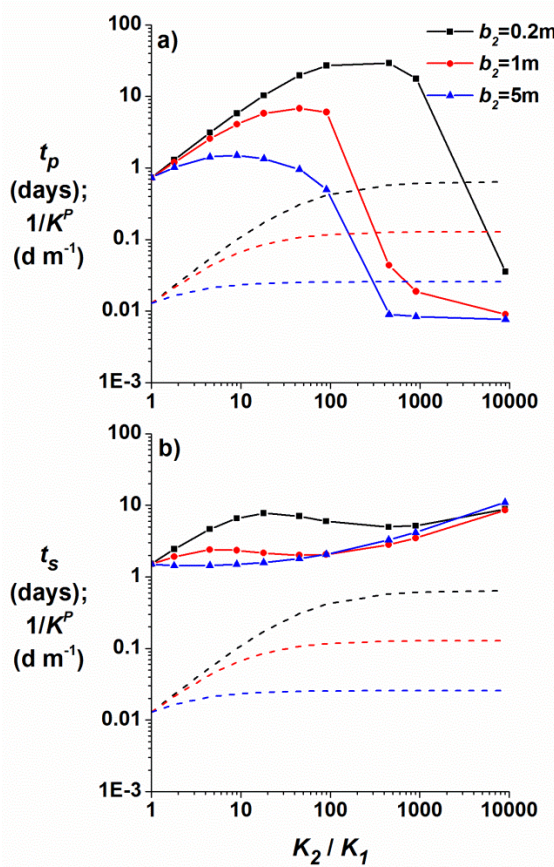


Figure 3-5 Comparison of numerical results for a) pressure travel times and b) solute travel times as a function of hydraulic conductivity contrast for different sand string thicknesses (b_2) ($K_2 = 77.76 \text{ m d}^{-1}$, $H = 5 \text{ m}$, $x = 30 \text{ m}$). The relationship between inverse average hydraulic conductivity of the system and the hydraulic conductivity contrast is also shown. Solid lines indicate travel time results and dashed lines indicate inverse hydraulic conductivity. For small values of K_2 / K_1 pressure travel time is proportional to $1/K^P$; for large values pressure travel time progressively decreases. The shift indicates the onset of semi-confined conditions in the sand string. Solute travel times are only proportional to the inverse of average hydraulic conductivity when b_2 is thin and K_2 / K_1 is small.

Solute travel times are less affected by changes in hydraulic conductivity contrast than pressure travel times. They vary over one order of magnitude, compared to pressure travel times which vary over three orders of magnitude (Figure 3-5). Solute travel times are only proportional to average hydraulic conductivity when $b_2/b < 0.5$ ($b_2 < 5 \text{ m}$), and for a much smaller range of K_2 / K_1 (compare $b_2 = 0.2 \text{ m}$ and $b_2 = 5 \text{ m}$ on Figure 3-5b). With the shift to semi-confined conditions solute travel times increase because rapid pressure propagation reduces the head gradient in the sand string.

3.3.3 Comparison to analytical solutions

3.3.3.1 Vertical clogging layer

Numerical results for the clogging layer model of heterogeneity were compared to the equivalent homogenous analytical solutions (equation (3.1) and equation (3.2) with average hydraulic conductivity obtained from equation (3.3)), and the analytical solution for pressure propagation in a heterogeneous system with a clogging layer (equation (B1)).

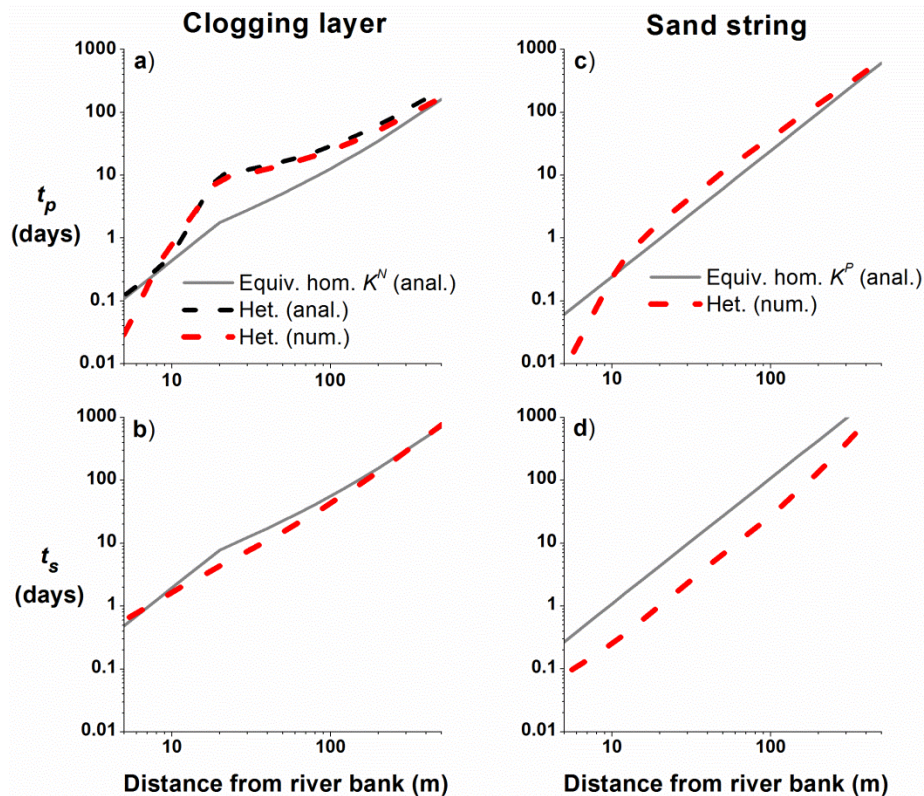


Figure 3-6 Comparison of pressure and solute travel times obtained from analytical solutions (equivalent homogenous, equations (3.1) and (3.2) and heterogeneous (equation B1)) with travel times obtained from numerical simulations of heterogeneous aquifers. Aquifer properties are as per Figure 4.

Pressure travel times predicted by equations (3.1) and (3.3) do not capture the retarding effect of the clogging layer, and systematically underestimate pressure travel times (Figure 3-6a). Hence, the ability of an equivalent homogenous hydraulic conductivity to capture the response of pressure travel times to this type of structure is limited by the proximity of a point of interest to the clogging layer / aquifer interface. Conversely, pressure travel times

obtained from the numerical simulation and equation (B1) are essentially equivalent at greater than 10 m from the river bank (Figure 3-6a). The divergence of analytical from numerical results at less than 10m from the river bank is due to explicit inclusion of the unsaturated zone in the numerical model rather than heterogeneity. Homogenous and heterogeneous numerical results are essentially indistinguishable in this zone (Figure 3-4a, b).

Solute travel times predicted by equations (3.2) and (3.4) essentially replicate the shift from control by the clogging layer to control by the aquifer with distance from the river bank observed for the numerical results, but at a slightly less rapid rate (Figure 3-6b). This confirms that solute travel time is influenced by more of the aquifer than the portion between the river and the observation point.

3.3.3.2 Horizontal sand string

Numerical results for the sand string conceptual model are compared to the equivalent homogenous analytical solutions with average hydraulic conductivity obtained from equation (3.4). The hydraulic conductivity contrast depicted on Figure 3-6 results in an unconfined sand string. Under these conditions average hydraulic conductivity controls pressure propagation, and hence the pressure travel times obtained from the numerical simulations are similar to those predicted by the equivalent homogenous solution, except very close to the river bank (Figure 3-6c). When the hydraulic conductivity contrast is large and the sand string is semi-confined, the numerical pressure travel times are substantially faster than the analytical results (not shown). Conversely, as indicated by the numerical results, solute travel times are controlled by the hydraulic conductivity of the sand string, and hence are substantially faster than results predicted by the equivalent homogenous solution (Figure 3-6d).

3.3.3.3 Sensitivity to parameter variation

In heterogeneous aquifers the sensitivities of travel times to variation in specific yield, porosity, river stage change, and saturated thickness are generally consistent with

equations (3.1) and (3.2) for homogenous aquifers. The homogeneous analytical solutions therefore provide a useful guide to the influence of system parameters on travel times in heterogeneous systems. The major exception occurs for semi-confined sand strings. In such cases travel times respond only minimally to changes in S_y , ϑ , H , and b . However, provided a constant hydraulic conductivity contrast is maintained, the ratio of hydraulic conductivities above which a string is semi-confined is independent of H , S_y , and the absolute magnitude of the string hydraulic conductivity.

3.3.4 Estimating hydraulic conductivity and flux

The differing influences of heterogeneity on pressure and solute travel times suggest that hydraulic conductivity and exchange flux estimates based on pressure and solute data will not be consistent. These inconsistencies were assessed by comparing hydraulic conductivity estimates from pressure and solute responses in the aquifer to the average value of hydraulic conductivity implemented in the numerical model. We then compared fluxes derived from the estimated and average hydraulic conductivity values (i.e., $Q = Kbi$, where i is calculated as the head gradient between the observation point and the river) to simulated fluxes across the river / aquifer interface at 5 d after the commencement of the simulation.

For the scenarios simulated, estimates of both hydraulic conductivity (from equations 3.1 and 3.2) and exchange flux obtained from travel time metrics are inaccurate at less than 10 m from the river bank due to processes related to the explicit inclusion of the unsaturated zone in the model (Figure 3-7a). When an unsaturated zone is explicitly simulated, pressure moves rapidly at early time (and is hence observed at small distances) because the delay in the movement of water into the unsaturated zone means that specific yield effectively increases with time (Welch et al., 2013). This region is therefore excluded from further analysis as the effects of unsaturated zone processes overwhelm the effects of hydraulic conductivity averaging in the near-river zone.

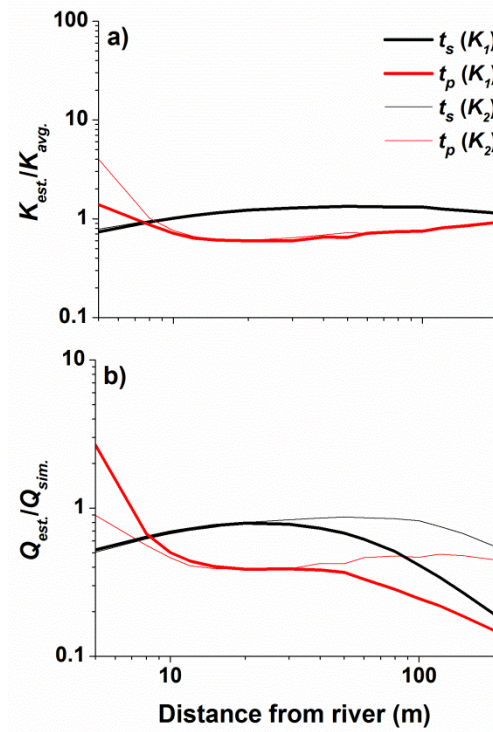


Figure 3-7 Comparison of a) hydraulic conductivities calculated with equation 3.1 (t_p) or equation 3.2 (t_s) and b) fluxes from solute and pressure travel times obtained from homogeneous aquifer simulations to actual (hydraulic conductivity) or model-derived (flux) values. $K_1 = 8.64 \text{ m d}^{-1}$ and $K_2 = 77.76 \text{ m d}^{-1}$.

In homogenous aquifers estimates of hydraulic conductivity obtained from observation points more than 10 m from the river bank indicate that using solute travel times overestimates aquifer hydraulic conductivity by 0-30%, and using pressure travel times underestimates aquifer hydraulic conductivity by 0-40%, irrespective of the magnitude of the hydraulic conductivity (Figure 3-7a). Flux estimates using hydraulic conductivity derived from solute travel times underestimate simulated fluxes by approximately 20%; using pressure travel times this increases to an underestimate of approximately 60%. The underestimate occurs in part because the head gradient between the river and the observation point is not a reliable indicator of the head gradient at the river bank. This is increasingly pronounced for aquifers with low hydraulic conductivities beyond 50 m from the river bank (Figure 3-7b).

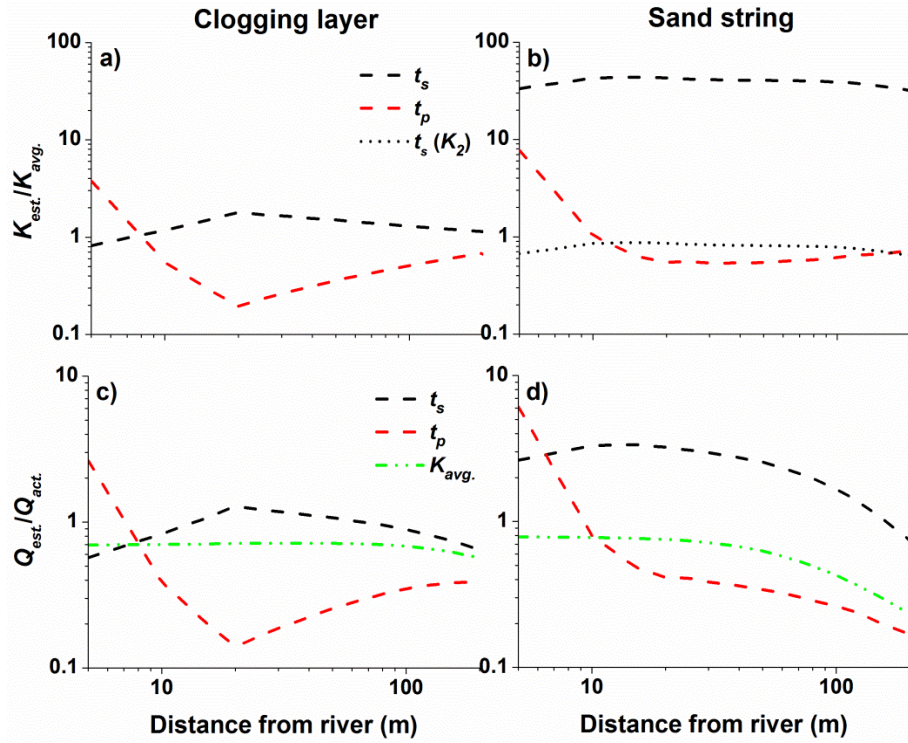


Figure 3-8 Ratios of a), b) estimated to average hydraulic conductivity and c), d) estimated to simulated flux from river to aquifer for clogging layer and sand string scenarios. Hydraulic conductivity estimates were derived from solute (t_s , equation 3.2) and pressure (t_p , equation 3.1) travel times and averages (equations 3.3 and 3.4). Flux was calculated at 5 d after the commencement of the simulation. Aquifer parameters are as per Figure 4; hence $K_2/K_1 = 9$. The most accurate estimates of flux in a clogging layer system are derived from solute travel times. The most accurate estimate in a sand string system is derived from average hydraulic conductivity; if this is unknown, then using pressure travel time when the hydraulic conductivity contrast is low and solute travel time when the contrast is high minimises error.

For the heterogeneous scenarios hydraulic conductivity estimates were compared to average hydraulic conductivities computed from equations (3.3) and (3.4) as appropriate.

For a clogging layer / aquifer system with a hydraulic conductivity contrast of approximately one order of magnitude, using solute travel times overestimates aquifer hydraulic conductivity by 20-80% (Figure 3-8a). Using pressure travel times underestimates hydraulic conductivity by 30-80%. Maximum error in hydraulic conductivity estimates is obtained at the interface of the clogging layer and the aquifer. For the sand string scenario, using solute travel times severely overestimates average aquifer hydraulic conductivity, but only

underestimates string hydraulic conductivity by 15-20% (Figure 3-8b). The latter confirms that solute travel time is representative of the hydraulic conductivity of the sand string. As for the clogging layer, using pressure travel times underestimates aquifer hydraulic conductivity, generally by approximately 40%. For the clogging layer scenario, flux estimates derived from pressure travel times range from 15% to 40% of the simulated flux between 10 and 100m from the river bank (Figure 3-8c). Estimates derived from solute travel times range from 85-130% of simulated fluxes over the same distance. Divergence from simulated flux is again greatest at the clogging layer/aquifer interface. Using average hydraulic conductivity produces a 30% underestimate of simulated flux. Each order of magnitude increase in the hydraulic conductivity contrast between clogging layer and aquifer increases the error in flux derived from pressure travel times and average hydraulic conductivity by approximately one order of magnitude (not shown). Conversely, flux estimates derived from solute travel times are essentially unaffected by the increase in contrast (not shown). Consequently, flux estimates derived from solute travel times provide the most accurate estimate of simulated flux for this type of system.

For the sand string scenario, flux estimates derived from pressure travel times decrease from 80% of the simulated flux at 10 m from the river to 35% at 50 m; estimates derived from solute travel times decrease from 330% to 255% (Figure 3-8d). Using average hydraulic conductivity underestimates simulated flux by 20-35%. Beyond 50m the low hydraulic conductivity of the aquifer controls flux estimates (compare Figure 3-8d and Figure 3-7b). When the sand string is semi-confined, flux estimates derived from both pressure and solute travel times overestimate simulated flux. For example, when the contrast is three orders of magnitude, flux estimates derived from pressure travel times overestimate simulated flux by three orders of magnitude, whereas the overestimate is limited to one order of magnitude when derived from solute travel times (not shown). Conversely, when the average hydraulic conductivity is used the percentage by which simulated flux is underestimated is unaffected. Thus, the most accurate flux estimate in this

type of system is derived from the average hydraulic conductivity. In practice, the average hydraulic conductivity will not be known with confidence, and hence, fluxes derived from solute travel times contain the smallest error across the broadest range of hydraulic conductivity contrasts.

3.3.5 Identifying heterogeneity from travel time ratios

Both generic types of subsurface structures retard pressure and solute propagation into an aquifer, but not equally. As the hydraulic conductivity of a clogging layer K_1 decreases, propagation through the clogging layer slows, travel times increase, and the travel time ratio decreases. For a given observation distance and clogging layer thickness, each t_s/t_p value corresponds to a single value of K_2/K_1 (Figure 3-9a). The relationship between t_s , t_p , t_s/t_p and K_2/K_1 in aquifers containing horizontal sand strings is more complex as the properties of the aquifer that control propagation change with K_2/K_1 and the ratio of string thickness to total saturated thickness b_2/b (Figure 3-9b). Hence, each travel time ratio corresponds to two possible values of hydraulic conductivity contrast for each string thickness. For example, for $b_2 = 5$ m K_2/K_1 values of 1 and 45 are obtained for a t_s/t_p of 2.

A solute travel time less than a pressure travel time ($t_s < t_p$, or $t_s/t_p < 1$) indicates that substantial water or solute advection into the aquifer (represented by t_s) precedes substantial pressure diffusion (represented by t_p). Such a condition is not possible in a homogeneous aquifer. While it might appear possible from equations (3.1) and (3.2) if the magnitude of the river stage rise exceeds the saturated thickness of the aquifer ($H > b$), such a combination of system parameters contravenes the assumption of linearity on which the solution is derived ($H < b$ so that aquifer transmissivity is approximately constant). However, a solute travel time to pressure travel time ratio less than unity may be obtained for both conceptual models of subsurface heterogeneity with reasonable sets of aquifer parameters (Figure 3-9). Consequently, $t_s/t_p < 1$ clearly signifies that heterogeneity is controlling pressure and solute propagation from a river into an adjacent aquifer. This

condition can be obtained with less than one order of magnitude contrast in hydraulic conductivities for both conceptual models.

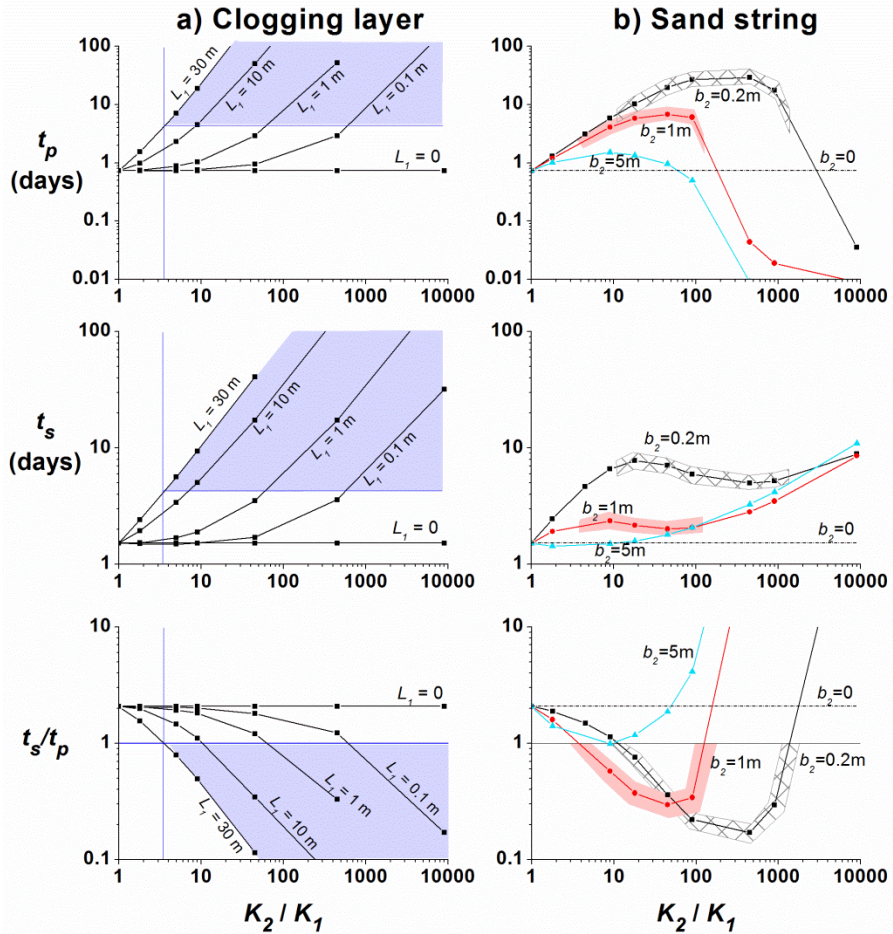


Figure 3-9 Numerically simulated solute and pressure travel times and their ratio at $x = 30 \text{ m}$ for a) clogging layers and b) sand strings of varying thickness across a range of hydraulic conductivity ratios ($K_2 = 77.76 \text{ m d}^{-1}$, $H = 5 \text{ m}$). Shaded areas correspond to the range of K_2/K_1 values and travel times that produce $t_s/t_p < 1$. In the case of a clogging layer, the hydraulic conductivity ratio where t_s/t_p drops below unity increases as the clogging layer thickness decreases. In the case of a sand string, the ratios of hydraulic conductivity that produce $t_s/t_p < 1$ overlap for thicknesses of 1 m (red shading) and 0.2 m (hatching) but are derived from distinct solute and pressure travel times. The sand string with a thickness of 5 m only achieves $t_s/t_p < 1$ when $K_2/K_1 = 9$.

For the clogging layer conceptual model, a plot of t_s/t_p against K_2/K_1 reveals that travel time ratios for all potential ratios of clogging layer thickness to observation distance (L_1/x) are contained within an envelope with the upper bound $L_1 = 0$ (homogenous aquifer) and the

lower bound $L_1 = x$ (observation point at clogging layer/aquifer interface, $L_1 = 30$ m on Figure 3-9a). As L_1 increases above x ($L_1 > 30$ m, observation point within the clogging layer), then the relationship decreases from that observed at the interface back towards that observed for a homogenous aquifer (not shown). Each t_s/t_p value corresponds to multiple combinations of K_2/K_1 and L_1/x ; for all clogging layer thicknesses there is a ratio of hydraulic conductivities that results in $t_s/t_p < 1$. In practice, the duration of river stage rise places an upper limit on measurable solute travel times. The position of the $L_1 = x$ curve, and consequently the value of K_2/K_1 at which $t_s/t_p < 1$, decreases as the ratio of specific yield to porosity and the ratio of river stage change to saturated thickness increase (not shown). The condition $t_s/t_p < 1$ signifies that flux estimated from pressure travel time will be substantially underestimated, the error increasing by an order of magnitude with each order of magnitude increase in hydraulic conductivity contrast.

For the sand string conceptual model the range of K_2/K_1 for which $t_s/t_p < 1$ (shaded regions in Figure 3-9b) has a lower limit determined by aquifer parameters and the magnitude of river stage rise, and an upper limit determined by the ratio at which semi-confined conditions commence. The latter is proportional to the ratio of string thickness to total saturated thickness of the aquifer b_2/b . To obtain $t_s/t_p < 1$ it is necessary for the sand string to be thin relative to the stage change ($b_2/H < 0.2$, not shown) and the saturated thickness ($b_2/b < 0.5$, Figure 3-9b), and for the ratio of specific yield to porosity to be close to unity (not shown). Sand strings become semi-confined when the hydraulic conductivity contrast is greater than one to three orders of magnitude. In this upper range, a sand string may be identified by a very fast pressure response (minutes) and realistically measurable solute response (hours to days), even though $t_s/t_p > 1$ (Figure 3-9b). In this case use of solute travel time to estimate flux will provide an overestimate, but it will be more accurate than using head data.

The conditions required to obtain $t_s/t_p < 1$ are not uniquely attributable to one type of subsurface heterogeneity. In order to differentiate between clogging layer and sand string conceptual models additional information is required, such as the hydraulic conductivity of different portions of the aquifer.

3.4 Field application

3.4.1 Site Description

The Mitchell River is a perennial river located in tropical North Queensland, Australia. It flows for 600 km from headwaters in the Daintree Rainforest on the Great Dividing Range through arid savannah to its discharge point in the Gulf of Carpentaria. Mean annual rainfall ranges from 1,620 mm in the tropical rainforest headwaters to 715 mm in the arid savannah (CSIRO, 2009). Rainfall is concentrated in the wet season, with 95% of precipitation falling between November and May. Relatively high rainfall intensity in the region results in rapid runoff. During the wet season flood peaks of 1 m to 6 m are common.

The field site is located in the upper reaches of the savannah part of the catchment, where the river is 10 m wide and incised 8 m into the floodplain. The riparian zone consists of a gallery forest of *Maleleuca spp.* and is surrounded by open woodland savannah dominated by *Eucalyptus spp.*. In this area the river flows through Quaternary alluvial sediments with outcrops of the Hodgkinson formation (Silurian – Devonian greywackes). Further catchment details are presented in Battle-Aguilar et al. (2014). A transect of piezometers was installed in the alluvium from 15 m to 1000 m from the river bank in 2010 and 2011 using truck-mounted and hand-held hydraulic augers and 50 mm hand-slotted PVC pipe. Piezometer screen lengths ranged from 0.2 m to 1 m. Drilling logs indicate that the local lithology consists of 0.3 – 1.5 m of sandy silty clay overlying interbedded silty sands and gravels with discontinuous clay lenses in some areas.

3.4.2 Analysis of field data

3.4.2.1 Determination of travel times and identifying heterogeneity

Pressure and electrical conductivity (EC) were measured and recorded throughout the wet season of 2011 – 2012 at intervals of 15 minutes using *In Situ* Aquatrolls. In general, pressure responses within the aquifer were significantly damped in comparison to the change in river stage, and lagged with horizontal distance into the aquifer, suggesting a reasonably low hydraulic conductivity. However, during large flow events when the river stage exceeded the water level in the aquifer substantial reduction in EC occurred at 15 m (GW1) and 30 m (GW2) from the low water level river bank (Figure 3-10). Large flow events at this site typically consist of stage rises of 3.5 m to 6 m, wave periods of 3 d to 10 d, and occur at least once each wet season. During low flow conditions the regional hydraulic gradient towards the river (measured perpendicular to the river bank) decreased from 0.1 $m\ m^{-1}$ for the first 15 m from the river to 0.008 $m\ m^{-1}$ between 15 m and 80 m from the river.

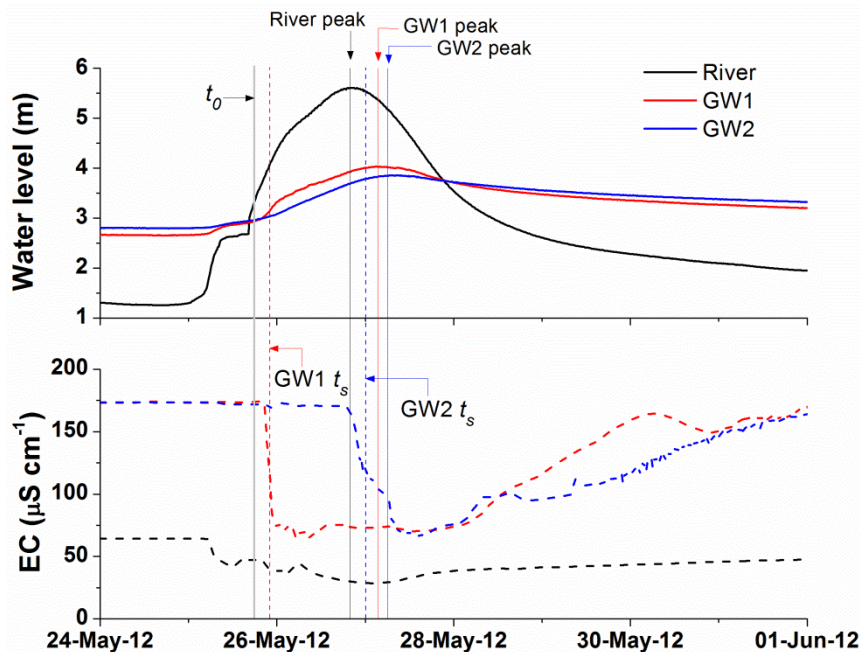


Figure 3-10 Field data for May 2012 for piezometers at 15 m (GW1) and 30 m (GW2) from the river bank. Dashed lines indicate groundwater EC or metrics. Note the damped groundwater level change compared to the river level change and the associated large drop in groundwater EC.

In May 2012 a 4.3 m flood wave passed the field site (Figure 3-10). The time to peak height in the river was 1.8 d. Prior to the flood event the river EC was $65 \mu\text{S cm}^{-1}$, and the groundwater EC was $175 \mu\text{S cm}^{-1}$. At 15 m from the river bank (GW1) the pressure measured in the piezometer increased by 1.37 m, peaking 0.33 d after the river, whereas EC decreased to $65 \mu\text{S cm}^{-1}$ one day before peak pressure rise at the piezometer, and hence also before the river peaked. At 30 m from the river bank (GW2) the maximum pressure rise of 1 m occurred 0.14 d after the peak at GW1. A similar minimum value in EC was observed at GW2, with the minimum occurring 0.25 d after the peak pressure rise.

Solute travel times were obtained from the data. Consistent with Welch et al. (2013), it was assumed that t_0 occurs at the time when $h_{river} = h_0 + 0.5H$, in this example on 25 May 2012 at 18:30 (Figure 3-10). For both piezometers the EC equal to a 50% decrease is $120 \mu\text{S cm}^{-1}$. This concentration was measured at GW1 on 25 May 2012 at 21:45, and at GW2 on 27 May 2012 at 00:00. Thus, measured solute travel times were 0.14 d at GW1 and 1.24 d at GW2.

Pressure travel times could not be determined because the river stage decreased before hydraulic head at the piezometers had increased by $0.5H$ (i.e., did not reach 2.15 m). Had the river stage not decreased, the head at the piezometers would have slowly continued to increase, and therefore, values for t_p are larger than the time from t_0 to the time when peak pressure rise is observed in the aquifer, that is, greater than 1.4 d (GW1) or 1.5 d (GW2). Hence, the solute travel time is less than the pressure travel time and minimum values for the ratio t_s/t_p are 0.1 (GW1) and 0.8 (GW2). Therefore, the aquifer may not be considered to be homogenous at the scale of the measurements.

3.4.2.2 Constraining aquifer properties and flux estimates

Aquifer properties at the site and flux estimates for the May 2012 event were constrained by comparing the calculated solute travel time (1.24 d) and minimum for pressure travel time (1.5 d) at GW2 (30 m from the river bank) to our limited simulation results (Figure 3-9, Section 3.3.5, observation point also at 30 m from the river bank) and considering

additional site information. A hydraulic conductivity value of 60 m d^{-1} was obtained from slug tests performed at piezometer GW2. Slug tests could not be performed at GW1 due to insufficient water depth ($<0.1 \text{ m}$), and therefore this piezometer was not considered further. High specific yield is expected in the sands and gravels encountered during installation of the piezometers. Constraints on aquifer properties depend on the type of subsurface structure considered.

If GW2 is screened in a sand string, the thickness of this string is likely to be close to 50% of the saturated thickness of the aquifer because the calculated solute travel time for GW2 (1.24 d) is close to that depicted for $b_2 = 5 \text{ m}$ on Figure 3-9b. Consequently, the ratio of hydraulic conductivities is most likely to be approximately 10, which means that the string is not semi-confined. Assuming that the slug test provided a realistic approximation of string hydraulic conductivity, the hydraulic conductivity of the surrounding aquifer is likely to be approximately 0.6 m d^{-1} .

If a clogging layer is present, Figure 3-9a indicates that aquifer porosity is likely 0.2, as follows: at 4 d, the lowest solute travel time in the shaded region (indicating travel times for which $t_s/t_p < 1$) is greater than the solute travel time measured at GW2 (1.24 d), whereas the pressure travel times in the shaded area are plausible ($> 1.5 \text{ d}$). Given that H and x are known, a porosity of 0.2 (compared to the 0.4 simulated) would reduce t_s but not t_p as required (refer equations (3.1) and (3.2)). Finally, the clogging layer is likely to have a hydraulic conductivity of at most 12 m d^{-1} , as a hydraulic conductivity contrast of five is the minimum feasible value to obtain a pressure travel time that exceeds the calculated solute travel time.

Theoretical simulations indicate that if a clogging layer is present, the solute travel time will provide the most accurate estimate of flux, but if an unconfined sand string is present then the pressure travel time (or head data) is the most appropriate approach to estimate flux and the solute travel time is the most appropriate tool to estimate the hydraulic

conductivity of the string (refer to section 3.3.4). As the type of structure is unknown, estimating flux from both solute and pressure data provides a range of potential fluxes at the site.

Given that the pressure travel time was longer than the wave period and hence is only known to be longer than 1.5 d, the pressure travel time cannot be used. As an alternative, the river data was simulated with the Hall and Moench (1972) solution to match the hydrograph at GW2. An estimated aquifer diffusivity of $500 \text{ m}^2 \text{ d}^{-1}$ was obtained. The diffusivity was converted to transmissivity using an assumed specific yield of 0.19. Subsequently, Darcy's Law was applied to obtain an estimate of the total flux from the river into the aquifer during the flow event of 265 m^3 per metre of bank over the duration of the flow event. The estimated saturated aquifer thickness of 10 m would result in a hydraulic conductivity estimate of 9.5 m d^{-1} however this conversion is not required for flux quantification.

The hydraulic conductivity was estimated from the solute travel time by rearranging equation (3.2). Using estimates of aquifer properties (saturated thickness of 10 m, porosity of 0.2 and specific yield of 0.19) and $t_s = 1.24 \text{ d}$, hydraulic conductivity was estimated at 80 m d^{-1} . This compares reasonably well to the estimate obtained from the slug test (60 m d^{-1}). The total flux from the river into the aquifer during the flow event was estimated using this technique as $2,300 \text{ m}^3$ per metre of bank over the duration of the flow event, one order of magnitude greater than that estimated from pressure propagation (265 m^3 per metre of bank).

3.5 Discussion

In homogeneous aquifers pressure will always propagate into an aquifer faster than water following river flow events. Water movement can be inferred from measurements of solutes, or a proxy such as EC. Co-measurement of pressure and a solute in a river and adjacent aquifer during flow events can be used to identify whether or not subsurface

heterogeneity dominates the propagation of pressure and water from the river to the aquifer. In this paper two generic conceptual models were investigated, a vertical clogging layer and horizontal sand string. The dominant influence of heterogeneity on pressure and solute propagation is readily identified when the measured solute travel time is less than the pressure travel time at an observation point within the aquifer. For both conceptual models the primary determining factor in obtaining a solute travel time faster than a pressure travel time is the ratio of hydraulic conductivities of the different parts of the system. Less than one order of magnitude difference in hydraulic conductivities is sufficient. Other key controls on pressure and solute travel times include the ratio of clogging layer thickness to the distance of the observation point from the river bank, and the ratio of string thickness to total saturated thickness.

Hydraulic conductivity estimates and subsequent estimates of exchange flux can be constrained by simultaneous consideration of time series solute data and head data in heterogeneous systems. Numerous studies have estimated aquifer properties on the basis of head measurements alone (e.g., Barlow et al., 2000; Ha et al., 2007). However, this work demonstrates that for the majority of types of heterogeneity and hydraulic conductivity contrasts that may be encountered, estimating hydraulic conductivity from solute data will provide a more accurate estimate of exchange flux. The maximum error in hydraulic conductivity estimates from pressure data, and hence exchange flux estimates, increases by approximately one order of magnitude with each order of magnitude increase in the ratio of high to low hydraulic conductivities. Similar results would be obtained where, for example, low hydraulic conductivity layers exist within an aquifer between the river and the observation point, regardless of whether or not the structure is contiguous with the river bank.

Our analysis of binary hydraulic conductivity systems does not consider temporal variability of aquifer parameters, within-zone heterogeneity, and the connectedness of heterogeneity

fields. Temporal variability of the hydraulic conductivity of the clogging layer can occur in high energy alluvial systems (Genereux et al., 2008). This variability may potentially be identified by variable t_s and t_p responses to flow events of similar magnitude. The effects on travel times of assuming a homogenous clogging layer requires further investigation given the wide range of heterogeneity reported for streambed deposits (e.g., Calver, 2001; Cardenas and Zlotnik, 2003). In these binary systems the contrast is more important than the absolute hydraulic conductivity values. Further research is required to confirm that increasing variance in a more complex heterogeneity field exacerbates the effects of heterogeneity on travel times and subsequent water flux estimates in the same way.

Consideration of within-zone heterogeneity of hydraulic conductivity raises the issue of connectivity of high and low hydraulic conductivity zones which may result from macropores and other preferential flow paths (Heeren et al., 2011; Poole et al., 2002).

Dynamic connectivity is typically assessed using metrics derived from artificially applied tracers. One example is the ratio of the average arrival and early (5%) arrival of particles flowing through a porous media (Knudby and Carrera, 2006). This ratio is generally applied to pumping tests (e.g., Renard and Allard, 2013) and based on a constant source model. Development of a similar metric based on transient inputs would facilitate use of data from flow events that naturally perturb alluvial systems. Combined with the metrics presented in this paper, the potential result would be an indication of the dominance of heterogeneity on pressure and solute propagation, and the connectivity of the hydraulic conductivity zones in the aquifer.

Finally, our analysis assumes that the river stage rise is the dominant driver for pressure propagation, water level change, and solute change within an aquifer, and that the river bank is vertical, and fully penetrates the aquifer. Principal component analysis is one technique that has been successfully applied to separate causes of forcing in alluvial environments (Lewandowski et al., 2009). Alternatively, locating a reference piezometer outside the zone of influence of the river pressure pulse may suffice. Observed and

modelled data presented by Wett *et al.* (2002) indicated that infiltration from rainfall can dominate both water level change and solute concentration where the solute (or proxy EC) is influenced by both precipitation and river water. It is therefore necessary to confirm that the tracer for which a time series is obtained is predominantly influenced by exchange with the river. In cases where it can be shown to be conservative, temperature may be useful as it is also readily measured at the event scale. Although Doble *et al.* (2012) demonstrated that flux into an aquifer during a flow event is relatively unaffected by bank slope unless banks are extremely flat, further analysis is required to clarify the effects of slope on calculation of travel times and subsequent estimates of hydraulic conductivity and exchange flux. Similarly, while solute travel times have been demonstrated to be relatively insensitive to the degree of aquifer penetration in homogenous aquifers (Welch *et al.*, 2013) this remains to be confirmed in heterogeneous systems.

3.6 Conclusions

Commonly pressure change alone is used to estimate surface water – groundwater exchange. Conventional theory says that pressure will propagate faster than water will move; that is, the physical exchange of water may be less than a pressure response suggests. However this work has demonstrated that it is possible to have more water exchange than indicated by pressure response alone when structures with contrasting hydraulic conductivities are present. The heterogeneity has unequal influences on pressure and solute propagation. A ratio of solute to pressure travel times less than unity clearly indicates the dominating influence of heterogeneity within an aquifer. Co-measurement of pressure and EC in transects of piezometers adjacent to rivers and calculation of travel time metrics is a simple method that can facilitate the identification of subsurface heterogeneity. Furthermore, such data can be used to constrain estimates of hydraulic conductivity and hence water flux in a way that is not possible with pressure measurements alone.

Acknowledgements

The authors thank the Australian Wildlife Conservancy – Brooklyn for site access and assistance during field work. Rebecca Doble and two anonymous reviewers provided constructive feedback on earlier drafts.

4 Influence of hydraulic gradient on bank storage exchange, penetration distance and return time

ABSTRACT

The hydraulic gradient between aquifers and rivers is one of the most variable properties in a river / aquifer system. Detailed process understanding of bank storage under hydraulic gradients is obtained from a 2-D numerical model of a variably saturated aquifer slice perpendicular to a river. Exchange between the river and aquifer occurs first at the interface with the unsaturated zone. Decreasing aquifer hydraulic conductivity, increasing partial penetration, and increasing hydraulic gradient redistribute exchange to the river bank. Hence, total exchange may be estimated to within 50% using existing analytical solutions provided that unsaturated zone processes do not strongly influence exchange. Bank storage is at a maximum when no hydraulic gradient is present, and increases as hydraulic conductivity increases. However, in the presence of a hydraulic gradient the largest exchange flux or distance of penetration does not necessarily correspond to the highest hydraulic conductivity, as a high hydraulic conductivity increases the components of exchange both into and out of the aquifer. Ambient groundwater discharge is not influenced by wave characteristics, and so higher hydraulic gradients are necessary to reduce bank storage when flow waves have large heights or periods. Practical measurement of bank storage exchange, penetration distance and return time is problematic due to the limitations of available measurement technologies and the nested processes of exchange that occur at the river – aquifer interface. Proxies, such as time series concentration data, require further development to be representative and quantitative.

4.1 Introduction

Bank storage is the process by which river water propagates into aquifers in response to river stage rise and subsequently contributes to the maintenance of baseflow in rivers after a flow event (e.g., Brunke and Gonser, 1997; Winter, 1998). The period of time that bank storage water resides in an aquifer and the distance it travels have important ramifications for biogeochemical cycling, contaminant mixing, and aerobic and anaerobic degradation, and assessment techniques that differentiate between surface and groundwater reservoirs (Sophocleous, 2002). Detailed understanding of the process is therefore beneficial to effective management of rivers and aquifers.

Theoretical investigations have considered various aspects of the bank storage process. It has been demonstrated that the volume (Pinder and Sauer, 1971) and storage zone (Chen and Chen, 2003) increase in proportion to aquifer hydraulic conductivity and the rate of stream level rise (Li et al., 2008), and reduce when vertical permeability reduces due to either less permeable river beds, aquitards or anisotropy (Chen and Chen, 2003). It has been suggested that consideration of the degree of penetration (Chen and Chen, 2003; Sharp Jr, 1977) and bank slope (Doble et al., 2012) are also crucial to accurate estimates of exchange flux. Theoretically, the time it takes for bank storage to return to a river is fastest for finite aquifers of limited horizontal extent, or when wave duration is long or aquifer diffusivity is high (Cooper and Rorabaugh, 1963). It has been shown numerically to range from days to years (Doble et al., 2012; McCallum et al., 2010).

Field-based studies have quantified volumes of bank storage exchange flux using hydraulic methods (Gerecht et al., 2011; Kondolf et al., 1987; Lewandowski et al., 2009; Sjodin et al., 2001), sometimes in combination with in-stream measurements of isotopes or water chemistry (McKenna et al., 1992; Meredith et al., 2009). Squillace (1996) presented one of the few examples where aquifer chemistry measurements clearly identified infiltration and exfiltration of river water. River water penetrated 30 m into the aquifer and completed discharging from the alluvium 5 weeks after peak river stage. In contrast, Schilling et al.

(2006) inferred that bank storage penetrated a mere 1.6 m into the aquifer from measurement of hydraulic gradients in near-river piezometers and estimation of the average linear velocity, and hence that near-river chemistry variability was due to other processes. In a study that only considered vertical infiltration below the river bed, Simpson and Meixner (2012) determined from chemistry measurements in the river and aquifer that flood water was generally retained for less than two months, but that the duration was related to the degree of gaining or losing, in other words, the hydraulic gradient between river and aquifer.

The hydraulic gradient between a river and an aquifer varies both spatially and temporally. Variability can be induced by changes within the aquifer such as recharge, extraction, and evapotranspiration, or changes in river level due to extraction or upstream management (Sophocleous, 2002). In theoretical studies hydraulic gradients between rivers and aquifers have tended to be either ignored or small. Chen and Chen (2003) suggested that hydraulic gradients of ± 0.003 had a minimal effect on bank storage. Chen et al. (2006) extended the analysis of positive hydraulic gradients up to 0.015 and demonstrated that the infiltration rate, and hence bank storage, could be reduced to zero for particular parameter combinations. McCallum et al. (2010) indirectly demonstrated that bank storage residence time reduces as the hydraulic gradient increases by establishing that the time for solute concentration to return to ambient groundwater concentration increases with higher aquifer recharge. However, the influence of a hydraulic gradient on exchange and return time in aquifers with a wide range of properties and wave characteristics has not previously been explored.

The objective of this study is to systematically assess the influence of aquifer and flow wave characteristics, and river shape and aquifer penetration, on (i) the water exchange between river and aquifer that results from a flow event (total exchange), (ii) the distance river water moves into an aquifer (penetration distance), and (iii) the time it takes river water to return

to the river from an aquifer (return time) when a range of hydraulic gradients are present. Using analytical and numerical methods we demonstrate that the distribution of exchange along the river bank and bed is a function of aquifer properties and partial penetration, and that the presence of a hydraulic gradient has a significant influence on these bank storage metrics.

4.2 Methods

The river – aquifer system was conceptualised as a 2-D cross-section perpendicular to a river bank (Figure 4-1).

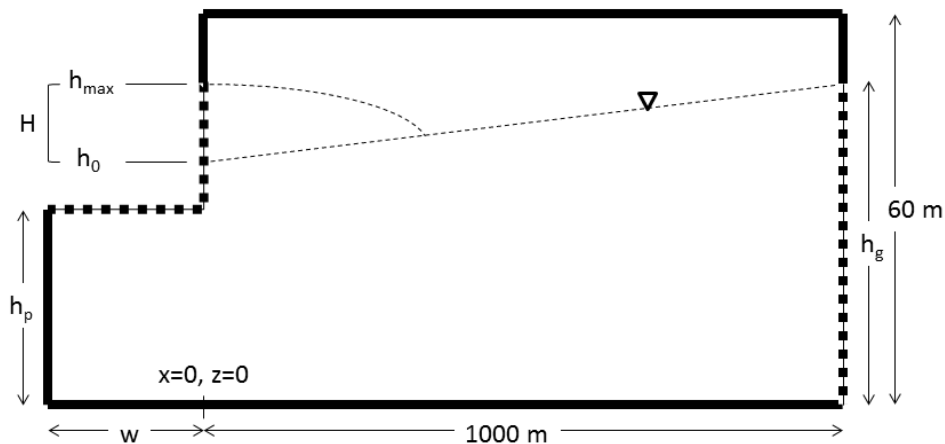


Figure 4-1 Conceptual model of river – aquifer system. Boundary conditions implemented in the numerical model are indicated with dashed lines. All other boundaries are no-flow boundaries. In the fully penetrating base case with no hydraulic gradient the water table is horizontal ($h_0 = b$), $w = 0$, the boundary condition representing the river extends to $z = 0$, and the boundary condition representing regional inflow is a no-flow boundary ($h_g = 0$). The river stage rise (H) is represented by time varying specified head and concentration boundaries from $z = 0$ or h_p to h_{max} .

Bank storage is defined as the movement of river water into and out of an aquifer in response to river stage rise and fall. Analytical solutions were used to illustrate the influence of aquifer and wave characteristics on estimates of bank storage exchange and return time in the presence of a hydraulic gradient. Numerical simulations of flow and transport were used to examine the influence of 1) an unsaturated zone, 2) dispersion, and

3) partial penetration of rivers on the process of exchange and to provide estimates of exchange and return time for comparison to analytical results. Numerical simulations were also used to examine river water penetration distances. In order to differentiate between river water and groundwater each water reservoir was tagged with a specific concentration of a conservative tracer in the numerical simulations. Consequently, mass outputs from the model correlate directly to volumes of river water exchanged with the aquifer but also incorporate the effects of mixing and spreading.

4.2.1 Analytical Solutions

The analytical solutions presented by Cooper and Rorabaugh (1963) for a finite aquifer were selected to obtain the rate of discharge from river to aquifer per unit width of aquifer, Q (equations (63) and (64)) and the total amount of river water held in the aquifer per unit width, V (equations (65) and (66)). These solutions are derived from the differential equation for non-steady flow of groundwater through Laplace transformation with respect to time and applying the principle of superposition to incorporate the effects of wave shape (Cooper and Rorabaugh, 1963). For application to unconfined aquifers it was assumed that aquifer transmissivity is constant and that the river fully penetrates the aquifer. The input function for river stage was a cosine wave. Note that the direction of flow described here has been reversed from the original definition (equations multiplied by negative 1).

The key assumption of the Cooper and Rorabaugh (1963) solution is that the water table within the aquifer is initially horizontal, and hence presents no resistance (or assistance) to the movement of river water into (or out of) an aquifer. For a water table with constant gradient towards or away from the river the principle of superposition provides

$$Q_{net}(t) = Q_{river}(t) - Q_{gw} \quad (4.1)$$

where Q_{net} is the net rate of river water discharge to the aquifer, Q_{river} is the total rate of river water discharge to the aquifer that would occur with no hydraulic gradient (i.e., that obtained directly from analytical solutions), and Q_{gw} is a steady state Darcy flux from the

aquifer to the river, $Q = iKb$, where i is hydraulic gradient from aquifer to river, K is hydraulic conductivity and b is saturated thickness of the aquifer. Hence, under gaining conditions the flow of river water into the aquifer is reduced ($-Q_{gw}$), while under losing conditions the flow of river water into the aquifer is increased ($+Q_{gw}$). The total volume of water in the aquifer V is obtained by summing the rate for each time step.

4.2.2 Numerical Simulations

A 2-D variably saturated flow and transport model was constructed in FEFLOW. In variably saturated mode FEFLOW solves the head-based form of the Richard's equation for flow and the convective form of the transport equation simultaneously across unsaturated and saturated portions of the model domain (Diersch, 2009). The base model domain is 60 m in height, 1000 m in length, and a default 1 m in width (Figure 1). Partially penetrating river models were constructed by extending the model domain length by half the river width, w . For the base case simulation the initial water table was horizontal, and the saturated aquifer thickness was equal to the height of the river (i.e., $h_0 = b$). In order to create a hydraulic gradient within the model the no flow boundary condition at $x = 1000$ m was replaced by a specified head boundary applied from $z = 0$ to $z = h_g$ with $h = h_g$ to represent regional groundwater discharge. The model was run to steady state to obtain a head distribution throughout the model, and then this condition was used as the initial condition for transient simulations of river stage rise and bank storage.

The river was represented by a time-varying head (TVH) boundary condition applied from the base of the river to maximum river stage ($z = 0$ or h_p to $z = h_{max}$). River stage was varied according to a cosine shaped wave, as per the analytical solution. A constant (specified) concentration boundary was applied along the same section of the model as the TVH and assigned a concentration of $C_{river} = 1 \text{ g m}^{-3}$. The concentration boundary condition was constrained such that it only applied when the direction of flux across the boundary was into the aquifer; otherwise it was removed and water was free to leave the model at any concentration. This allowed infiltrated river water to be distinguished from water that was

in the aquifer prior to river stage rise. The aquifer was assigned an initial concentration of $C_{aquifer} = 0 \text{ g m}^{-3}$.

4.2.3 Initial Conditions and Metrics

The base models for the analytical and numerical approaches were both assigned a saturated thickness equal to the river stage of $h_0 = 20 \text{ m}$, and other aquifer parameters selected to represent a sandy alluvial aquifer. Ranges for parameters were selected to represent a variety of alluvial environments consisting of silty sands to gravels and a common range of flow events (Table 1).

Table 4-1 Parameter variation.

Parameter	Base case	Range
Hydraulic conductivity, $K (\text{md}^{-1})$	10	1-100
Saturated thickness, $b (\text{m})$	20	10, 20
Dispersivity (m)	0.01	0.001-1
River half width (m)	0	0-45
River depth (m)	20	2-20
Aspect ratio (half width : height; -)	0	1/3 – 9
Hydraulic gradient, $i (\text{m/m})$	0	0 ± 0.05
Wave height (m)	1	1, 5
Wave period (d)	5	1, 5

Three metrics were selected to compare and contrast scenarios:

1. Total exchange: the total volume of river water that enters the aquifer and subsequently returns to the river. For gaining river scenarios all infiltrating water eventually returns to the river; for losing river scenarios this does not occur. Total exchange was obtained from the flow (analytical) or mass (numerical) balance. In gaining rivers total exchange is the maximum value observed in the aquifer during the flow event, in losing rivers total exchange is the difference between the maximum value observed during the flow event and the value in the aquifer when the river returns to losing conditions. This metric is of use when considering total load (e.g., contaminant, oxygen) on an aquifer as a result of a flow event;

2. Penetration distance: defined herein for gaining rivers as both the maximum horizontal distance from the river bank and the maximum vertical distance from the river bed of infiltrating water, as defined by the 0.5 concentration contour. For losing rivers it is defined as the maximum distance travelled into the aquifer by a water particle that also returns to the river. The latter was obtained using pathline analysis. The distance water travels into an aquifer is directly linked to ecological function and has ramifications for siting monitoring wells; and
3. Return time: time taken for a certain percent of total exchange to return to the river, given as time after commencement of simulation. As for total exchange the return time was obtained from the mass balance. Three classifications were used: 10% return time to represent rapid exchange; 50% return time to represent the median time water resides in aquifer; and 90% return time to represent longer residence time water. The return time represents the period of time for which introduced river water and its constituents can affect groundwater chemistry.

4.3 Results

First we describe the process of bank storage using numerical simulations with a variably saturated model. Second, we describe relationships between hydraulic gradient, aquifer and wave properties for the metrics total exchange and return time (analytical and numerical methods), and penetration distance (numerical only). Third, we assess the relationships between hydraulic gradient, river shape and aquifer penetration and the bank storage metrics.

4.3.1 Process of Exchange

Prior to a flow event, groundwater discharges through the entire river bank of a gaining river (Figure 4-2a). In the initial phase of river stage rise, there is minimal flow of water into the aquifer as the rising head in the river is quickly transferred to the aquifer. However, the rising stage in the river progressively reduces flux from the river to the aquifer because it reduces the head gradient. After some time, river stage rise at the interface with the

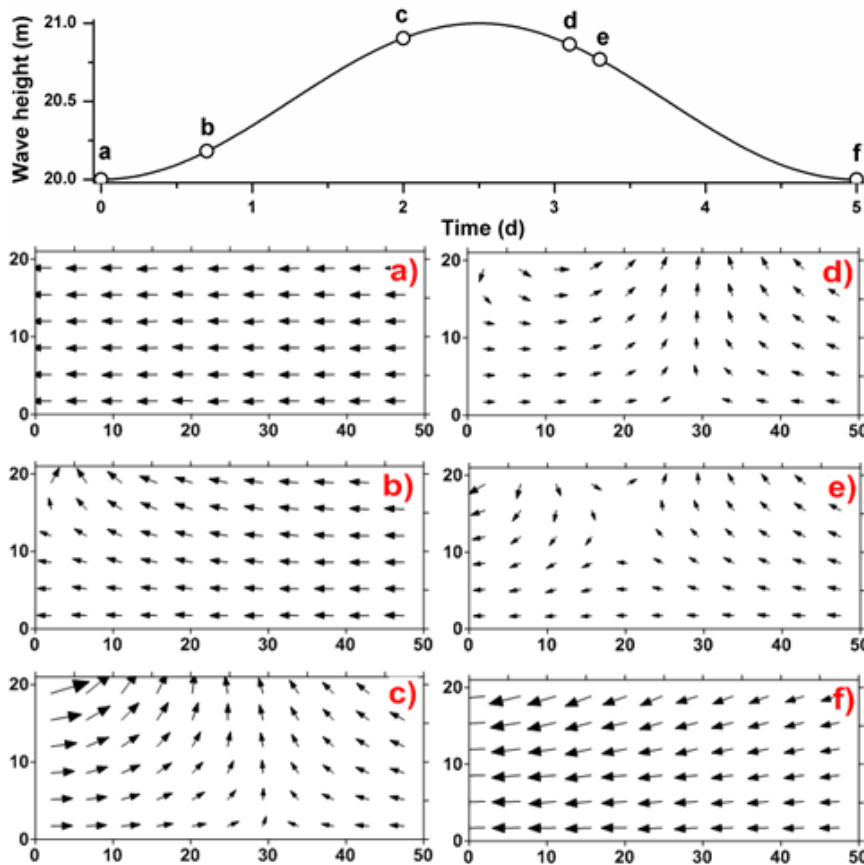


Figure 4-2 Velocity vectors from the simulation of a wave 1 m high with a period of 5 days under a hydraulic gradient of 0.01 depicting the process of river water movement into and out of an aquifer. Other aquifer parameters are as per the base case. The flood wave and the points at which velocity vectors are shown are indicated in the top panel. Initially, groundwater discharges to the river (a). River water first moves into the aquifer close to the interface with the unsaturated zone (b). After some time, river water flows into the aquifer over the whole cross-section (c). As the river stage falls the process occurs in reverse. Initially, return of river water occurs only at the interface with the unsaturated zone (d), but over time over the whole cross-section (e). Finally, steady state groundwater discharge to the river is re-established (f).

unsaturated zone exceeds the rate of pressure rise in the aquifer and river water begins to flow into the aquifer at this interface (Figure 4-2b). That is, water flows both into and out of the river bank, and both away from and towards the river within the aquifer. As time progresses, the elevation of the interface between water flowing in and out of the river bank lowers, and simultaneously, the groundwater divide within the aquifer moves further way from the river bank (Figure 4-2c). The magnitude of exchange and duration of the

period when exchange occurs both into and out of the river increases with hydraulic gradient. At high gradients river water discharge is confined to the upper section of the river bank.

The process is repeated in reverse as the flow wave passes. The water level in the aquifer adjacent to the river bank initially reduces at approximately the same rate as the river stage then commences discharging to the river from the bank section at the unsaturated zone interface (Figure 4-2d). A second groundwater divide develops in the aquifer close to the river. In this period there are three zones of groundwater movement in the aquifer – 1) between river and first divide close to unsaturated zone interface, towards river; 2) between divides and at depth, into aquifer; 3) beyond second divide, towards river. With time the section of the river bank over which water is discharging back to the river extends downward (Figure 4-2e). In the lower section of the aquifer groundwater flow in the direction of the river is quickly re-established. In the upper half of the aquifer the divides propagate away from and towards the river respectively. After they merge groundwater moves solely in the direction of the river (Figure 4-2f) and regional flow observed prior to the flow event is re-established.

In a losing river the rising river stage of the first half of a flow event simply increases the rate of river water flux into the aquifer. The rate is consistently highest at the interface with the unsaturated zone. The bank storage process during a falling river stage is similar to the positive gradient scenario, but lagged, and only a single groundwater divide is created. Initially the reduction in river stage and head in the aquifer occur at the same rate. Flux out of the aquifer is first observed at the interface with the unsaturated zone, before extending downward to cover the entire river bank, before once again moving up the river bank until flow is solely from the river to the aquifer.

Even when no hydraulic gradient is present, as the river stage reduces during flow events water flows simultaneously into the aquifer from the river at the base of the aquifer and

out of the aquifer into the river near the water table surface (Figure 4-2b-e) in variably saturated aquifers. As a consequence, the total volume of river water or mass that is exchanged with the aquifer is slightly larger than the maximum net exchange (i.e., the maximum amount of water or mass that is observed in the system during the flow event, defined herein as total exchange) for both water and mass (not shown). The difference is 5 – 10% for scenarios simulated in this study.

4.3.2 Aquifer and Wave Properties, Exchange and Return Time

4.3.2.1 Analytical results

Imposing a hydraulic gradient on the analytical solution reveals complex relationships to variation in hydraulic conductivity and wave height and period. In general, both the volume of exchange of bank storage and the return time of bank storage from aquifer to river reduce as the absolute magnitude of the hydraulic gradient increases (Figure 4-3). Total exchange is smaller in a losing river (compared to equivalent gradient for gaining river) because not all the river water that enters the aquifer in response to river stage rise returns to the river before losing conditions are re-established. The distribution of return times, identified from the relative change in 10%, 50%, and 90% return times, reduces as hydraulic gradient increases for gaining rivers, however in losing rivers it is essentially constant for hydraulic gradients smaller than -0.005 (not shown).

In a system with no hydraulic gradient, total exchange is directly proportional to the square root of the hydraulic conductivity (refer to equations 64 and 65 in Cooper and Rorabaugh (1963)). Total exchange increases from 4.06 m^3 with $K = 1 \text{ m d}^{-1}$ to 40.6 m^3 with $K=100 \text{ m d}^{-1}$ (Figure 4-3a). However, under a constant regional gradient total discharge from (or to) an aquifer is directly proportional to hydraulic conductivity (V is the integral over time of $Q = iKb$). Consequently, for bank storage under a regional gradient changes in hydraulic gradient (HG) have increasingly pronounced impacts on total exchange at higher hydraulic conductivities (Figure 4-3a). For example, at $\text{HG} = 0.02$, $V = 2.8 \text{ m}^3$ with $K = 1 \text{ m d}^{-1}$, while $V = 1.15 \text{ m}^3$ with $K = 10 \text{ m d}^{-1}$ and no exchange occurs for an aquifer with $K = 100 \text{ m d}^{-1}$. In a

losing system with $HG = -0.02$, $V = 0.9 \text{ m}^3$ with $K = 1 \text{ m d}^{-1}$, while no exchange occurs for aquifers with $K = 10 \text{ m d}^{-1}$ and $K = 100 \text{ m d}^{-1}$. Hence, when a hydraulic gradient is present, the largest total exchange does not necessarily correspond to the highest hydraulic conductivity.

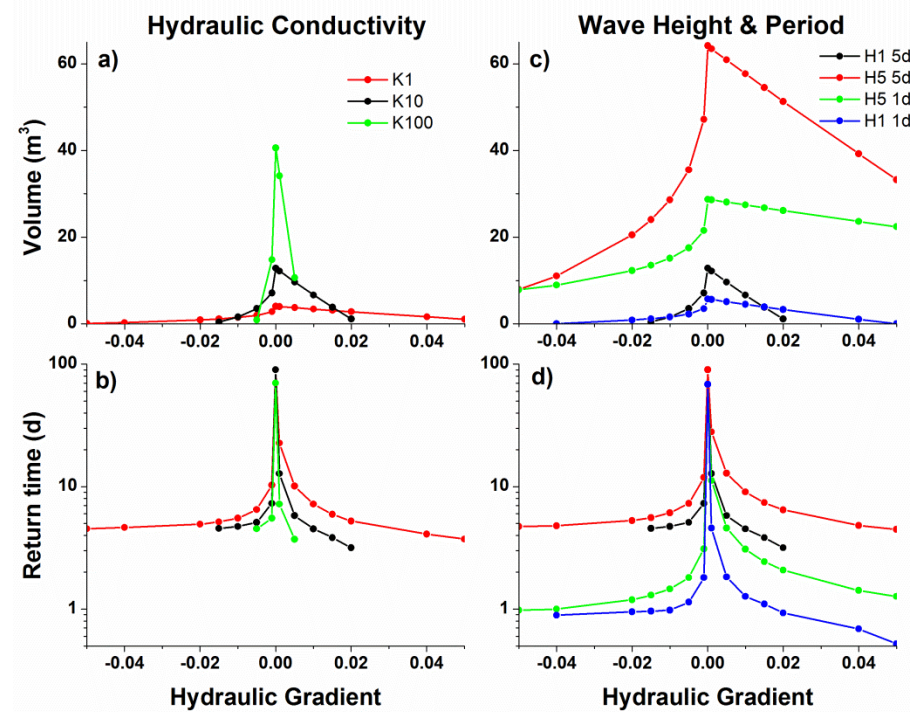


Figure 4-3 Total volume of water exchange per unit width of aquifer and return times obtained from analytical solutions for a range of hydraulic conductivity (K), wave height (H) and wave period values at a range of hydraulic gradients. Where no data is plotted for a hydraulic gradient zero exchange occurs. K1 refers to a hydraulic conductivity of 1 m d^{-1} , H5 refers to a wave height of 5 m , and 1d refers to a wave period of 1 d .

Return time decreases as aquifer hydraulic conductivity increases (Figure 4-3b). When no hydraulic gradient is present 90% return times range from 70 to 90 d for the hydraulic conductivity values tested; with a positive gradient of only 0.001 these reduce by factors of four ($K = 1 \text{ m d}^{-1}$) to ten ($K = 100 \text{ m d}^{-1}$) (Figure 4-3b). In losing rivers the time for 90% return also decreases with increasing hydraulic conductivity. It is consistently less than 10 d, and for the scenarios tested, commonly less than the 5 d wave period. In contrast, short (10%) and median (50%) return times are essentially independent of hydraulic conductivity

in losing rivers (not shown). Similar to total exchange, differences in return time observed for aquifers with very different hydraulic conductivities are less than differences for different hydraulic gradients.

With no hydraulic gradient, total exchange is directly proportional to wave height whereas steady state discharge from (or to) an aquifer under a regional gradient is independent of wave height. Consequently, total exchange is less sensitive to hydraulic gradient at large wave heights (compare 1 m wave heights to 5 m wave heights on Figure 4-3c). The impact of the hydraulic gradient is also lower for more rapid increases in river stage, achieved, for example, by reducing the wave period for a constant wave height (compare 1 d and 5 d wave periods on Figure 4-3c). At a gradient of 0.15, waves with a height of 1 m and periods of 5 d and 1 d introduce the same amount of water into aquifer; for waves with a height of 5m the gradient where this equivalence occurs is greater than 0.05. In losing systems this occurs at smaller hydraulic gradients. Similarly, increasing wave height and period both increase return time (Figure 4-3d) and reduce the sensitivity of the return time distribution to increasing hydraulic gradient, whether positive or negative (not shown).

4.3.2.2 Numerical results

Numerical simulations indicate that the relationships between hydraulic gradient, hydraulic conductivity, wave height and period, and total exchange and return time determined from the analytical solutions are also apparent in variably saturated systems (compare Figure 4-3 and Figure 4-4). However, a number of discrepancies in the magnitude of exchange and return time were identified.

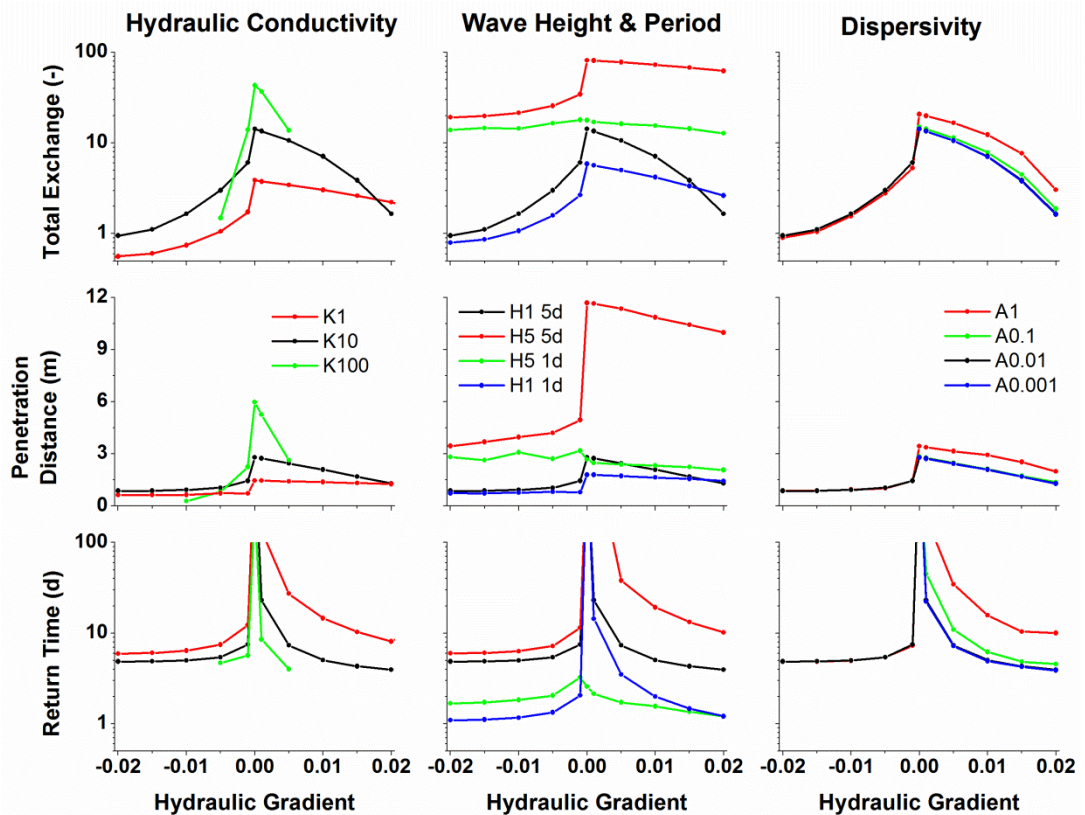


Figure 4-4 Dependency of total exchange per unit width of aquifer, penetration distance, and 90% return time on variation in hydraulic gradient and hydraulic conductivity (K), wave height (H) and period, and dispersivity (A). Penetration distance is plotted at the time maximum exchange occurs. $A1$ refers to a longitudinal dispersivity value of 1 m.

For total exchange the percentage error in analytical results compared to the numerical results is generally less than 20% (Figure 4-5a). Exceptions occur for scenarios where the rate of exchange and hence the total volume is substantially enhanced or retarded by unsaturated zone processes. In gaining rivers this occurs when there is a rapid increase in river stage (H5 1d). In losing rivers this occurs at low hydraulic gradients ($K = 1 \text{ m d}^{-1}$) and moderate rates of river stage rise (H5 5d and H1 1d). Irrespective of the direction of the hydraulic gradient, larger errors also occur at the greatest hydraulic gradient for which exchange is observed (i.e., no exchange is observed for the subsequent hydraulic gradient simulated). This maximum hydraulic gradient is generally greater in numerical simulations than indicated by the analytical solution, particularly for negative gradients.

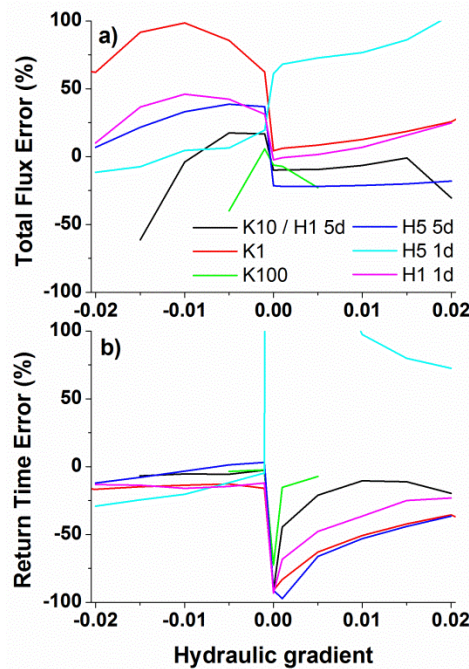


Figure 4-5 Percentage error in analytical results compared to numerical results for a) total flux and b) 90% return time. Errors for 50% return times are substantially lower than for 90% return times.

Return times are generally underestimated by the analytical solution (Figure 4-5b).

Percentage errors are greatest when no hydraulic gradient is present and range from 20-80% for 50% return times and 70-90% for 90% return times. These values generally reduce to <20% at hydraulic gradients with an absolute magnitude greater than 0.005. Across all hydraulic gradients 10% return times are underestimated by at most 20% (not shown). The longer numerical return times are a function of the retarding effect of the unsaturated zone and dispersion, neither of which the analytical solution considers. Numerical return times are presented in detail on Figure 4-6.

Decreasing dispersivity decreases the total exchange between a gaining river and the aquifer, return time, and the distribution of return times (Figure 4-4 and Figure 4-6). Within the range proposed by Gelhar (1992) as appropriate for transport at the scale under consideration (0.001-0.1) dispersivity variation has minimal influence on exchange and return time (Figure 4-4). Under losing conditions altering dispersivity causes minimal variation in exchange and return time.

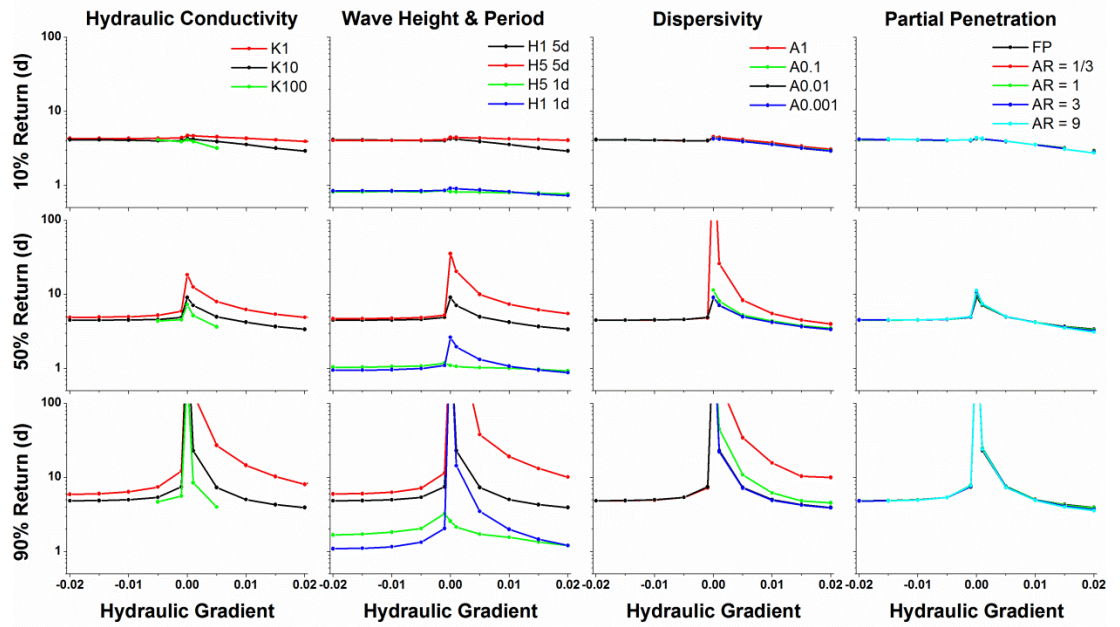


Figure 4-6 10%, 50% and 90% return times after commencement of river stage rise for variation in hydraulic conductivity (K), wave height (H) and period (d), dispersivity (A), and partial penetration with varying aspect ratios (AR). FP refers to a fully penetrating river.

Numerical simulations demonstrate that the vertical distribution of exchange along the fully penetrating river bank is not even (Figure 4-7). A large proportion of exchange occurs in the upper quarter of the river bank, and this proportion increases as the hydraulic gradient increases and the hydraulic conductivity decreases. That is, as hydraulic conductivity increases, the distribution becomes more uniform. For example at $HG = 0$, with $K = 10 \text{ m d}^{-1}$ the percentage of exchange in the top 25% of the river bank is 40% and with $K = 1 \text{ m d}^{-1}$ it is 50%. With an increase to $HG = 0.01$ percentages increase by 10% and 5% respectively. This behaviour is the result of faster pressure propagation and hence lack of vertical gradients within the aquifer at higher hydraulic gradients. Similarly, reducing wave period and height increase the skew of exchange to the upper portion of the river bank, and imposing a hydraulic gradient provides a further increase (not shown). Trends are similar for equivalent negative gradients (not shown).

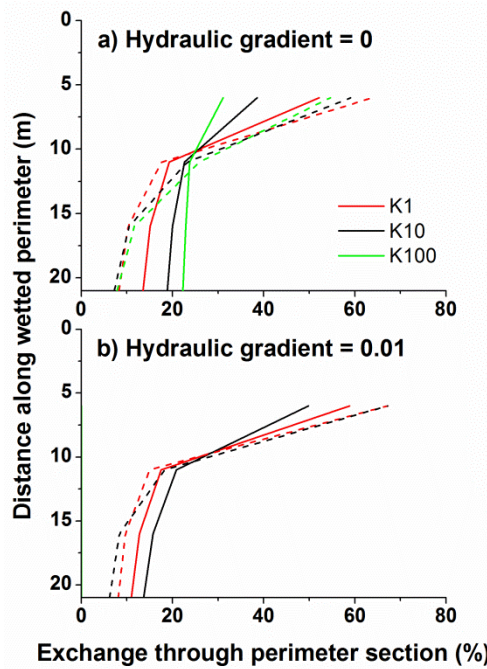


Figure 4-7 Vertical distribution of exchange along the wetted perimeter on entry to the aquifer for a range of hydraulic conductivities at a) hydraulic gradient = 0 and b) hydraulic gradient = 0.01. The dashed lines represent the percentage exchange for a partially penetrating system with an aspect ratio of 3 (river bed half width = 15m; river bank height = 5m). Irrespective of penetration, there is no exchange of river water with an aquifer with $K = 100 \text{ m d}^{-1}$ at a hydraulic gradient of 0.01.

4.3.2.3 Penetration Distance

For all scenarios tested, imposing a hydraulic gradient reduces the penetration distance as it does water exchange (Figure 4-4). In losing scenarios the most pronounced reduction in penetration distance occurs between HG = 0 and HG = 0.001. Comparison of the 0.5 concentration contour (dispersivity = 0.01 m) used to assess gaining rivers to pathlines used to assess losing rivers indicated that in a gaining river the 0.5 concentration contour approximately represents the maximum distance that water particles travel into the aquifer. Consequently, the use of different metrics does not introduce any appreciable bias into the comparison between losing and gaining rivers.

The maximum penetration distance is at the interface with the unsaturated zone in all scenarios. The relationships between penetration distance, hydraulic conductivity, wave

height, wave period, dispersivity and hydraulic gradient follow the same trends as total exchange. For the scenarios tested the maximum penetration distance was generally less than 3 m, with the exception of 5 m high and 5 d period waves where it extended to 12 m.

4.3.3 River Shape and Aquifer Penetration

Potential errors introduced by assuming a fully penetrating river in comparison to varying degrees of partial penetration are assessed by comparing numerical results from a fully penetrating river to partially penetrating rivers with different aspect ratios (ratio of river bed half width to river bank height). In general the wetted perimeter is maintained as a constant, the bank height reduced, and half width increased. As for aquifer and wave characteristics, the models are assessed using the metrics of total exchange, distance of penetration and return time for a range of hydraulic gradients.

4.3.3.1 Total Exchange

As long as the wetted perimeter is constant, the aspect ratio of a river does not have a major influence on the total exchange with the river in comparison to reductions due to hydraulic gradient (Figure 4-8a) and other parameters (Figure 4-4). However, the percentage change between the fully penetrating and partially penetrating rivers does increase with the absolute magnitude of the hydraulic gradient. Reduction in total exchange only occurs when the aspect ratio increases above unity. In comparison to the fully penetrating scenario, increasing the aspect ratio to 9 (18 m river bed half width and 2 m bank) results in a 10% decrease in total exchange at HG = 0 and a 25% decrease in total exchange at HG = 0.01. For a partially penetrating river a greater portion of exchange occurs through the bank than observed for the corresponding bank section of the fully penetrating river bank. For example, with an aspect ratio of 9 the proportion entering the aquifer through the bank is 45% compared to 20% through the top 2 m of a fully penetrating river bank. Similar results are observed for losing rivers (negative gradients).

The relative influence of the aspect ratio and partial penetration on the vertical distribution of exchange along the river bank is dependent on the hydraulic conductivity of the aquifer.

It decreases as hydraulic conductivity decreases because the largest effect of partial penetration is to redistribute exchange to the bank (Figure 4-7), and as described for the fully penetrating river, at lower hydraulic conductivities a larger proportion of the exchange already occurs through the top quarter of the river bank. For example, at $HG = 0$ in a scenario with an aspect ratio of 3 (15 m river bed half width and 5 m river bank) and $K = 100 \text{ m d}^{-1}$, exchange through the top 25% of the river bank increases by 25% in comparison to the fully penetrating scenario; with $K = 1 \text{ m d}^{-1}$ it increases by <10% (Figure 4-7).

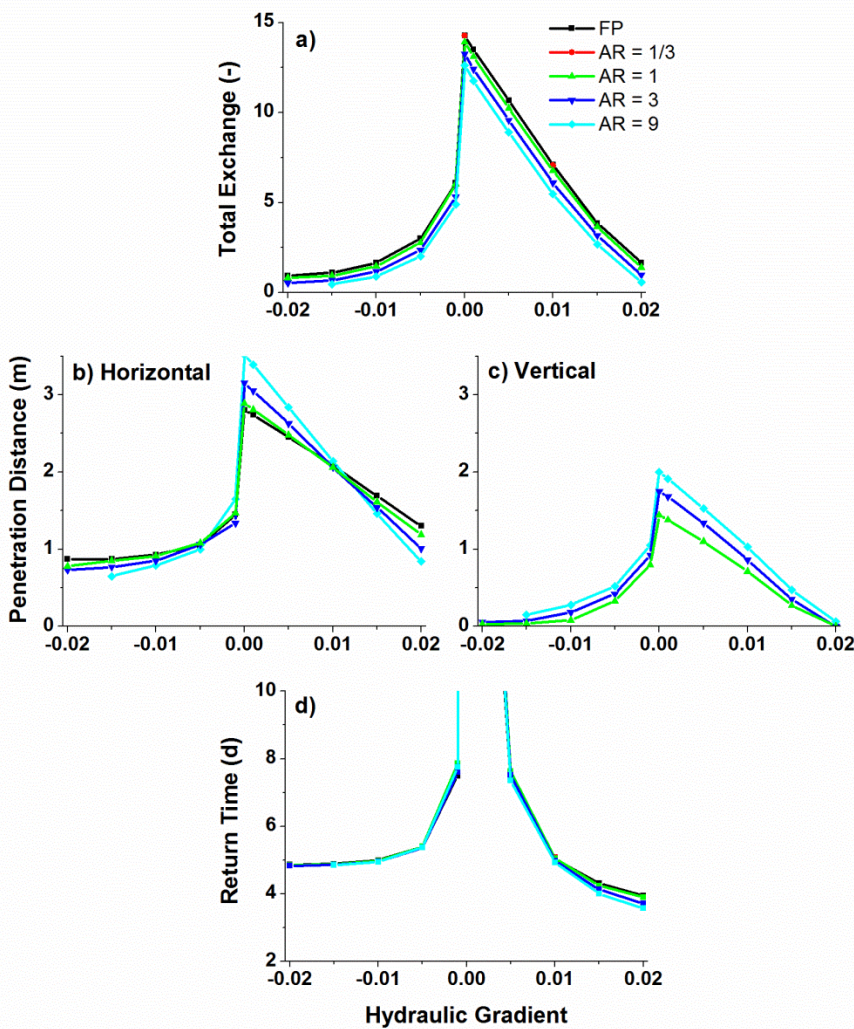


Figure 4-8 Dependency of a) total exchange per unit width of aquifer, b) horizontal penetration distance, c) vertical penetration distance, and d) return time on variation in hydraulic gradient and partial penetration. The wetted perimeter is constant at 20m and the aspect ratio (river bed half width : river bank height, AR) varied from 1/3 to 9. Only aspect ratios >1 are plotted for distance and return time. There is no vertical component of exchange for the fully penetrating (FP) case.

4.3.3.2 Penetration Distance

At hydraulic gradients between -0.005 and +0.01, the maximum horizontal penetration distance increases as the aspect ratio increases once the aspect ratio is greater than unity (Figure 4-8b). With no hydraulic gradient the distance increases from 2.8 m to 3.2m for aspect ratios between 3 and 9 (Figure 4-8b, Figure 4-9). At higher gradients the horizontal distance of penetration is lower for models with higher aspect ratios. The difference in penetration distance between partially and fully penetrating models is at most ± 0.7 m for the parameters simulated (25-50%).

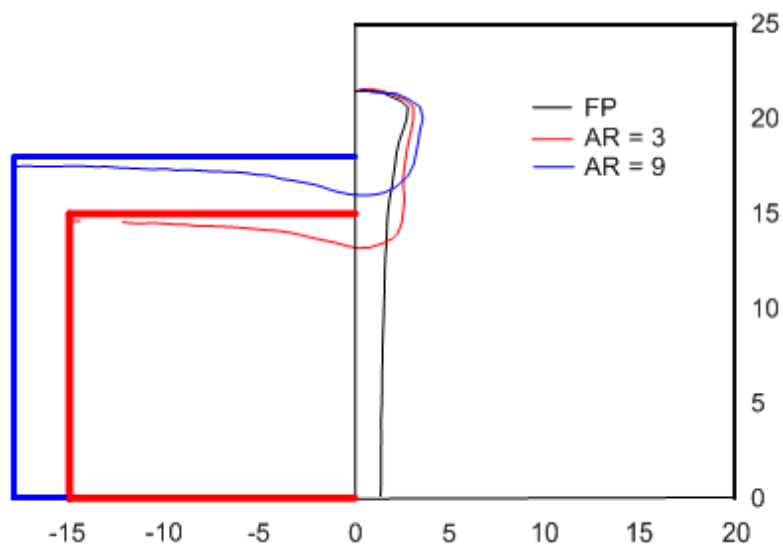


Figure 4-9 Close up of the spatial variation in penetration distance of the 0.5 concentration contour for a fully penetrating river (FP, black line), aspect ratio (AR) of 3 (red line) and 9 (blue line) with no hydraulic gradient present. Thick red and blue lines indicate the extension of the model domain for partially penetrating models. Distances are in metres.

In all cases simulated, the maximum vertical penetration distance occurs below the river bank / bed corner. It is larger for larger aspect ratios, but reduces as the absolute magnitude of the hydraulic gradient increases so that at $HG = \pm 0.02$ water penetrates less than 0.05 m below the river bed (Figure 4-8c). The penetration distance below the river bed of partially penetrating rivers is consistently lower than the penetration distance adjacent to the corresponding section of a fully penetrating river bank (Figure 4-9). The minimum vertical penetration distance is located beneath the centre of the river.

4.3.3.3 Return Time

When no hydraulic gradient is present, return times increase as the aspect ratio increases

(Figure 4-8, Figure 4-6). However, when a hydraulic gradient is present the influence of partial penetration on return time (median and distribution) is extremely minor, and essentially non-existent beyond a gradient of 0.001 (at least up to aspect ratio of 9, Figure 4-8d, 6). Even at lower gradients there is no difference in the first 10% of return.

Differences between partially penetrating cases and the fully penetrating case are insignificant compared to the differences imposed by hydraulic gradients.

4.4 Discussion

The presence of a hydraulic gradient between river and aquifer reduces total water exchange and penetration distance during bank storage, and reduces the return time of river water from an aquifer. Analytical estimates of bank storage exchange and return time as a function of parameter and hydraulic gradient variation compare favourably with trends predicted by numerical simulations of a variably saturated aquifer, except where there is an extremely rapid river stage rise. Changes in metrics as a function of hydraulic gradient equal, and in some cases exceed, changes induced by the range of other parameters tested.

The presence of a positive hydraulic gradient creates a hydraulic boundary to flow within an aquifer, and hence, similar to aquifers of limited lateral extent, return times reduce as the hydraulic gradient increases (Cooper and Rorabaugh, 1963). Hence, in addition to large river stage, high hydraulic conductivity and storage identified by Kondolf et al. (1987), a low hydraulic gradient is also necessary for river stage change to lead to substantial bank storage exchange. In typical alluvial environments with hydraulic conductivities up to 100 m d^{-1} , wave heights less than 5 m, wave periods less than 5 d and hydraulic gradients less than 0.01, penetration distances will commonly be less than 20 m, and return times less than 15 days.

Partial penetration and bank slope have been identified as potentially significant limitations to the use of analytical solutions for estimating bank storage exchange (Chen and Chen,

2003; Doble et al., 2012; Sharp Jr, 1977). In the case of partial penetration the magnitude of the discrepancy has not previously been systematically quantified. Compared to the changes in bank storage metrics as a function of other parameters, our work indicates that the aspect ratio of a river (degree of aquifer penetration) has a minor influence on total exchange (when compared to a fully penetrating river with equivalent wetted perimeter). This is predominantly a function of the redistribution of exchange from the river bed to the river bank. Hence, analytical solutions can provide a useful estimate of exchange in partially penetrating systems as long as the entire wetted perimeter is considered, not only the bank section. The influence of bank slope has not been considered in this work. In the absence of a hydraulic gradient, Doble et al. (2012) demonstrated that with a bank slope of 3.4° from the horizontal the volume of bank storage increased by 40%, and with a bank slope of 8.5° return times increased fourfold. The combined influence of bank slope and hydraulic gradient on bank storage exchange volume and return time will be complex due to competing alterations to the flow field and requires further assessment.

Although the three metrics applied are useful for the assessment of hypothetical environments, in practice exchange, penetration distance and return time are difficult to measure directly. Solute change over time at an observation point within an aquifer can provide a useful proxy for bank storage return time. Provided that river water of a different concentration to ambient groundwater reaches an observation point, the rate of concentration change is related to the hydraulic gradient. For positive gradients (gaining rivers) the rate of recovery back to the pre-event concentration at the observation point also increases as the hydraulic gradient increases. Although this method does not enable a direct estimation of return time, such time series data is readily attainable and therefore provides a simple method for inferring relative return times for flow events that occur when different hydraulic gradients are present. Welch et al. (2014) presented such data for a flow event in 2012 with a hydraulic gradient of 0.05 (Figure 4-10a). Return to the pre-event concentration in the monitoring well took 7 d. Monitoring in 2013 (Welch,

unpublished) identified that the hydraulic gradient had reduced to 0.02, and the recovery time after a large flow event increased to 20 d (Figure 4-10b). Analytical assessment using site characteristics suggests that 40% of the increase in return time may be attributed to changes in wave characteristics, and the remainder the reduction in hydraulic gradient.

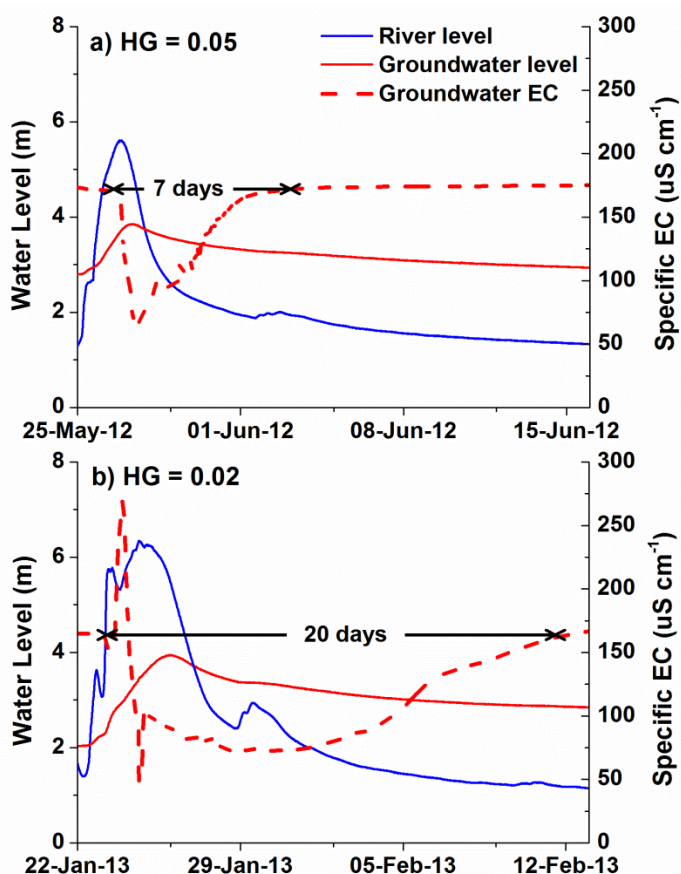


Figure 4-10 Comparison of river flow events in a) 2012 and b) 2013 and the groundwater level (solid red line) and specific electrical conductivity (EC, dashed red line) at a field site adjacent to the Mitchell River in tropical north Queensland, Australia. The monitoring bore is 30 m from the river bank. In 2012 there was a hydraulic gradient (HG) of 0.05 towards the river; in 2013 the gradient had reduced to 0.02.

Practical measurement of bank storage metrics directly is further complicated by the nested processes that occur at the river – aquifer interface. In order to isolate exchange due to bank storage, it is necessary to distinguish between this exchange, hyporheic exchange that occurs during steady state flow, and regional groundwater discharge. Combination of hydraulic measurements with noble gases, isotopes of water and water

chemistry can provide first-order estimates of relative contributions to discharge (Cook et al., 2006; Gardner et al., 2011). Penetration distance may be estimated using time series measurements of concentration change (Welch et al., 2013), but can only be measured directly by a fine network of piezometers. In addition to the method described above, return time can be inferred from time series measurement of tracers of aquifer residence time, particularly if the observation point is located adjacent to the river bank. However, all these methods are point measurements in space or time and hence struggle to reflect heterogeneity inherent in alluvial systems. Repeating geophysical imaging of the near-river aquifer throughout a flow event provides one avenue for partially overcoming these limitations (Cardenas and Markowski, 2010; Ward et al., 2010). Further development of analysis techniques is required to convert geophysical images to quantitative estimates of exchange flux. Alternatively, an integrated catchment return time can be inferred from chemistry measurements of river water, if exchange with groundwater is the dominant process affecting the river chemistry.

Finally, the analysis presented in this paper assumed that the hydraulic gradient is independent of hydraulic conductivity. This may have exaggerated the relative influence of hydraulic conductivity and gradient on the bank storage metrics, since usually hydraulic gradients are large when hydraulic conductivity is low. Also, our analysis has only considered single flow events. In many systems multiple events may occur before bank storage has returned to the river. This complicates both measurement techniques and assessment metrics, and has been shown to increase the distance of penetration of river water into an aquifer (McCallum et al., 2010). Preferential flow paths due to aquifer heterogeneity have also not been considered. Welch et al. (2014) clearly identified heterogeneity as controlling the relative rates of solute and pressure propagation, and aquifer responses clearly indicate travel of river water into the aquifer further into the aquifer than homogeneous simulations suggest.

4.5 Conclusions

When hydraulic gradients are present in alluvial environments our results indicate that the process of bank storage will generally cause river water to move on the scale of metres into an adjacent aquifer, for periods of days to weeks. Under the conditions tested total exchange may be estimated with less than 50% error using existing analytical solutions, provided that unsaturated zone processes do not have a pronounced influence on exchange, and that the entire wetted perimeter is considered. The influence of partial river penetration on total exchange and return time is small in comparison to other parameters as it simply causes redistribution of exchange from the river bed to the river bank. The penetration distance of river water into an aquifer is greatest near the water table, and increasingly so with increasing hydraulic gradient. Knowledge or manipulation of the hydraulic gradient close to the river / aquifer interface is essential to effective restoration of riparian corridors or contaminant mixing or natural attenuation driven by river stage change.

Acknowledgements

The authors thank Marc Leblanc for coordinating the field component of this research, Jordi Batlle Aguilar, Nick Rockett, Tony Forsyth and Joel Bailey for assistance in the field, and the Australian Wildlife Conservancy – Brooklyn for site access and general assistance during field work.

5 Conclusions, Research Contribution and Future Work

Previous studies of bank storage have predominantly relied on hydraulic assessment techniques as pressure data is readily available, analytical relationships directly relate pressure propagation to aquifer properties, and numerical assessment is relatively straightforward. Through systematic assessment of the movement of pressure and solutes during bank storage, this work has increased understanding of the process of bank storage. It has also developed new tools for the assessment of river – aquifer exchange during flood events that use a combination of time series measurement of pressure and solutes within aquifers.

Analytical and numerical techniques have established that new relationships between aquifer and flood wave characteristics and water/solute travel times and distances in response to flood events may be used with reasonable confidence in variably saturated aquifers. Furthermore, as the ratio of solute travel time to pressure travel time is independent of hydraulic conductivity, it provides a new method by which aquifer properties may be estimated from time series solute data under specific hydrogeological settings. Given that it is based on an assumption of homogeneity, results may be best viewed as first-order estimates, but in any case, provide valuable insights to the controls of individual aquifer and flood wave characteristics on solute propagation.

In practice, alluvial environments are rarely homogenous. Numerical investigation of conceptual models of two common alluvial structures, clogging layers and sand strings, identified that pressure and solute propagation are unequally affected by heterogeneity. In homogeneous systems the rate of pressure propagation always exceeds the rate of solute propagation from a river into an aquifer. Hence, substantial change in pressure within an aquifer following a flow event always precedes substantial change in solute concentration. However, in heterogeneous systems, the rate of solute propagation can exceed the rate of pressure propagation. As a consequence, substantial change in solute concentration may

be measured prior to substantial change in pressure at an observation point within an aquifer. The controlling presence of heterogeneous structures may therefore be identified by a ratio of solute to pressure travel time less than unity. Flux estimates derived from solute travel times and the new analytical relationship were demonstrated to be more accurate than those derived from pressure responses in heterogeneous environments. The magnitude of the error contained in estimates derived from pressure responses is proportional to the hydraulic conductivity contrast between the clogging layer or sand string and remainder of the aquifer. Combining solute and pressure time series measurements substantially strengthens any assessment of river – aquifer exchange in response to river flow events.

One of the most variable parameters between rivers and groundwater prior to flood events is the hydraulic gradient. Application of the principle of superposition to an existing analytical solution for bank storage identified that variability in hydraulic gradient is at least as influential on bank storage exchange and return time as anticipated variability in aquifer and wave characteristics. The relationships were generally reproduced in numerical simulations of a variably saturated model. Numerical simulations further identified that exchange is greatest in the section of the river bank closest to the interface with the unsaturated zone, and that this increases with increasing hydraulic gradient, reducing hydraulic conductivity, and increasing aspect ratio of partially penetrating rivers. Due to the redistribution of exchange from the river bed to the river bank, the overall amount of exchange is similar to a fully penetrating river with equivalent wetted perimeter, and hence, analytical solutions can still provide reasonable estimates of bank storage in partially penetrating rivers, so long as the river bank and river bed length are considered. The presence of a hydraulic gradient is a key control that must be considered in any estimate of bank storage exchange.

Heterogeneity of aquifer characteristics requires further consideration. The binary heterogeneity fields investigated had distinct influences on pressure and solute propagation during bank storage. Such simple heterogeneity fields may not always appropriately represent an environment at the scale of interest. The influence of more complex heterogeneity may in the first instance best be investigated numerically using geostatistical methods, sensitivity and uncertainty analysis. However, field techniques that can directly consider travel times and sophisticated visualisations of the subsurface are equally warranted.

Field application of the theoretical developments has been limited to a common proxy for solute, electrical conductivity. This simple tracer will not be appropriate in all environments, and does not enable a definite correlation between a particular river flow event and groundwater chemistry change to be made. Future investigations that combine tracers that can unequivocally represent river water and physical measurements of flow direction would enable more robust quantification of relationships between solute and pressure travel times, flow paths, and distances in a wider variety of hydrogeological settings. Appropriate tracers must have distinct concentrations in river water and the adjacent aquifer, be able to be measured at an appropriate temporal resolution, and ideally, indicate the residence time of water in the aquifer. Further development of geophysical imaging techniques such that they can be converted to quantitative estimates would also assist explicit consideration of field-scale heterogeneity.

Appendix A Theoretical development of solute travel time

A one dimensional analytical solution to equation (2.1), subject to initial conditions $h = h_0$ at $x \geq 0, t = 0$ and the boundary condition $h = h_0 + H$ at $x = 0, t = 0$, is given by (Carslaw and Jaeger, 1959)

$$h = h_0 + H \cdot erfc\left(\frac{x}{\sqrt{4Dt}}\right), \quad (A1)$$

where D is aquifer diffusivity. At this stage x and t are independent.

The water particle (or solute) travel velocity v_s is defined by Darcy's Law:

$$v_s = \frac{dx}{dt} = -\frac{K}{\theta} \frac{\partial h}{\partial x}, \quad (A2)$$

where θ is aquifer porosity, diffusion and dispersion are neglected, and there is assumed to be no lag time. Forming the partial x derivative of h from equation (A1), then

$$\frac{dx}{dt_s} = c \sqrt{\frac{D}{\pi t}} e^{-\frac{x^2}{4Dt}}, \quad \text{where } c = \frac{KH}{D\theta}, \quad (A3)$$

and x and t are no longer independent. Subsequently, the subscript s is added to either x or t to indicate their dependence. A solution for x as a function of t that is non-linear in x and t was developed numerically using the robust procedure LSODA of the numerical package ODEPACK, as solution was otherwise analytically intractable without variable transformation. It was found that a plot of x against \sqrt{Dt} produced a straight line passing through the origin $x = 0, Dt = 0$. In terms of aquifer parameters, the distance-time relationship obtained is

$$x = a\sqrt{Dt}, \quad (A4)$$

where a is a constant determined by the gradient of the straight line.

By rearrangement, the solute (water particle) travel time obtained is

$$t = \frac{x^2}{a^2 D} . \quad (\text{A5})$$

Hence, equation (A3) becomes

$$\frac{dx}{dt_s} = \frac{a}{2} \sqrt{\frac{D}{t}} = c \sqrt{\frac{D}{\pi t}} e^{-\frac{a^2}{4}} , \quad (\text{A6})$$

that is,

$$a = \frac{2}{\sqrt{\pi}} c e^{-\frac{a^2}{4}} , \quad (\text{A7})$$

so that for $a^2/4 \ll 1$, then $a \rightarrow 2c/\sqrt{\pi}$, provided that $c \ll \sqrt{\pi}$. Equation (A7) provides an alternative way of finding a from the numerically determined line gradient. By defining a new constant w within

$$a = \frac{2}{\sqrt{\pi}} w c \quad (\text{A8})$$

a transcendental equation for finding w is then

$$w = e^{-\frac{w^2 c^2}{\pi}} . \quad (\text{A9})$$

This was solved using the Muller (1956) – Frank (1958) method, which does not require function derivatives as in the Newton-Raphson method, both methods converging rapidly near the ultimate value of w . A plot of a against c is given on Figure 2-1. Comparison of a values from a selection of c values determined by the numerical line gradient and the transcendental equation solution method provided perfect agreement within tolerable numerical round-off errors, that is, $\approx 10^{-6}$.

With $D = Kb/S$, the expression for c of equation (A3) becomes

$$c = \frac{HS}{b\theta} , \quad (\text{A10})$$

and finally, from equation (A5) the travel time of a solute (water), $t = t_s$, as a function of x :

$$t_s = \frac{x^2 S}{a^2 Kb} . \quad (\text{A11})$$

Appendix B Analytical solutions for pressure propagation through a clogging layer

The most common analytical solution for pressure propagation applied to surface water – groundwater problems (Hall and Moench, 1972) uses the retardation coefficient of Hantush (1965) which describes the retardation of flow or head propagation by the clogging layer in terms of clogging layer thickness and clogging layer and aquifer hydraulic conductivities.

This solution assumes that the flux across the boundary is proportional to the head difference between the boundary and the surrounding medium (Carslaw and Jaeger, 1959).

The physical dimensions and properties of the clogging layer are not represented.

Modification of a solution for heat propagation into a semi-infinite composite solid (Carslaw and Jaeger, 1959) allows explicit consideration of the influence of the physical properties of the clogging layer, including storage (S), on pressure propagation. In response to an instantaneous increase in river stage, head change h at a distance of x m from the river bank with a hydraulic conductivity boundary at $x = L_1$ is given by

$$h(x,t) = \begin{cases} h_0 + H \sum_{n=0}^{\infty} \alpha^n \left\{ \operatorname{erfc} \frac{(2n+1)L_1 + (x - L_1)}{\sqrt{4D_1 t}} - \alpha \cdot \operatorname{erfc} \frac{(2n+1)L_1 - (x - L_1)}{\sqrt{4D_1 t}} \right\}, & 0 < x < L_1 \\ h_0 + \frac{2H}{1+\sigma} \sum_{n=0}^{\infty} \alpha^n \operatorname{erfc} \frac{(2n+1)L_1 + k(x - L_1)}{\sqrt{4D_1 t}}, & x > L_1 \end{cases} \quad (\text{B1})$$

where

$$k = \sqrt{\frac{D_1}{D_2}}, \quad \sigma = \frac{K_2 k}{K_1}, \quad \alpha = \frac{\sigma - 1}{\sigma + 1},$$

and D is hydraulic diffusivity ($= Kb/S$). Solution in the region $x > L_1$ (i.e., not in the clogging layer) provides results essentially equivalent to results from the expression presented by Hall and Moench (1972) with the retardation coefficient defined as per Hantush (1965).

Appendix C Synoptic sampling results from the Cockburn River

Synoptic river sampling was conducted along the Cockburn River and its tributaries to assess, in general, the spatial variation in losing and gaining reaches. The Cockburn River is formed at the junction of Swamp Oak and Jamiesons Creek. Flow gauging was conducted using a portable electromagnetic flow meter. Additional readings were obtained from the permanent gauging stations operated by the NSW Office of Water (NOW). Flow and chemistry results are only presented for the dates and times collected and analysed. Times are in Australian Eastern Standard Time.

Table C-1 Sampling locations along the Cockburn River and tributaries. “SO” indicates Swamp Oak Creek, “C” indicates the main branch of the Cockburn River, “J” indicates Jamiesons Creek and “MM” indicates Mulla Mulla Creek, and “GS” indicates a permanent gauging station.

Location	Easting	Northing	River distance (m)
River			
SO1	331629	6561391	0
SO1A	328945	6563043	7190
SO2	327947	6563297	9480
SO3	325391	6564817	14240
SO GS	325401.7	6564748.7	14260
COA	3243601	6564628	16430
COB	323590	6563538	18170
COC	322805	6563190	19670
COD	322313	6562194	21100
COE	322173	6562053	21290
COF	321944	6561976	21525
C1	321277	6562153	22350
MullaXing GS	321245.4	6562261.5	22410
C1A	319749	6562569	25400
C1B	319593	6563704	26650
C2	318550	6563513	27830
C2A	318458	6563113	28228
C3	317002	6563329	30050
C3A	316693	6563311	30378
C4	314815	6561651	33880
C4A	314650	6561721	34064
Kootingal Bridge GS	314470.4	6561726.8	34240
C4B	314424	6561785	34305
C5	313229	6560486	36190
C5A	312829	6560317	36693
C6	310612	6558076	41420
C7	308593	6555001	46820
Tributaries			
J1	324455	6565738	15720
MM2	322104	6561989	21400
MM1A	322536	6560541	2230M
MM1	323332	6656611	7820M

Radon samples were collected using the PET method described by Leaney and Herczeg (2006). EC results were obtained using a handheld EC meter calibrated prior to use. Radon analyses were conducted at the CSIRO Land and Water analytical laboratory in Adelaide using a Qantulus liquid scintillation counter.

Table C-2 Sampling results October 2010.

Location	Date	Time	Flow (ML/d)	EC (µS/cm)	Rn (Bq/L)	Date	Time	Flow (ML/d)	EC (µS/cm)	Rn (Bq/L)
SO1	26/10/10	8:20	219.8	182.6	0.13	27/10/10				
SO2	26/10/10	9:15	256.2	232.6	0.22	27/10/10				
SO3	26/10/10	10:05	256.9	247.5	0.18	27/10/10				
SO GS	26/10/10	10:00	299.178	240		27/10/10	10:00	148.003	238	
C1	26/10/10	13:05	476.0	243.5	0.16	27/10/10				
MullaXing GS	26/10/10	13:00	505.526	241.97		27/10/10	10:00	303.698	224.738	
C2						27/10/10	10:40	305.7	234.5	0.38
C3	26/10/10	16:50	485.5	257	0.5	27/10/10				
C4						27/10/10	13:40	221.7	244	1.87
KB GS	26/10/10	17:00	354.002	250.633		27/10/10	13:00	234.486	234.117	
J1	26/10/10	11:10	34.9	330	1.14	27/10/10				
MM2	26/10/10	15:50	131.2	195	0.1	27/10/10				
MM1	26/10/10	14:30	148.2	175.8	0.12	27/10/10	7:50	92.6	170	0.12

Table C-3 Sampling results January and April 2011

Location	Date	Time	Flow (ML/d)	EC (µS/cm)	Rn (Bq/L)	Date	Time	Flow (ML/d)	EC (µS/cm)	Rn (Bq/L)
SO1	13/01/11	9:15	59.3	332	0.23					
SO1A	13/01/11	9:50		347	0.35					
SO2	13/01/11	10:05	68.6	343	0.31	13/04/11	8:00	7.2	541	0.6
SO3	13/01/11	10:45	63.2	343	0.23	13/04/11	8:35	4.3	501	0.61
SO GS	13/01/11	11:00	76.4	343		13/04/11	9:00	6.5		
COA	13/01/11	12:20		334	0.27	13/04/11	9:35		493	0.4
COB	13/01/11	14:00	110.4	337	0.29	13/04/11	9:45	4.8	500	1.04
COC	13/01/11	14:00		341	0.27	13/04/11	10:15		498	0.56
COD	13/01/11	14:10		341	0.22					
COE						13/04/11	10:35		495	
COF						13/04/11	11:20		282	
C1	13/01/11	15:45	179.4	305	0.17	13/04/11	11:30	42.7	282	0.24
MullaXing GS	13/01/11	16:00	172.9	314.261		13/04/11	12:00	44.8	274	
C1A	13/01/11	16:40		304	0.28	13/04/11	13:50		288	0.5
C1B						13/04/11	14:40		304	0.63
C2	13/01/11	16:30	185.6	305	0.45	13/04/11	13:45	35.9	322	0.57
C3	13/01/11	18:20		304	1.25	13/04/11	14:50		337	2.79
C4	13/01/11	18:50	192.1	308	2.78	13/04/11	15:10	33.3	369	4.47
KB GS	13/01/11	18:00	177.4	317.233		13/04/11	15:30	37.6	355	
C5						13/04/11	16:00	32.1	415	4.26
C6						13/04/11	16:55		479	2.48
C7						13/04/11	17:20	17.3	499	3.91
J1	13/01/11	11:50	40.3	318	1.11	13/04/11	9:05	0.3	552	19.69
MM2	13/01/11	15:00	66.2	249	0.15	13/04/11	10:30	36.5	254	0.16
MM1A						13/04/11	12:55		244	0.14
MM1	13/01/11	17:40	63.0	224	0.15	13/04/11	12:15	38.8	219	0.19

Table C-4 Sampling results April 2012

Location	Date	Time	Flow (ML/d)	EC (µS/cm)	Rn (Bq/L)
C1	25/04/2012	8:50	62.1	448	0.25
MullaXing GS	25/04/2012	9:00	62.1	441	
C1A	25/04/2012	10:00		452	1.85
C1B	25/04/2012	10:20		459	0.52
C2	25/04/2012	10:50	74.2	458	0.74
C2A	25/04/2012	11:10		454	0.75
C3	25/04/2012	12:10	52.8	445	1.96
C3A	25/04/2012	12:33		447	3.36
C4	25/04/2012	14:15	69.6	432	4.42
C4A	25/04/2012	14:40		433	3.64
KB GS	25/04/2012	15:00	99.6	428	
C4B	25/04/2012	15:20		450	4.68
C5	25/04/2012	16:15	58.9	438	2.59
C5A	25/04/2012	16:30		438	2.58
C7	25/04/2012	17:05	69.7	465	1.32

Table C-5 Additional chemistry results 13 April 2011: major ions

Location	Time	pH	EC dS/m	Total Alkalinity meq/L	Cl⁻ mg/L	SO₄⁼ mg/L	Ca mg/L	K mg/L	Mg mg/L	Na mg/L
SO2	8:30	8.1	0.54	3.0	17	79	41	2.35	23.4	35.9
C1	12:20	8.1	0.29	1.9	7.7	23	21.2	2.33	14.5	16.1
C2	14:40	8.2	0.33	2.1	8.9	28	23.6	2.35	15.5	19.2
C6	17:25	7.9	0.48	2.9	25	38	33.6	1.94	22.4	32.5
J1	9:45	7.9	0.55	3.8	19	37	42	2.07	23.1	41.9
MM1	12:50	8.0	0.23	1.5	6.1	16	15.4	2.28	11.4	11.5
MM2	11:30	7.9	0.26	1.7	6.8	20	18.1	2.34	13.2	13.6

Ion samples were filtered through a 45µm filter in the field. Cation samples were acidified in the field with nitric acid.

Table C-6 Additional chemistry results 13 April 2011: minor ions and metals

Location	Time	F⁻ mg/L	Br⁻ mg/L	NO₃⁻ mg/L	S⁻ mg/L	Mn mg/L	Si mg/L	Sr mg/L
SO2	8:30	0.10	0.06	<0.05	25.3	<0.05	4.67	0.385
C1	12:20	0.06	<0.05	<0.05	7.54	<0.05	2.69	0.165
C2	14:40	0.07	<0.05	<0.05	9.13	<0.05	3.25	0.188
C6	17:25	0.12	0.10	1.5	12.2	<0.05	7.29	0.291
J1	9:45	0.20	0.14	<0.05	11.7	0.0655	10.4	0.324
MM1	12:50	0.05	<0.05	<0.05	5.04	<0.05	2.43	0.116

As, Al, Cd, Co, Cr, Cu, Mo, Ni, Pb, Se, and Zn were below the detection limit of 0.05 mg L⁻¹. B, Fe, P, and Sb were below the detection limit of 0.1 mg L⁻¹.

Appendix D Time series data from the Cockburn and Mitchell Rivers

This data is contained on a CD. Pressure, temperature, and specific electrical conductivity were obtained using *In Situ* Aquatrolls.

Table D-1 Cockburn River monitoring locations

Location	Type	Easting	Northing	Installation date
Groundwater				
93039*	Observation well	314500.35	6561765.38	25/10/2010
273218-1	Observation well	314502.29	6561762.35	12/08/2011
273218-2	Observation well	314509.04	6561745.87	12/08/2011
273218-3	Observation well	314507.66	6561744.62	12/08/2011
273033	Observation well	307977.98	6554247.9	27/04/2012
93038	Observation well	314529.19	6561618.47	25/10/2010
Cosmic	Observation well	314761	6561767	25/10/2010
273219-1	Observation well	317032.20	6563365.86	12/08/2011
273219-2	Observation well	317014.54	6563383.43	12/08/2011
273034*	Observation well	317020.70	6563350.77	25/10/2010
93030	Observation well	308508	6554677	14/04/2011
93559	Observation well	318548.20	6563460.94	14/01/2011
BL2	Drivepoint	318508.09	6563479.31	12/01/2011
BL3	Drivepoint	318514.56	6563468.29	12/01/2011
River				
SO3*	Stilling well	325391	6564827	26/10/2010
MM1	Stilling well	323337	6556623	27/10/2010
MM1	Stilling well	323326	6557216	11/08/2011
J1	Stilling well	324455	6565738	13/04/2011
C3	Stilling well	317072.57	6563342.80	12/08/2011
C2	Stilling well	318450.46	6563468.85	27/10/2010

*Barometric loggers for pressure compensation were installed at these locations

Table D-2 Mitchell River monitoring locations

Location	Type	Easting	Northing	Installation date
Groundwater				
1A	Observation well	304449.3	8164939	27/02/2011
1B	Observation well	304452.4	8164937	26/02/2011
1C*	Observation well	304451	8164938	27/02/2011
1D	Observation well	304450.2	8164939	12/12/2012
1E	Observation well	304450.4	8164939	12/12/2012
2A	Observation well	304567	8165072	28/02/2011
2B	Observation well	304567	8165072	28/02/2011
2C	Observation well	304567	8165072	27/02/2011
3A	Observation well	304776	8165282	28/02/2011
3B	Observation well	304776	8165282	26/02/2011
4*	Observation well	305158	8165601	26/02/2011
ST1A	Observation well	304433.2	8164935	12/12/2012
ST1B	Observation well	304430	8164937	22/07/2011
ST1C	Observation well	304431.6	8164936	12/12/2012

Location	Type	Easting	Northing	Installation date
<i>Groundwater</i>				
ST2	Observation well	304436	8164946	22/07/2011
ST3	Observation well	304465	8164952	22/07/2011
ST4	Observation well	304492	8164968	22/07/2011
ST5	Observation well	304421.5	8164927	12/12/2012
ST6A	Observation well	304424.6	8164931	12/12/2012
ST6B	Observation well	304424.8	8164930	12/12/2012
<i>River</i>				
BROOKLYN	Stilling well	304414	8164927	26/02/2011
MARYCK	Stilling well	306552	8166815	28/02/2011
MITCHELLDS	Stilling well	303474	8165318	28/02/2011
MITCHELLUS	Stilling well	305205	8163705	28/02/2011

*Barometric loggers for pressure compensation were installed at these locations

Appendix E Groundwater chemistry and isotope results

E1 Cockburn River

One-off sampling and chemical analysis of select piezometers in the Cockburn River catchment was conducted in April 2011.

Table E-1 Cockburn River groundwater chemistry and isotope results

Location	Date	Time	pH	EC dS/m	Total Alkalinity meq/L	Cl ⁻ mg/L	SO ₄ ⁼ mg/L	Ca mg/L	K mg/L	Mg mg/L	Na mg/L
93030	12/04/11	18:15	7.5	1.01	6.0	86	79	84.3	1.11	45.2	73.6
93038	12/04/11	12:10	7.2	0.45	3.0	14	31	28.2	2.54	19.2	34.6
93039	12/04/11	12:55	6.9	0.69	4.0	130	41	45.1	2.49	28.4	59.2
93559	14/04/11	16:45	7.4	1.31	7.0	120	170	106	2.94	61.4	108
273033	12/04/11	9:45	7.2	0.70	4.6	41	33	58.6	0.732	37.5	53.2
273034	12/04/11	15:50	7.3	0.79	4.1	77	24	44.7	2.83	29.2	78.8
BL 1	12/04/11	16:50	7.8	0.35	2.3	10	29	26.5	2.15	16.2	20.4
BL 2	12/04/11	17:15	8.0	0.35	2.3	9.8	28	26	2.1	16	20.5
Cosmic	12/04/11	14:50	7.2	0.59	3.2	23	79	39.6	1.42	25.8	48.7
UBL	14/04/11	10:30	7.6	0.33	2.1	8.8	25	22.4	2.36	11.5	17.3

Location	F ⁻ mg/L	Br ⁻ mg/L	NO ₃ ⁻ mg/L	S mg/L	Al mg/L	Fe mg/L	Mn mg/L	P mg/L	Si mg/L	Sr mg/L	Zn mg/L	²²² Rn Bq/L	Error Bq/L
93030	0.11	0.29	13	26.1	<0.05	<0.1	<0.05	<0.1	12.2	0.744	<0.05	39.1	0.9
93038	0.73	0.06	0.10	9.93	<0.05	<0.1	0.275	<0.1	19.8	0.237	<0.05	83	1.5
93039	0.46	0.18	30	13	<0.05	<0.1	0.0556	0.342	24.4	0.431	0.127	72.2	1.4
93559	0.28	0.46	27	55.5	<0.05	<0.1	1.81	<0.1	15.5	1.04	<0.05	39.2	1.4
273033	0.10	0.14	28	16.4	<0.05	<0.1	<0.05	0.102	12.7	0.625	<0.05	18.8	0.5
273034	0.51	0.32	50	7.18	<0.05	<0.1	<0.05	0.324	21.4	0.468	<0.05	245.4	3.7
BL 1	0.10	<0.05	0.50	8.88	<0.05	<0.1	<0.05	<0.1	4.39	0.214	<0.05	3.3	0.2
BL 2	0.10	<0.05	0.93	9.05	<0.05	<0.1	<0.05	<0.1	4.5	0.21	<0.05	3.6	0.2
Cosmic	0.08	0.11	11	25.7	<0.05	<0.1	<0.05	<0.1	8.63	0.339	<0.05	31.1	0.8

As, Cd, Co, Cr, Cu, Mo, Ni, Pb, and Se were below the detection limit of 0.05 mg L⁻¹. B and Sb were below the detection limit of 0.1 mg L⁻¹.

E2 Mitchell River

Sampling of the piezometer transect installed adjacent to the Mitchell River was conducted in February/March 2011 (wet season) and October 2011 (dry season) to assess seasonal effects of bank storage on aquifer chemistry. All analyses were conducted at the CSIRO Land and Water laboratory in Adelaide, except strontium, which was analysed at the University of Adelaide.

Table E-2 Mitchell River groundwater chemistry and isotope results

Location	Date	pH	EC μS/m	Temp °C	DO mg/L	CO ₂ mg/L	HCO ₃ mg/L	¹⁸ O	² H	¹³ C	CFC11 pptv	CFC12 pptv	SF ₆ Year
1C	27/02/11	6.19	135.4	26.4	3	78.0	68.2	-8.62	-56.79	-9.7	<25	107	2006
1B	26/02/11	6.3	148.2	26.4	3.5	84.0	67.0	-8.69	-56.98	-7.0	32	325	2006
2C	27/02/11	6.7	21120	27	5	544.0	1522.5	-5.87	-39.94	-12.5	<25	87	1992
2B	1/03/11	6.63	21690	27.2		544.0	1534.6	-6.13	-43.31	-12.0	<25	111	1986
3B	1/03/11	6.48	1419	27.9		344.0	682.1	-7.22	-50.21	-13.0			1995
3A	26/02/11	6.3	18080	27	1.2	316.0	584.6	-6.67	-47.13	-12.2	30	54	1990
4	26/02/11	7.2	176	25.7	4	74.0	82.8	-8.13	-50.97	-8.6	212	587	2008
Brooklyn	26/02/11	6.76	36.3	22.7		15.3	108.4	-6.74	-40.55	-14.7	280	532	2003

CFC results are presented as equivalent atmospheric concentration. Recharge years for SF₆ results were determined using the piston flow model. Sampling for these analyses was not conducted in the dry season.

Location	Date	pH	EC dS/m	Total Alkalinity meq/L	Cl ⁻ mg/L	SO ₄ ⁼ mg/L	Ca mg/L	K mg/L	Mg mg/L	Na mg/L	²²² Rn Bq/L	Error Bq/L	^{87/86} Sr
1C	27/02/11	7.86	0.15	0.9	9.9	2.9	1.22	0.794	1.21	22.5	30.9	0.9	.729950
1B	26/02/11	7.91	0.15	0.9	9.9	2.6	1.08	0.731	1.28	23.1	34.9	1	.728745
2C	27/02/11	7.94	19.9	17.8	6600	220	65.7	3.26	191	3680	190.5	3	.727321
2B	1/03/11	7.73	20.0	15.7	6900	220	122	5.89	275	3640	187.3	3	.726742
3B	1/03/11	8.16	15.1	7.1	5300	62	74.5	8.18	176	2610	98.2	1.8	.728653
3A	26/02/11	8.08	16.6	6.9	6100	70	92.8	11.7	224	2830	131.7	2.4	.727868
4	26/02/11	8.10	0.17	1.1	7.4	2.5	2.96	1.19	2.24	21.8	33.5	0.9	.729270
Brooklyn	26/02/11	7.26	0.07	0.2	6.9	0.68	<0.1	<0.1	<0.1	<0.1	0.77	0.05	0.7268
1C	12/10/11	6.60	0.16	1.1	8.6	1.7	3.19	1.46	2.61	23	30.2	0.9	.729990
1B	14/10/11	6.53	0.18	1.3	9.5	1.5	3.42	1.16	2.57	27.7	29.5	1	.729611
1A	12/10/11	7.19	0.41	1.5	61	1.4	10.3	8.47	3.34	58.4	-	-	-
2C	13/10/11	7.21	18.8	19.0	6600	230	66.7	6.21	195	3760	96.2	2.2	.727267
2B	13/10/11	7.07	18.8	18.4	6800	230	115	6.08	261	3590	148.9	3	-
2A	14/10/11	7.17	8.6	7.8	2700	65	44.3	3.58	115	1490	20.4	0.8	-
3B	13/10/11	6.83	6.9	4.8	2400	36	47.7	5.33	84.2	1340	112.9	2.4	-
3A	13/10/11	6.80	17.5	7.3	6500	81	105	13.7	256	3150	79.3	1.9	-
4	13/10/11	6.79	0.18	1.1	9.7	2.5	5.54	1.83	1.5	26.1	33.6	0.9	.729928
ST1	13/10/11	6.68	0.16	1.1	8.2	1.5	5.59	1.4	2.73	22.9	24.2	0.7	-
ST3	14/10/11	6.70	0.39	2.1	43	2.6	0.244	2.07	2.01	75	6.9	0.6	-
ST4	14/10/11	7.31	3.0	10.5	570	48	3.26	0.859	12.1	565	46.6	1.3	-
Brooklyn	14/10/11	6.98	0.08	0.3	12	0.83	1.78	1.32	1.21	8.61	0.55	0.04	.726396

Location	F ⁻ mg/L	Br ⁻ mg/L	NO ₃ ⁻ mg/L	S mg/L	Al mg/L	B mg/L	Fe mg/L	Mn mg/L	P mg/L	Si mg/L	Sr mg/L	Zn mg/L
1C	0.10	<0.05	0.65	0.812	0.639	<0.1	0.195	<0.05	<0.1	19.2	<0.05	<0.05
1B	0.13	<0.05	0.91	0.769	0.779	<0.1	0.218	0.143	<0.1	20.2	<0.05	<0.05
2C	0.91	16	0.08	63.7	<0.25	<0.5	0.861	2.28	<0.5	24.2	2.54	<0.25
2B	0.98	17	0.12	65.1	<0.25	<0.5	<0.5	1.01	<0.5	30.3	3.64	<0.25
3B	0.21	12	0.11	19.6	<0.25	<0.5	1.17	2.49	<0.5	33.8	2.17	<0.25
3A	0.27	14	0.09	21.8	<0.25	<0.5	<0.5	1.27	<0.5	28.1	2.65	<0.25
4	0.10	<0.05	0.34	0.707	0.837	<0.1	0.3	<0.05	<0.1	19.8	<0.05	<0.05
Brooklyn	<0.05	<0.05	<0.05	<0.1	<0.05	<0.1	<0.1	<0.05	<0.1	<0.1	<0.05	<0.05
1C	0.06	<0.05	0.12	0.544	<0.05	<0.1	<0.1	<0.05	<0.1	18.4	<0.05	0.208
1B	0.08	<0.05	<0.05	0.471	<0.05	<0.1	0.226	0.223	<0.1	17.9	<0.05	0.0615
1A	0.29	0.13	0.87	0.458	<0.05	<0.1	0.107	0.564	<0.1	28.5	<0.05	0.384
2C	<1	14	<1	66.5	<0.25	<0.5	<0.5	2.1	<0.5	25.9	2.62	<0.25
2B	<1	14	<1	65.4	<0.25	<0.5	<0.5	1.11	<0.5	30.7	3.49	<0.25
2A	0.56	5.50	0.19	18.5	<0.25	<0.5	<0.5	2.5	<0.5	29.5	1.31	0.334
3B	<0.5	4.8	<0.5	10.5	<0.25	<0.5	0.507	0.557	<0.5	32.8	0.894	<0.25
3A	<1	13	<1	24.9	<0.25	<0.5	<0.5	1.18	<0.5	29	3	<0.25
4	0.06	<0.05	0.08	0.82	<0.05	<0.1	<0.1	<0.05	<0.1	18	<0.05	0.163
ST1	0.07	0.05	<0.05	0.507	<0.05	<0.1	<0.1	<0.05	<0.1	18.3	<0.05	0.146
ST3	0.66	0.09	0.27	0.756	43.5	<0.1	9.21	<0.05	<0.1	66.3	<0.05	0.0663
ST4	2.0	1.2	<0.2	14.4	<0.05	0.115	<0.1	0.242	0.126	32.5	0.0802	0.15
Brooklyn	<0.05	<0.05	<0.05	0.376	<0.05	<0.1	0.359	0.0567	<0.1	7.44	<0.05	<0.05

Appendix F Published conference proceedings

F1 Effects of bank storage on near-stream groundwater – an investigation of the hydraulics and chemistry in the Cockburn River, NSW

Presented at the 11th Australasian Environmental Isotope Conference and 4th Australasian Hydrogeology Research Conference, Cairns, July 2011.

Chani Welch¹ and Peter G. Cook^{1,2}

¹National Centre for Groundwater Research and Training (NCGRT), Flinders University, School of the Environment, Adelaide, Australia

²Water for a Healthy Country National Research Flagship, Commonwealth Scientific and Industrial Research Organization, Division of Land and Water, Glen Osmond, Adelaide, South Australia, Australia.

Of prime importance to water managers is the quantification of fluxes between surface water and groundwater reservoirs. One technique that is commonly used to quantify fluxes from groundwater to gaining rivers is chemical baseflow separation, a mass balance approach. One major drawback of this technique is that it assumes constant groundwater discharge chemistry (c_g).

It was posited that bank storage causes surface water and groundwater to mix in the near-stream zone, and, as water resumes discharging to the river, results in a predictable temporal variation in the chemistry of groundwater discharge that varies markedly from 'regional' groundwater. If this process is significant, estimates of groundwater discharge from mass balance methods could vary substantially, as the selection of c_g has a large influence on the flux estimate.

This project investigated the process of bank storage in the Cockburn River in Northern NSW. The Cockburn River has a catchment area of approximately 1100km², and is underlain

in the upper part of the catchment by fractured rock before flattening out onto an alluvial floodplain. Time series level and electrical conductivity (EC) measurements were obtained at locations within the river and adjacent groundwater at varying distances from the riverbank to capture responses to passing flood waves. Results from a piezometer located approximately 10m from the riverbank show delays between peak level in the river and groundwater of hours, whereas delays between EC minima were days. This substantially longer lag in arrival of the EC response indicated that while the head change was transmitted rapidly to the aquifer, actual water movement occurred much more slowly.

A FEFLOW model was constructed to investigate the stream and aquifer parameters influencing the delay between movement of the hydraulic and solute fronts. The model was used to interpret results from additional monitoring locations along the river.

F2 Estimating aquifer parameters from time series EC and pressure data collected during river flow events

Presented at the 2012 NGWA Ground Water Summit, Garden Grove, May 2012.

C. Welch¹, P.G. Cook^{1,2}, Glenn Harrington^{1,2}, and Neville Robinson¹

¹ National Centre for Groundwater Research and Training (NCGRT), School of the Environment, Flinders University, GPO Box 2100, Adelaide, SA 5001, Australia

² Water for a Healthy Country National Research Flagship, Commonwealth Scientific and Industrial Research Organization, Division of Land and Water, Glen Osmond, Adelaide, SA, Australia

Numerous analytical models have been developed for predicting pressure responses in aquifers resulting from water level variations in rivers. These models have also been used for estimating aquifer parameters from observed responses in bores adjacent to the river.

Where the river and aquifer have distinct chemistries, then this same process can also produce a water quality (solute) response in the adjacent aquifer. However, there are few

observations of such responses in bores following river flow events, and limited theoretical development in the use of solute data to estimate aquifer parameters.

We present a new semi-analytical solution that relates travel distance and time for movement of a solute into a confined aquifer to the increase in river stage (H), and aquifer parameters hydraulic conductivity, storativity (S), porosity (θ), and aquifer thickness (b).

Combining solute travel time with an existing solution for pressure travel time yields a ratio that is solely a function of H , S , θ , and b .

A 2D numerical model of an aquifer slice perpendicular to a river was constructed in FEFLOW. Simulations of a confined system indicate good agreement with t_s and t_p predicted by the analytical solutions. The applicability of the relationships to unconfined systems in which rivers are generally located is evaluated through simulations in an equivalent model that explicitly includes the unsaturated zone. Sensitivity analysis indicates that the predicted relationships generally hold, providing that unsaturated zone storage is appropriately represented.

The utility of the method for estimating aquifer thickness and storage is tested using extended time series data from an observation bore. The field example indicates that co-measurement of pressure and EC and application of the analytical relationships can reasonably estimate aquifer thickness using standard ratios for storage parameters, or conversely, if aquifer thickness is known, can provide an estimate of the storage parameters.

F3 Interpreting aquifer pressure and solute responses to river flood events in the presence of alluvial heterogeneity

*Presented at the International Association of Hydrogeologists 40th International Congress,
Perth, September 2013.*

Chani Welch*^{1,2}, Glenn Harrington^{1,3}, Marc LeBlanc^{1,4} & Peter G. Cook^{1,2,3}

¹National Centre for Groundwater Research and Training, c/o Flinders University GPO Box 2100, Adelaide SA 5001, Australia

²School of the Environment, Flinders University, GPO Box 2100, Adelaide SA 5001, Australia

³CSIRO Water for a Healthy Country Flagship, Private Bag 2, Glen Osmond SA 5064, Australia

⁴School of Earth and Environmental Sciences, James Cook University, PO Box 6811, Cairns, QLD-870, Australia

Two commonly used tools for assessing river – aquifer interaction are pressure and salinity responses at monitoring bores during flood events. We demonstrate that responses observed within alluvial aquifers are a function of the dominant type of sub-surface structure through numerical simulations of two stylised conceptual models, firstly streambed clogging layers, and secondly, horizontal high hydraulic conductivity sand layers between less conductive materials. The presence of a clogging layer significantly retards pressure propagation at smaller thicknesses and higher hydraulic conductivity than solute propagation. Consequently, the rate of head rise is reduced within the aquifer, a large hydraulic head difference across the clogging layer is maintained, and water and solute transport proceeds relatively unaffected despite the lower hydraulic conductivity. This may be identified from monitoring data at an observation point within the aquifer by a substantial change in solute concentration at almost the same time as the pressure response. Furthermore, the rate of pressure propagation is sensitive to the hydraulic conductivity of the aquifer at up to double the distance from the observation point to the

river; however the rate of solute propagation can be sensitive to the hydraulic conductivity at hundreds of times this distance. Pressure and solute responses within high hydraulic conductivity sand layers approach that which would be expected in an aquifer with saturated thickness equivalent to the thickness of the sand layer at a particular ratio of layer to aquifer hydraulic conductivities. However, further decreasing the ratio of hydraulic conductivities causes the gravel layer to begin to behave as a confined-type system with little change in water table surface despite faster pressure and slower solute responses.

Time series pressure and EC data from a transect of piezometers in an alluvial aquifer bordering the Mitchell River in tropical North Queensland are used to demonstrate how this new understanding of pressure and solute propagation can be used to infer the dominant type of structural heterogeneity of a system. Such information is critical for quantifying river – aquifer exchange fluxes, and for identifying probable contaminant transport rates and pathways.

References

- Baillie, M.N., Hogan, J.F., Ekwurzel, B., Wahi, A.K., Eastoe, C.J., 2007. Quantifying water sources to a semiarid riparian ecosystem, San Pedro River, Arizona. *Journal of Geophysical Research: Biogeosciences*, 112(G3): G03S02. doi: 10.1029/2006jg000263.
- Barlow, P.M., DeSimone, L.A., Moench, A.F., 2000. Aquifer response to stream-stage and recharge variations. II. Convolution method and applications. *Journal of Hydrology*, 230: 211-229. doi: 10.1016/s0022-1694(00)00176-1.
- Battle-Aguilar, J., Harrington, G.A., Leblanc, M., Welch, C., Cook, P.G., 2014. Chemistry of groundwater discharge inferred from longitudinal river sampling. *Water Resources Research*, 50(2): 1550-1568. doi: 10.1002/2013wr013591.
- Bear, J., 1972. *Dynamics of Fluids in Porous Materials*. American Elsevier.
- Bertin, C., Bourg, A.C.M., 1994. Radon-222 and Chloride as Natural Tracers of the Infiltration of River Water into an Alluvial Aquifer in Which There Is Significant River/Groundwater Mixing. *Environmental Science & Technology*, 28(5): 794-798. doi: 10.1021/es00054a008.
- Brunke, M., Gonser, T.O.M., 1997. The ecological significance of exchange processes between rivers and groundwater. *Freshwater Biology*, 37(1): 1-33. doi: 10.1046/j.1365-2427.1997.00143.x.
- Calver, A., 2001. Riverbed Permeabilities: Information from Pooled Data. *Ground Water*, 39(4): 546-553. doi: 10.1111/j.1745-6584.2001.tb02343.x.
- Cardenas, M.B., Markowski, M.S., 2010. Goelectrical Imaging of Hyporheic Exchange and Mixing of River Water and Groundwater in a Large Regulated River. *Environmental Science & Technology*, 45(4): 1407-1411. doi: 10.1021/es103438a.
- Cardenas, M.B., Zlotnik, V.A., 2003. Three-dimensional model of modern channel bend deposits. *Water Resources Research*, 39(6): 1141. doi: 10.1029/2002wr001383.
- Carsel, R.F., Parrish, R.S., 1988. Developing joint probability distributions of soil water retention characteristics. *Water Resources Research*, 24(5): 755-769. doi: 10.1029/WR024i005p00755.
- Carslaw, H.S., Jaeger, J.C., 1959. *Conduction of Heat in Solids*. Oxford at the Clarendon Press, London.
- Chen, X., Chen, D.Y., Chen, X.-h., 2006. Simulation of baseflow accounting for the effect of bank storage and its implication in baseflow separation. *Journal of Hydrology*, 327: 539-549. doi: 10.1016/j.jhydrol.2005.11.057.
- Chen, X., Chen, X.-h., 2003. Stream water infiltration, bank storage, and storage zone changes due to stream-stage fluctuations. *Journal of Hydrology*, 280: 246-264. doi: 10.1016/s0022-1694(03)00232-4.
- Cirpka, O.A. et al., 2007. Analyzing Bank Filtration by Deconvoluting Time Series of Electric Conductivity. *Ground Water*, 45(3): 318-328. doi: 10.1111/j.1745-6584.2006.00293.x.
- Cook, P.G., Lamontagne, S., Berhane, D., Clark, J.F., 2006. Quantifying groundwater discharge to Cockburn River, southeastern Australia, using dissolved gas tracers ^{222}Rn and SF_6 . *Water Resources Research*, 42(10): W10411. doi: 10.1029/2006wr004921.
- Cooper, H.H.J., Rorabaugh, M.I., 1963. Ground-water movements and bank storage due to flood stages in surface streams. U.S.G.S. Water Supply Paper 1536-J: 343-366. doi:
- CSIRO, 2009. Water in the Mitchell Region, CSIRO Water for a Healthy Country Flagship, Australia.
- Dentz, M., Le Borgne, T., Englert, A., Bijeljic, B., 2011. Mixing, spreading and reaction in heterogeneous media: A brief review. *Journal of Contaminant Hydrology*, 120–121: 1-17. doi: 10.1016/j.jconhyd.2010.05.002.
- Diersch, H.J., 2009. FEFLOW Reference Manual, Finite Element Subsurface Flow & Transport Simulation System. DHI-WASY GmbH, Berlin.

- Doble, R., Brunner, P., McCallum, J., Cook, P.G., 2012. An Analysis of River Bank Slope and Unsaturated Flow Effects on Bank Storage. *Ground Water*, 50(1): 77-86. doi: 10.1111/j.1745-6584.2011.00821.x.
- Engdahl, N.B., Vogler, E.T., Weissmann, G.S., 2010. Evaluation of aquifer heterogeneity effects on river flow loss using a transition probability framework. *Water Resources Research*, 46(1): W01506. doi: 10.1029/2009wr007903.
- Fleckenstein, J.H., Niswonger, R.G., Fogg, G.E., 2006. River-Aquifer Interactions, Geologic Heterogeneity, and Low-Flow Management. *Ground Water*, 44(6): 837-852. doi: 10.1111/j.1745-6584.2006.00190.x.
- Frank, W.L., 1958. Finding zeros of arbitrary functions. *Journal of the ACM (JACM)*, 5(2): 154-160. doi: 10.1145/320924.320928.
- Gardner, W.P., Harrington, G.A., Solomon, D.K., Cook, P.G., 2011. Using terrigenic ^{4}He to identify and quantify regional groundwater discharge to streams. *Water Resources Research*, 47(6): W06523. doi: 10.1029/2010wr010276.
- Gelhar, L.W., Welty, C., Rehfeldt, K.R., 1992. A critical review of data on field-scale dispersion in aquifers. *Water Resources Research*, 28(7): 1955-1974. doi: 10.1029/92wr00607.
- Genereux, D.P., Leahy, S., Mitasova, H., Kennedy, C.D., Corbett, D.R., 2008. Spatial and temporal variability of streambed hydraulic conductivity in West Bear Creek, North Carolina, USA. *Journal of Hydrology*, 358: 332-353. doi: 10.1016/j.jhydrol.2008.06.017.
- Gerecht, K.E. et al., 2011. Dynamics of hyporheic flow and heat transport across a bed-to-bank continuum in a large regulated river. *Water Resources Research*, 47(3): W03524. doi: 10.1029/2010wr009794.
- Gilfedder, B.S., Hofmann, H., Cartwright, I., 2012. Novel Instruments for in Situ Continuous Rn-222 Measurement in Groundwater and the Application to River Bank Infiltration. *Environmental Science & Technology*, 47(2): 993-1000. doi: 10.1021/es3034928.
- Guinn Garrett, C., Vulava, V.M., Callahan, T.J., Jones, M.L., 2012. Groundwater-surface water interactions in a lowland watershed: source contribution to stream flow. *Hydrological Processes*, 26(21): 3195-3206. doi: 10.1002/hyp.8257.
- Ha, K., Koh, D.-C., Yum, B.-W., Lee, K.-K., 2007. Estimation of layered aquifer diffusivity and river resistance using flood wave response model. *Journal of Hydrology*, 337: 284-293. doi: 10.1016/j.jhydrol.2007.01.040.
- Hall, F.R., Moench, A.F., 1972. Application of the convolution equation to stream-aquifer relationships. *Water Resources Research*, 8(2): 487-493. doi: 10.1029/WR008i002p00487.
- Hantush, M.S., 1961. Discussion of Paper by P. P. Rowe, "An Equation for Estimating Transmissibility and Coefficient of Storage from River-Level Fluctuations". *Journal of Geophysical Research*, 66(4): 1310-1311. doi: 10.1029/JZ066i004p01310.
- Hantush, M.S., 1965. Wells near streams with semipervious beds. *Journal of Geophysical Research*, 70(12): 2829-2838. doi: 10.1029/JZ070i012p02829.
- Heeren, D.M. et al., 2011. Stage-dependent transient storage of phosphorus in alluvial floodplains. *Hydrological Processes*, 25(20): 3230-3243. doi: 10.1002/hyp.8054.
- Hill, M.C., Tiedeman, C.R., 2007. Effective groundwater model calibration: with analysis of data, sensitivities, predictions, and uncertainty. John Wiley & Sons, Inc, Hoboken, New Jersey, 455 pp.
- Hornberger, G.M., Ebert, J., Remson, I., 1970. Numerical Solution of the Boussinesq Equation for Aquifer-Stream Interaction. *Water Resources Research*, 6(2): 601-608. doi: 10.1029/WR006i002p00601.
- Hunt, R.J., Coplen, T.B., Haas, N.L., Saad, D.A., Borchardt, M.A., 2005. Investigating surface water-well interaction using stable isotope ratios of water. *Journal of Hydrology*, 302: 154-172. doi: 10.1016/j.jhydrol.2004.07.010.

- Kalbus, E., Reinstorf, F., Schirmer, M., 2006. Measuring methods for groundwater – surface water interactions: a r;review. *Hydrological Earth System Sciences*, 10(6): 873-887. doi: 10.5194/hess-10-873-2006.
- Kirchner, J.W., 2003. A double paradox in catchment hydrology and geochemistry. *Hydrological Processes*, 17(4): 871-874. doi: 10.1002/hyp.5108.
- Knudby, C., Carrera, J., 2006. On the use of apparent hydraulic diffusivity as an indicator of connectivity. *Journal of Hydrology*, 329: 377-389. doi: 10.1016/j.jhydrol.2006.02.026.
- Kondolf, G.M., Maloney, L.M., Williams, J.G., 1987. Effects of bank storage and well pumping on base flow, Carmel River, Monterey County, California. *Journal of Hydrology*, 91: 351-369. doi: 10.1016/0022-1694(87)90211-3.
- Leaney, F.W., Herczeg, A.L., 2006. A rapid field extraction method for determination of radon-222 in natural waters by liquid scintillation counting. *Limnology and Oceanography: Methods*, 4: 254-259.
- Lewandowski, J., Lischeid, G., Nützmann, G., 2009. Drivers of water level fluctuations and hydrological exchange between groundwater and surface water at the lowland River Spree (Germany): field study and statistical analyses. *Hydrological Processes*, 23(15): 2117-2128. doi: 10.1002/hyp.7277.
- Li, H., Boufadel, M.C., Weaver, J.W., 2008. Quantifying Bank Storage of Variably Saturated Aquifers. *Ground Water*, 46(6): 841-850. doi: 10.1111/j.1745-6584.2008.00475.x.
- Mächler, L., Brennwald, M.S., Kipfer, R., 2012. Membrane Inlet Mass Spectrometer for the Quasi-Continuous On-Site Analysis of Dissolved Gases in Groundwater. *Environmental Science & Technology*, 46(15): 8288-8296. doi: 10.1021/es3004409.
- McCallum, J.L., Cook, P.G., Brunner, P., Berhane, D., 2010. Solute dynamics during bank storage flows and implications for chemical base flow separation. *Water Resources Research*, 46(7): W07541. doi: 10.1029/2009wr008539.
- McKenna, S.A., Ingraham, N.L., Jacobson, R.L., Cochran, G.F., 1992. A stable isotope study of bank storage mechanisms in the Truckee river basin. *Journal of Hydrology*, 134: 203-219. doi: 10.1016/0022-1694(92)90036-u.
- Meredith, K.T. et al., 2009. Temporal variation in stable isotopes (^{18}O and ^2H) and major ion concentrations within the Darling River between Bourke and Wilcannia due to variable flows, saline groundwater influx and evaporation. *Journal of Hydrology*, 378: 313-324. doi: 10.1016/j.jhydrol.2009.09.036.
- Meyboom, P., 1961. Estimating ground-water recharge from stream hydrographs. *Journal of Geophysical Research*, 66(4): 1203-1214. doi: 10.1029/JZ066i004p01203.
- Muller, D.E., 1956. A Method for Solving Algebraic Equations Using an Automatic Computer. *Mathematical Tables and Other Aids to Computation*, 10(56): 208-215. doi: 10.2307/2001916.
- Nevill, C., 2009. Managing Cumulative Impacts: Groundwater Reform in the Murray-Darling Basin, Australia. *Water Resour Manage*, 23(13): 2605-2631. doi: 10.1007/s11269-009-9399-0.
- Page, R.M., Lischeid, G., Epting, J., Huggenberger, P., 2012. Principal component analysis of time series for identifying indicator variables for riverine groundwater extraction management. *Journal of Hydrology*, 432–433: 137-144. doi: 10.1016/j.jhydrol.2012.02.025.
- Pinder, G.F., Bredehoeft, J.D., Cooper, H.H., Jr., 1969. Determination of Aquifer Diffusivity from Aquifer Response to Fluctuations in River Stage. *Water Resources Research*, 5(4): 850-855. doi: 10.1029/WR005i004p00850.
- Pinder, G.F., Sauer, S.P., 1971. Numerical Simulation of Flood Wave Modification Due to Bank Storage Effects. *Water Resources Research*, 7(1): 63-70. doi: 10.1029/WR007i001p00063.

- Poole, G.C., Stanford, J.A., Frissell, C.A., Running, S.W., 2002. Three-dimensional mapping of geomorphic controls on flood-plain hydrology and connectivity from aerial photos. *Geomorphology*, 48(4): 329-347. doi: 10.1016/S0169-555X(02)00078-8.
- Renard, P., Allard, D., 2013. Connectivity metrics for subsurface flow and transport. *Advances in Water Resources*, 51: 168-196. doi: 10.1016/j.advwatres.2011.12.001.
- Rorabaugh, M.I., 1960. Use of water levels in estimating aquifer constants in a finite aquifer. International Association of Scientific Hydrology(Publication 52): 314-323. doi:
- Rowe, P.P., 1960. An Equation for Estimating Transmissibility and Coefficient of Storage from River-Level Fluctuations. *Journal of Geophysical Research*, 65(10): 3419-3424. doi: 10.1029/JZ065i010p03419.
- Sawyer, A.H., Bayani Cardenas, M., Bomar, A., Mackey, M., 2009. Impact of dam operations on hyporheic exchange in the riparian zone of a regulated river. *Hydrological Processes*, 23(15): 2129-2137. doi: 10.1002/hyp.7324.
- Schilling, K.E., Li, Z., Zhang, Y.-K., 2006. Groundwater-surface water interaction in the riparian zone of an incised channel, Walnut Creek, Iowa. *Journal of Hydrology*, 327: 140-150. doi: 10.1016/j.jhydrol.2005.11.014.
- Sharp Jr, J.M., 1977. Limitations of bank-storage model assumptions. *Journal of Hydrology*, 35: 31-47. doi: 10.1016/0022-1694(77)90075-0.
- Simpson, S.C., Meixner, T., 2012. The influence of local hydrogeologic forcings on near-stream event water recharge and retention (Upper San Pedro River, Arizona). *Hydrological Processes*. doi: 10.1002/hyp.8411.
- Sjodin, A., Lewis, W.M., Saunders, J.F., 2001. Analysis of groundwater exchange for a large plains river in Colorado (USA). *Hydrological Processes*, 15(4): 609-620. doi: 10.1002/hyp.173.
- Solomon, D.K., Genereux, D.P., Plummer, L.N., Busenberg, E., 2010. Testing mixing models of old and young groundwater in a tropical lowland rain forest with environmental tracers. *Water Resources Research*, 46(4): W04518. doi: 10.1029/2009wr008341.
- Sophocleous, M., 2002. Interactions between groundwater and surface water: the state of the science. *Hydrogeology Journal*, 10(1): 52-67. doi: 10.1007/s10040-001-0170-8.
- Squillace, P.J., 1996. Observed and Simulated Movement of Bank-Storage Water. *Ground Water*, 34(1): 121-134. doi: 10.1111/j.1745-6584.1996.tb01872.x.
- Todd, D.K., 1956. Ground-water flow in relation to a flooding stream. American Society of Civil Engineers.
- Trinchero, P., Sánchez-Vila, X., Fernández-García, D., 2008. Point-to-point connectivity, an abstract concept or a key issue for risk assessment studies? *Advances in Water Resources*, 31(12): 1742-1753. doi: 10.1016/j.advwatres.2008.09.001.
- Vogt, T. et al., 2010. Fluctuations of electrical conductivity as a natural tracer for bank filtration in a losing stream. *Advances in Water Resources*, 33(11): 1296-1308. doi: 10.1016/j.advwatres.2010.02.007.
- Ward, A.S., Gooseff, M.N., Singha, K., 2010. Imaging hyporheic zone solute transport using electrical resistivity. *Hydrological Processes*, 24(7): 948-953. doi: 10.1002/hyp.7672.
- Welch, C., Cook, P.G., Harrington, G.A., Robinson, N.I., 2013. Propagation of solutes and pressure into aquifers following river stage rise. *Water Resources Research*, 49(9): 5246-5259. doi: 10.1002/wrcr.20408.
- Welch, C., Harrington, G.A., Leblanc, M., Batlle-Aguilar, J., Cook, P.G., 2014. Relative rates of solute and pressure propagation into heterogeneous alluvial aquifers following river flow events. *Journal of Hydrology*, 511: 891-903. doi: 10.1016/j.jhydrol.2014.02.032.
- Wett, B., Jarosch, H., Ingerle, K., 2002. Flood induced infiltration affecting a bank filtrate well at the River Enns, Austria. *Journal of Hydrology*, 266: 222-234. doi: 10.1016/S0022-1694(02)00167-1.

- Whiting, P.J., Pomeranets, M., 1997. A numerical study of bank storage and its contribution to streamflow. *Journal of Hydrology*, 202: 121-136. doi: 10.1016/s0022-1694(97)00064-4.
- Winter, T.C., Judson W. Harvey, O. Lehn Franke, William M. Alley, 1998. Ground Water and Surface Water: A Single Resource. U.S. Geological Survey Circular, 1139.
- Woessner, W.W., 2000. Stream and fluvial plain ground water interactions: Rescaling hydrogeologic thought. *Ground Water*, 38(3): 423-423-429. doi: 10.1111/j.1745-6584.2000.tb00228.x.
- Yeh, T.-C.J. et al., 2009. River stage tomography: A new approach for characterizing groundwater basins. *Water Resources Research*, 45(5): W05409. doi: 10.1029/2008wr007233.
- Zlotnik, V.A., Huang, H., 1999. Effect of Shallow Penetration and Streambed Sediments on Aquifer Response to Stream Stage Fluctuations (Analytical Model). *Ground Water*, 37(4): 599-605. doi: 10.1111/j.1745-6584.1999.tb01147.x.